

SOLUBILIZATION AND MOBILIZATION OF PERCHLOROETHYLENE BY
COSOLVENTS IN POROUS MEDIA

By

MICHAEL EDWARD VAN VALKENBURG

A DISSERTATION PRESENTED TO THE GRADUATE SCHOOL
OF THE UNIVERSITY OF FLORIDA IN PARTIAL FULFILLMENT
OF THE REQUIREMENTS FOR THE DEGREE OF
DOCTOR OF PHILOSOPHY

UNIVERSITY OF FLORIDA

1999

This dissertation is dedicated to each person who gave his or her life so valiantly and courageously for our country. I know this is but a little gesture, but nonetheless their sacrifices have moved me so deeply, that any acknowledgement of them in remembrance is the least that each of us can do. I hope in just reading this, you will remember them.

ACKNOWLEDGMENTS

I would certainly not be in the position to be even writing these acknowledgements if it were not for the support of my family throughout the years. Through several times of self-evaluation and self re-direction, they have always been supportive and helpful, providing motivation when I had very little – especially my Mom. I am thankful for my Dad, for “buying me books and teaching me all he knew.” I know he was far from perfect, so am I, but he was, is, and always will be my Dad.

My wife, Kim, and our three children, Joseph, Lauryn, and Kelley have been so understanding about times devoted away from them when they have wanted me the most, and my attentiveness that could have always been better. There was always something else on my mind – to finish this! I wish I could have been there even more. I will always try to be a better father and husband. There is more to come.

I extend my sincere appreciation to the U.S. Air Force (and the American taxpayer) for sponsoring my education and completion of this dissertation. I thank the Biomedical Sciences Corps for its flexibility and thank the U.S. Air Force Academy and the Department of Chemistry for having the faith in me to complete this degree and wanting me back to work in what has to be one of the nicest environments in the world! Special thanks go to Col. Hans Mueh, Col. Clifford Utermoehlen, Lt. Col. Ron Furstenau, and Maj. Rob Racicot.

Obvious thanks go to Dr. Mike Annable and my committee members for their guidance in my completion of this project. Special thanks go to Dr. Joe Delfino for taking the time to sit down for lunch with me in a deli in Denver, Colorado during an ACS convention and encouraging me to become a Gator! Also, I valued his graduate program guidance and wise advice that I took on numerous occasions. Thanks are given to Dr. Bill Wise for his many hours of exchanging knowledge, in the lab and in the office, and to Dr. Suresh Rao for his confidence building. Finally, special gratitude to Mike Annable for being so understanding, supportive, and always open to my impromptu office visits seeking guidance and tutelage.

Thanks also go to my fellow lab partners, Michael Brooks, Jaehyun Cho, Clayton Clark, and Rick Young for their many instances of assistance and showing patience with me, and to Randy Switt for all his computer help. To my fellow 2-D boxer and final lab inmate – Jim Jawitz – I appreciate the use of “the box,” his motivational assistance, the hours of practical knowledge, and the many laughs. He will not be “forgotten” in this document.

One final person, who I am sure does not get recognized enough and whose expertise I am grateful for, is Lynn LaBauve, of the Marston Science Library Reference Desk. Over the last three years she has sought me out numerous times to help in searching the vast reference databases used in completing research. Those needing reference help at the University of Florida should find her and they will reap the benefits.

TABLE OF CONTENTS

	<u>page</u>
ACKNOWLEDGMENTS	iii
LIST OF TABLES	viii
LIST OF FIGURES	ix
ABSTRACT	xiii
 CHAPTERS	
1. INTRODUCTION.....	1
Background.....	1
Selection of DNAPL	5
Study Objectives	5
Dissertation Organization.....	8
2. INVESTIGATIONS OF THE RELATIONSHIP OF COSOLVENT FRACTION TO PERCHLOROETHYLENE (PCE) SOLUBILITY AND EQUILIBRIUM INTERFACIAL TENSION	9
Introduction.....	9
Comparison of the Molecular Structures of Water and Low Molecular Weight Alcohols.....	10
Solubility of Hydrocarbons into Water/alcohol Mixtures and its Relationship to Amount of Cosolvent	13
Log-linear relationship.....	15
Cosolvency power.....	17
Other methods for solubility estimation	17
Choice of solubility estimation method	21
Interfacial Tension of Ternary Alcohol/water/PMOS Mixtures	21
Relation to amount of cosolvent	22
Different interfacial tension prediction methods	23
Relation of IFT to Solubility of Organic Solute	27
Materials and Methods.....	27
Results and Discussion.....	29
Log Linear Solubility Estimation.....	29
Ethanol	29

Isopropanol (IPA).....	30
UNIFAC Method.....	31
Extended Hildebrand Method.....	31
Minor cosolvent addition.....	35
Interfacial Tension Measurements and Predictions.....	36
Conclusions.....	39
3. MOBILIZATION OF RESIDUAL PERCHLOROETHYLENE DURING COSOLVENT FLOODING.....	42
Introduction.....	42
Solubilization vs. Mobilization	45
The Trapping Number Relationship.....	47
Study Objective	49
Materials and Methods.....	50
GC Analysis.....	50
Physical Measurements	51
Sand Column Preparation.....	51
PCE Saturation.....	52
Hydrodynamic Parameters	52
Sand Column Mobilization Studies.....	53
Results and Discussion.....	54
Equilibrated Gradient Column Studies.....	54
Blank Equilibrated Gradient Study	55
Non Equilibrated Column Studies	55
Generation of Mobilization Curves.....	58
Swelling Effects of Cosolvents.....	62
Conclusions.....	64
4. ENTRAPMENT VERSUS MOBILIZATION OF RESIDUAL PERCHLOROETHYLENE DURING COSOLVENT FLOODING.....	66
Introduction.....	66
Solubilization, Mobilization and the Trapping Number Relationship	68
Mobilization and Entrapment of Residual Non-Aqueous Phase Liquid.....	68
Study Objective	70
Materials and Methods.....	70
Physical Measurements	71
Sand Column Preparation.....	71
PCE Saturation and Generation of Trapping Curves.....	72
Mobilization studies	72
Entrapment studies.....	74
Hydrologic Parameters.....	74
Results and Discussion.....	76
Entrapment in Homogeneous Sand Column	77
Effect of Pore Size Heterogeneity on the Entrapment of PCE.....	80

Conclusions	83
5. MOBILIZATION AND ENTRY OF DNAPL POOLS INTO FINER SAND MEDIA: TWO-DIMENSIONAL BOX STUDIES.....	85
Introduction.....	85
Materials and Methods.....	90
General Packing Procedure	91
Dye Tracer Displacement	93
DNAPL Introduction	94
Hydraulic Controls During 2-D Box Experiments.....	94
Results and Discussion.....	95
No. 100-140 Fine Layer	95
Step input of 100% alcohol	95
One-dimensional horizontal sand column experiments.....	98
Step input of 80% alcohol	99
No. 60-70 Fine Layer.....	101
Step input of 80% alcohol.....	101
Gradient Injection (10-90%) of Alcohol	101
No. 40-50 Fine Layer.....	105
Background dye flush after DNAPL injection.....	105
Step input of 80% alcohol.....	106
No. 30-40 Fine Layer.....	107
Step input of 80% alcohol.....	107
Step input of 70% alcohol.....	109
Step input of 50% alcohol.....	110
Two-Dimensional Studies with t-Butyl Alcohol.....	110
Step input of 30% TBA: #30-40 finer layer	111
Step input of 40% TBA: #100-140 finer layer	111
Systematic Quantitative Evaluation and Prediction of Mobilization into Finer Layers.....	116
Conclusions	120
6. SUMMARY AND CONCLUSIONS	122
APPENDICES	
A MOISTURE RELEASE CURVES FOR SAND MEDIA.....	127
B TWO-DIMENSIONAL BOX SCHEMATICS	134
REFERENCES.....	147
BIOGRAPHICAL SKETCH	156

LIST OF TABLES

Table	<u>page</u>
2-1. Solubility parameters for study components (Barton 1975)	32
3-1. Physical Measurements of PCE Saturated Cosolvent Solutions	57
3-2. Physical properties of solutions used in swelling mobilization studies.	64
4-1. Results of linear regression of entrapment studies	79
5-1. Particle size ranges of sands used.....	92
5-2. Summary of Experimental Runs in 2-Dimensional Box Studies	96
5-3 – Summary of desaturation profile curve fitting parameters. Beit Netofa Clay values (α , n , and m) are from van Genuchten (1980). Pore radius for the clay is taken from Wise (1992).	117
5-4 – Results of globule force balance calculations. Mobilization of globule is predicted if $h_{dnapl} > h_d^{cs / dnapl}$. Permeability of 20-30 medium measured to be $6.35E-7 \text{ cm}^2$. “Clay” scenario based on Beit Netofa clay (van Genuchten 1980) is shown for comparison. Fluid property values shown are approximate and for illustrative purposes.	119

LIST OF FIGURES

Figure	page
2-1. Graph of data from Franks and Ives (1966), relating concentration of hydrogen bonds to volume fraction of ethanol.....	12
2-2. Solubility of PCE as a function of cosolvent volume fractions (initial phase volumetric phase ratio 1:1).....	30
2-3. Comparison of Measured Solubility Data and those predicted by the UNIFAC Method.	32
2-4. PCE Solubility Prediction of the Hildebrand and Extended-Hildebrand Theories for the IPA Cosolvent Mixtures.	34
2-5. Solubility of PCE as a function of various cosolvent volume fractions (initial phase volumetric phase ratio 1:1).....	36
2-6. Relationship of equilibrated interfacial tension of PCE/alcohol/water ternary systems as a function of initial cosolvent volume fraction.	37
2-7. Logarithmic plot of the IFT of ternary PCE/cosolvent/water mixtures versus initial volume fraction of cosolvent. Additional data for addition of 10% isobutanol is shown for reference.....	38
2-8. Interfacial tension of PCE/cosolvent/water mixtures related to solubility of PCE in the aqueous phase. Numbers above selected data points indicate initial volume fraction of cosolvent.	40
3-1. Gradient effluent profile for saturated PCE run (influent %'s shown are ethanol volume fractions prior to saturation).	56
3-2. Gradient effluent profile using unsaturated ethanol mixtures - percent of mobilization shown.	56
3-3. Gradient effluent profile using unsaturated ethanol cosolvent mixtures with PCE saturation reduction shown.	57

3-4. Mobilization curves showing effect of a cosolvent (ethanol) flushing phase which is pre-equilibrated with PCE (gradient 2 and 4) and a flushing phase with full solubilization potential (non-equilibrated 1). All are gradient runs.....	59
3-5. PCE Desaturation Curves – PCE saturated ethanol cosolvent runs compared with data from Pennell et al. (1996).	60
3-6 Ethanol mobilization curves with surfactant run superimposed.	61
3-7. Results from mobilization studies using pre-equilibrated IPA solutions, superimposed on the ethanol study results.	63
3-8. Results of mobilization of PCE during gradient TBA column flushing; TBA pre-equilibrated with PCE.	63
4-1. Moisture release curve for No. 30-40 silica sand used for these studies, conducted via Tempe cell. van Genuchten (1980) and Brooks & Corey (1964) fits are based on minimizing the sum of squares of the difference between the actual data and the fitted line.....	75
4-2. Relative permeability to the wetting phase at less than normal nonwetting phase residual saturations: Morrow and Songkran (1982) data shown with regression ($R^2 = 0.907$) and fit of this study's Tempe cell data based on van Genuchten (1980) parameters and the Mualem (1976) method.....	76
4-3. PCE Desaturation curve – experimental ethanol data only compared to those of Pennell et al. (1996).	77
4-4. PCE desaturation curves for both mobilization and entrapment studies, with linear regressions shown for the entrapment experiments	79
4-5. Effective saturation of study 30-40 mesh sand as a function of capillary pressure, resulting slope of regressed line is the Brooks and Corey lambda, $\lambda = 3.65$	81
4-6. Results of entrapment experiments on the heterogeneous packing (#20-100 sand), shown with homogeneous entrapment and mobilization results for reference.	82
5-1. Schematic of DNAPL contamination of subsurface aquifer systems, showing free phase and residual DNAPL.	87
5-2. Typical 2-D box setup after injection of PCE, prior to any flushing.	93
5-3. Dyed PCE injected into Number 20-30 medium (approximately 2.7 ml) pooled over a 1 cm layer of Number 100-140 medium.	97

5-4. Removal of residual dyed PCE by gradient ethanol injection (0-100% v/v) over one pore volume. Darker band at interface is highly saturated PCE which is mobilizing toward the lower left and pooling.....	99
5-5. Progression of DNAPL pool collapse – Nos. 20-30 background medium, Nos. 100-140 finer layer - after 0.8 PV of 80% v/v ethanol/water step input. Downstream direction is to the right in all pictures.....	100
5-6. Spreading of DNAPL pool downstream on top of finer Nos 100-140 layer. No breakthrough occurred during this run – 1.1 PV after 80% v/v ethanol/water step input.	100
5-7. Schematic of step input of 80% alcohol - No. 60-70 finer layer.....	103
5-8. Horizontal spreading of PCE pool upstream from injection zone - Nos. 20-30 background media, 60-70 finer layer, 1.1 PV after gradient injection of 10 – 90% v/v ethanol/water over 1PV. Blue band is location of 58% (leading edge) to 76% ethanol.....	104
5-9. Highly concentrated cosolvent phase in which dye has partitioned, entering finer Nos. 60-70 layer. This is not free phase mobilization. Blue band above is from a post gradient step input to 100% reagent alcohol	104
5-10 – Breakthrough of highly concentrated PCE containing cosolvent phase into finer layer and subsequent reestablishment of DNAPL below the finer layer due to lower alcohol concentrations.....	105
5-11. Water tracer study for 40-50 finer layer experiment. Note the significant holdup of tracer in lower portions of PCE pool and noticeable progression of dye in finer layer underneath.	106
5-12. Collapsing of PCE pool and spreading of DNAPL along 40-50 layer. No breakthrough of DNAPL observed.....	107
5-13. Schematic for step input of 80% alcohol – No. 30-40 finer layer.	109
5-14. Schematic for step input of 70% alcohol – No. 30-40 finer layer.	109
5-15. Mobilization of DNAPL into finer 30-40 layer at two locations, upstream from injection zone (small + mark in picture) – 0.45 PV after step input of 80% v/v ethanol/water mixture. Mobilization also occurred later at one other location downstream of pool (see text).....	109

5-16. Mobilization of the PCE pool by a 40% v/v TBA cosolvent mixture (0.6 PV) resulting in the trapping of a volume of the cosolvent mixture on top of the finer layer.....	113
5-17. PCE and TBA elution profiles from 2D Box after a step input of 40% v/v TBA/H ₂ O. TBA profile data are shown as GC peak areas for reference.....	114
5-18. DNAPL pool shape after the injection of one pore volume of 40% v/v TBA cosolvent mixture.....	115
A-1. Moisture release curve for Nos. 20-30 sand.	128
A-2. Pore size frequency distribution of Nos. 20-30 sand.	128
A-3. Moisture release curve for Nos. 30-40 sand	129
A-4. Pore size frequency distribution of Nos. 30-40 sand	129
A-5. Moisture release curve for Nos. 40-50 sand.	130
A-6. Pore size frequency distribution of Nos. 40-50 sand.	130
A-7. Moisture release curve for Nos. 60-70 sand.	131
A-8. Pore size frequency distribution of Nos. 60-70 sand.	131
A-9. Moisture release curve for Nos. 100-140 sand.....	132
A-10. Pore size distribution of Nos. 100-140 sand.	132
A-6-11. Moisture release curve for wide distribution (#20-100) sand.	133
A-12. Pore size distribution of wide distribution (#20-100) sand.	133

Abstract of Dissertation Presented to the Graduate School
of the University of Florida in Partial Fulfillment of the
Requirements for the Degree of Doctor of Philosophy

SOLUBILIZATION AND MOBILIZATION OF PERCHLOROETHYLENE BY
COSOLVENTS IN POROUS MEDIA

By

Michael E. Van Valkenburg

May 1999

Chairman: Dr. Michael D. Annable
Major Department: Environmental Engineering Sciences

Batch equilibrium studies conducted for perchloroethylene (PCE)/cosolvent systems determined that the log-linear solubility relationship is not a completely accurate method to predict solubility of PCE in cosolvent mixtures over an entire range of volume fractions. Batch studies resulted in cosolvency powers of 3.73 and 4.13 for ethanol and isopropanol, respectively. However, log-linear predictions may be adequate for estimations necessary for remediation efforts. The use of the Extended Hildebrand model is recommended.

The interfacial tension (IFT) resulting from cosolvent mixtures when compared to the initial volume fraction of cosolvent showed a relationship, similar to the log-linear model. An "IFT reduction power" was determined for ethanol to be -3.60, and isopropyl alcohol, -5.80, describing the ability of cosolvents to reduce IFT with increasing volume

fraction. IFT values are accurately estimated by PCE solubility in regimes conducive to cosolvent flushing.

Onset of residual PCE mobilization was found to begin at a trapping number (N_t) of 2×10^{-4} . Solubilization of residual PCE is dominant at ethanol volume fractions less than 85% and mobilization of PCE is avoided. Under severe conditions, mobilization via cosolvents can occur. These include large step inputs of high cosolvent fractions (greater than 85%), when DNAPL saturation is great enough for IFT reduction to cause mobilization. Behavior of surfactant and cosolvent systems was similar on a mobilization curve and is independent of alcohol type.

Entrapment and mobilization of residual NAPL are separate and distinct processes. The entrapment process appeared to be log-linearly related to the trapping number for homogeneous media. This is believed to be associated with the log-linear dependence of saturation with capillary pressure. However, for heterogeneous media, increased saturations with decreasing IFTs was observed.

Two-dimensional studies revealed that pooled DNAPL was found to collapse under reducing IFT conditions and mobilized downward and up gradient along overriding cosolvent fronts. This caused significant build-up of DNAPL on the lower confining layer. The most significant production of DNAPL through any fine layer in these studies was actually up stream from the source zone. Gradient injection to remove pooled DNAPLs did not appear to provide significant benefit over step inputs. Entry pressure calculations predicted breakthrough of PCE into the finer media in excellent fashion. Breakthrough of PCE under typical ethanol flooding conditions (80% by volume) can generally be assumed to occur in homogeneous sand media when the cosolvent/DNAPL entry pressure of the

finer media ($h_d^{cs/dnapl}$) is less than 0.35 cm. A swelling alcohol (t-butanol) used to remove pooled DNAPL resulted in trapped cosolvent zones on top of finer layer due to density effects. Partitioning of TBA into DNAPL allowed for more accumulation on finer layer before entry was observed. Calculations for an example clay estimated that approximately a half a meter worth of equilibrated PCE-type DNAPL would have to accumulate before entry into the clay pores under extreme cosolvent flooding conditions.

CHAPTER 1 INTRODUCTION

Background

Due to our industrial society's ever-increasing use of chemicals during the last 50 years, it has been increasingly necessary to manage the corresponding waste products from these industrial operations. The management of these waste streams at various times throughout this half-century has evolved from "drum it up and bury it in the back 40" type methods to highly regulated disposal and stream reduction. Unfortunately, prior to the 1980's, industry did not realize the environmental and health impacts of our decisions, which we thought were proper at the time. As a result, there are hundreds of thousands of disposal sites in the United States alone, thousands of which are severe enough to be on the Environmental Protection Agency's (EPA) National Priority List. A large number of these sites are contaminated with a class of chemicals known as dense nonaqueous phase liquids (DNAPLs), some of which are known carcinogens. These chemicals, immiscible with water, include polychlorinated biphenyls (PCBs), creosotes, and halogenated solvents. Prior to the early 1990s, this class of contaminants received minimal attention from environmental engineers and hydrogeologists.

Until recently, remediation technologies for the removal of these DNAPLs from subsurface environments focused on pumping of groundwater and subsequent treatment of this stream. Risk reduction to possible receptors was the driving force behind these

actions. However, due to the solubility limitations of these types of treatment, remedial action time-scales were long and expensive. The source of contamination is very slowly removed due to solubilization into water. In the last few years, research efforts and technology demonstrations have become more focused on source removal. These include surfactant flooding and cosolvent flushing (Annable et al. 1996; Falta et al. 1997; Fortin et al. 1997; Jawitz et al. 1998b; Lunn and Kueper 1997; Pennell and Abriola 1996; Pennell et al. 1994; Pope and Wade 1995; Rao et al. 1997). Although these techniques tend to be more aggressive and have high initial costs, the removal of a possible long-term source is beneficial from risk reduction, economic, and legal perspectives.

The major concern with the use of surfactants and cosolvents is the possibility of DNAPL movement during these remediation operations. The natural driving force behind any movement of DNAPL in the subsurface is gravity. Downward DNAPL movement of any kind is undesirable as this increases the likelihood of the contaminant leaving the more accessible and shallower geologic zones and entering deeper drinking water aquifers. Furthermore, once collected on top of a finer layer, entry, and subsequent breakthrough presents severe risks to aquifers below. Remediation techniques using surfactant and/or cosolvents increase solubility of the DNAPL into the aqueous phase, but concurrently increase the possibility of DNAPL movement due to a decrease in interfacial forces between the DNAPL and the aqueous phase. In fact, some remediation techniques using surfactants have as their main objective the bulk movement of the DNAPL towards recovery wells for extraction. This technology has been modified from the enhanced oil recovery (EOR) field, where surfactants are used to move oil previously trapped in

reservoir rock. The movement of any non-aqueous phase liquid in the subsurface has been labeled 'mobilization' and will be hereafter referred to as such.

The use of alcohols to enhance recovery of oils or NAPLs via miscible displacement has long received attention (Morse 1952). Several other references to alcohol use appear in early literature on the topic, including Gatlin (1959), Gatlin and Slobod (1960), Kamath (1960), Paulsell (1953), Sievert (1958), and Slobod et al. (1958).

Due to the inherent risks of downward mobilization of DNAPLs, the use of cosolvents to remove them via miscible displacement has increased in popularity. This is due to the primary objective of 'cosolvent flushing' being solubilization of the DNAPL, rather than mobilization. However, this is not to say that mobilization does not occur if cosolvents are used. Since the solubility of a contaminant increases generally logarithmically with addition of a cosolvent to water, use of cosolvents (such as ethanol or isopropyl alcohol) in their pure state, or at least at high volume fractions, would appear to be a consistently wise choice. Nevertheless, mobilization of DNAPL at these high volume fractions (>80% by volume) of cosolvents is very possible, especially if DNAPL saturations are above residual levels.

DNAPLs in the subsurface can also be residually trapped in the vadose and phreatic zones of the subsurface. Here the DNAPL exists as discrete globules in the pore of the soil medium. Eventually, the draining DNAPL in the saturated zone can become 'pooled' on top of a layer of soil that is more restrictive to downward flow of any fluid. It is less permeable than the surrounding layers. Here, it can spread laterally along the less-permeable layer until equilibrium is achieved. Alternatively, continuing quantities of

DNAPL can accumulate and the height of the pool becomes great enough to where gravity forces the DNAPL to enter the smaller pores of the less-permeable layer.

Mobilization of DNAPL can occur during the remediation of both these types of sources, residual and pooled. Mobilization of a residual DNAPL, like PCE, can create banks that can move ahead of the rich cosolvent flushing phase, or can move downward along the cosolvent front, depending on the difference in gravity between the DNAPL and the aqueous flushing phase. Pooled DNAPL can mobilize as described above, but the presence of an underlying layer can prevent downward movement if the permeability is low enough (high entry pressure), accumulation is small enough, and therefore entry pressures into the finer media not exceeded. Under extreme conditions of low entry pressure, low interfacial forces, and large pool thickness, entry of the DNAPL in to the pores is possible. Eventual breakthrough into lower regions is then probable, depending on the layer thickness and amount of DNAPL present.

Because of the complexities of DNAPL source removal briefly introduced above, several questions arise: 1) is there an optimum amount of a cosolvent that can be used to maximize solubilization, yet minimize the chance of mobilization; 2) can predictions be made as to when mobilization of residual DNAPL will occur; 3) what DNAPL will be left behind, or "entrapped," if the entire amount is not removed with the cosolvent used; 4) can predictions be made as to whether pooled DNAPL will enter an underlying layer under certain flushing conditions; and 5) are there better flushing methods to minimize the chance of mobilization of either residual or pooled DNAPL? There are a variety of chemical, physical, and hydrogeologic factors that can influence the outcome of these questions. Several of these will be discussed in the chapters that follow.

Selection of DNAPL

A common solvent used throughout the last few decades is tetrachloroethylene, also known as perchloroethylene, or "perc" (PCE, C_2Cl_4 , Chemical Abstract Number (CAS) 127-18-4). This solvent has been used as an industrial degreaser, but a more common use even today is as a dry cleaning solvent. The former use has led to the better-known industrial hazardous waste sites. Perchloroethylene has been found in at least 330 of the 1117 National Priorities List (NPL) hazardous waste sites. However, it is increasingly evident that the thousands of dry cleaner establishments in the United States had their share of mismanagement of PCE. There are over 600 contaminated dry cleaner sites in Florida alone. Due to the sheer number of potential contaminated sites, the toxicity of PCE (a drinking water equivalent level (DWEL) of 0.5 mg/L has been established by the EPA), and often close proximity of these establishments to residential areas, there is growing concern of the impact of long-term subsurface sources of PCE contamination.

Study Objectives

Based on the background summarized above, the following paragraphs describe the objectives of this research.

Determine solubility relationship of PCE to amount of cosolvent. This objective is to determine the solubility relationships (log-linear relationship or other) for a few common alcohols used to remediate NAPLs, and justify the quantities used under different remediation regimes. Due to the unique nature of water and the various intermolecular interactions which occur when a solute is added (or when enough solute is added to become a cosolvent), the scientific basis for the solubility relationship can become

complicated. Once a relationship has been established, an explanation for its features will be proposed based on the chemical literature and this study's observations.

Measure the effects of the type of alcohol(s) and amount(s) on interfacial tension (IFT) and develop a relatively simple, yet useful relationship between the two. As the mutual solubility between two phases increases, the interfacial tension between them decreases. A critical feature of cosolvent flushing in the field is the rate of decrease in IFT with increasing cosolvent volume fractions. This study will measure the relationship between the amount of alcohol added and the IFT between the equilibrated phases.

Propose a relationship between the solubility of PCE into various cosolvent mixtures and the resulting equilibrated IFT. It would be beneficial for field applications to have an understanding of the expected solubility of PCE into the aqueous phase and the corresponding IFT that results from this mixture. Mobilization of NAPL is a strong function of IFT. To have an estimate of the aqueous phase concentration of PCE at various IFT values would provide information helpful in determining if mobilization will occur under a given flow regime. This study will attempt to establish this relationship to possibly be used in further studies and field applications.

Development of a trapping number relationship using cosolvents. IFT is not the only parameter governing mobilization. Relationships have been established (Pennell et al. 1996b) and applied to surfactant use in porous media. These relationships describe the amount of NAPL removed from a given media via mobilization as a function of a dimensionless "trapping number", which includes contributions from viscous, capillary, and buoyancy forces. However, a similar relationship verified with cosolvents has not been found in the literature. Sand column experiments were performed similar to Pennell

et al. (1996) using a cosolvent mixture(s) found from the previous bench top experiments to develop and verify the dependence of DNAPL (PCE) saturation on the trapping number.

Determine the relative amounts of mobilization due to purely IFT reduction and to possible swelling of DNAPL. During cosolvent flooding both solubilization and mobilization of the NAPL can occur. Mobilization occurs due to a variety of hydrogeologic and physical parameters. A critical parameter during these remediation operations is the IFT. To isolate the effects of reduction of IFT on mobilization of PCE, soil column experiments were conducted with the influent cosolvent phase pre-equilibrated with PCE.

Determine the relationship of entrapment of DNAPL to the trapping number and the difference between entrapment and mobilization of residual PCE using cosolvents. The entrapment of a NAPL in the pore structure after being exposed to reduced interfacial tensions is important to evaluate, since a high removal efficiency is desired. The entrapment process of PCE in a one-dimensional homogeneous sand column under various trapping number environments will be evaluated and compared to the mobilization experiments. Additionally, the effect of sand pore size heterogeneity on entrapment were observed.

Qualitatively observe the effects of various cosolvent mixtures on the removal of PCE pooled above various finer sand layers. Two-dimensional studies were conducted varying the amount of cosolvent in the flushing phase and the mode of injection (step input versus gradient input). General observations and conclusions were made to improve removal of pooled systems using cosolvents.

Confirm the quantitative prediction of entry of DNAPL into finer pores below DNAPL pools, during cosolvent flushing processes. Entry of DNAPLs into finer more “impermeable” layers is undesirable during removal of DNAPL plumes. Prediction of entry of these DNAPLs into finer layers is straightforward via basic force balance calculations. However, under cosolvent flooding conditions, parameters used to calculate entry pressures (density contrast and interfacial tension between the two fluids) are changing during flooding processes, especially for strongly partitioning alcohols like t-butyl alcohol. It is possible that the entry predictions can be made assuming equilibrium density and interfacial tension values.

Dissertation Organization

Each of the following chapters (Chapters 2–5) is written to essentially be a stand-alone document. Thus, a similar format of Introduction, Methods and Materials, Results and Discussion, and Conclusions is used throughout. Chapter 2 includes the results of the bench top solubility and interfacial tension studies (first through third objectives). Chapter 3 discusses the results of the mobilization studies of residual perchloroethylene (fourth and fifth objectives). Chapter 4 further expands on the process of mobilization and its comparison to the entrapment of DNAPL after exposure to reduced interfacial tension conditions (sixth objective). Finally, Chapter 5 outlines the results of the two-dimensional box studies to evaluate flooding processes on pooled DNAPL system and predict their entry into a finer medium below (final two objectives). Chapter 6 summarizes the major conclusions of the entire dissertation and identifies areas of future research.

CHAPTER 2
INVESTIGATIONS OF THE RELATIONSHIP OF COSOLVENT FRACTION TO
PERCHLOROETHYLENE (PCE) SOLUBILITY AND EQUILIBRIUM
INTERFACIAL TENSION

Introduction

Optimization of remediation technologies is a prime concern to engineers, scientists and environmental regulators. This optimization involves engineering, scientific, economic, environmental impact and health risk considerations. One recent technology for Non-Aqueous Phase Liquid (NAPL) or Dense Non-Aqueous Phase Liquid (DNAPL) removal from subsurface environments is the use of cosolvents to increase the solubilization of contaminants and to flush the mixtures (and NAPL if mobilization occurs) into recovery wells. Cosolvents are commonly binary alcohol-water mixtures and less commonly ternary alcohol A-alcohol B-water mixtures. The exact "recipes" for these mixtures are rather loosely chosen. Relationships between the solubilities of the contaminants of interest and the resulting interfacial tensions (IFTs) for different amounts of cosolvent would be beneficial to optimization of these technologies. Hereafter, the term IFT, and IFT measurements presented in the results section, are defined (or measured) at the interface between the cosolvent mixture and the DNAPL phase. One common DNAPL is perchloroethylene (PCE), a historically common industrial degreaser and dry cleaning solvent. An objective of this investigation was to determine the effects of

various cosolvents and cosolvent mixtures on the solubility of PCE and the resulting equilibrium interfacial tension between the two phases (organic and aqueous). From these results, it is desired to develop a simple predictive relationship between these factors. An accurate understanding of the IFTs of these mixtures also allows better prediction of the mobilization of a separate PCE phase. This situation is a concern due to the density of PCE (approximately 1.62 g/ml) and its possible downward movement (mobilization), out of the control of the remediation scheme.

Comparison of the Molecular Structures of Water and Low Molecular Weight Alcohols

Cosolvents typically used for cosolvent flooding operations are monohydric (contain only one alcohol group, e.g., ethanol or isopropyl alcohol). When these monohydric alcohols are present in binary alcohol/water mixtures, deviations from ideal solution behavior are seen, especially at lower volume fractions (Franks and Ives 1966). These deviations can be attributed in a general way to the bifunctional nature of these types of solute molecules. It is a push-and-pull effect where the small hydrophobic portion of the molecule resists the pull exerted by the hydrophilic hydroxyl group. This hydroxyl group, either as a proton donor or acceptor, can hydrogen bond with the solvent (water) molecules. Although hydrogen bonding plays a role in the behavior of these systems, it cannot account for all observed phenomena. Other structural differences need consideration. Deviations from ideal behavior is noticeably lessened if a second hydroxyl group is added to the molecule (e.g., glycols) which shifts the balance of forces in favor of a more "aqueous behavior" (Franks and Ives 1966).

The structure of water is tetrahedral in shape, with the polar O-H bonds being approximately sp^3 hybridized. Thus, each oxygen atom can form approximately four

tetrahedrally-disposed hydrogen bonds (Frank and Wen 1957). Formation of these hydrogen bonds is energetically favorable, until it suffers collective destruction by high energy fluctuation. Thus, a three-dimensional cluster of water molecules is formed, which lifetime is on the order of 10^{-11} seconds (Franks and Ives 1966). Although this lifetime is short, it is still two or three orders of magnitude greater than the period of molecular vibration. Liquid water is considered to be a mixture of these clusters (which can be open) and a dense fluid composed of non-hydrogen bonded water molecules (Franks and Ives 1966). This order-disorder balance in water is sensitive and is highly significant to its properties. This is particularly the case in the reaction of water with hydrophobic parts of bifunctional molecules, like alcohols.

For aliphatic alcohols, like ethanol, the C-H bonds are sp^3 hybridized, with the O-H again being close to the same hybridization. Similar to water, it can form hydrogen bonds between alcohol molecules, but generally no more than two hydrogen bonds can form (each oxygen acting as a proton donor and as an electron acceptor). Linear polymers of 5-7 molecules (or less for sterically hindered alcohols) are formed, with lifetimes on the order of 10^{-11} to 10^{-9} seconds (Magat 1959). It is clear that hydrogen bonding has a significant effect on the properties of alcohols, but not in the same way as water, in which increasing hydrogen bonding leads to more cavity formation, or an "openness" of structure. Franks and Ives (1966) consider an 80% mole fraction ethanol/water mixture (similar to the concentrations used in cosolvent flooding processes) and note that the number of "moles" of hydroxyl group per mole of liquid phase for pure water, the mixture, and pure ethanol (EtOH) are 2, 1.2, and 1, respectively. Even more

significant are the concentrations of protons available for hydrogen bonding in these liquids - 111, 24, and 17 moles/l (Franks and Ives 1966), as shown in Figure 2-1.

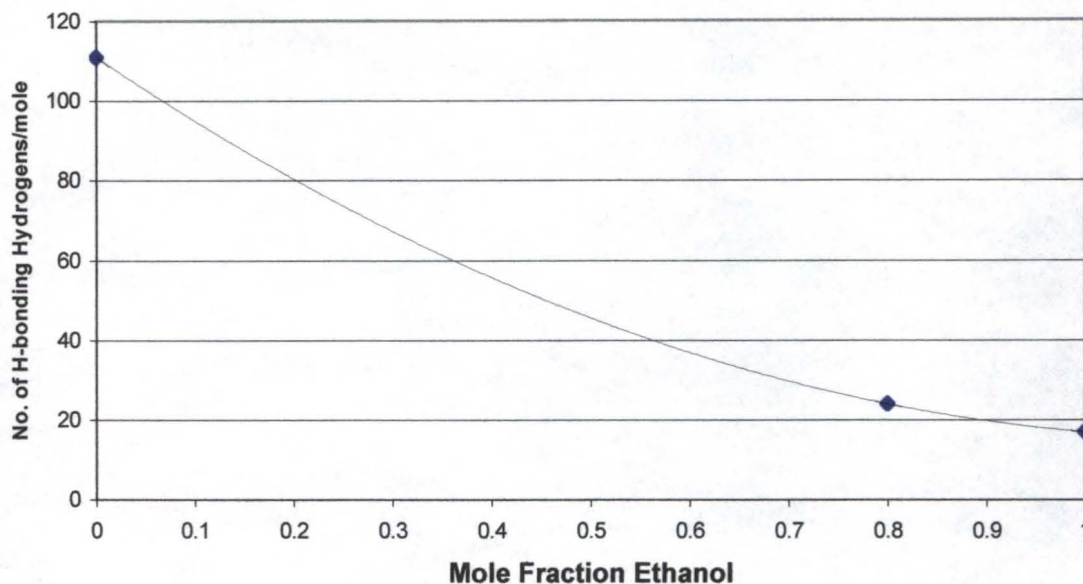


Figure 2-1. Graph of data from Franks and Ives (1966), relating concentration of hydrogen bonds to volume fraction of ethanol.

It is therefore much more difficult for a hydrophobic solute like PCE to enter into this network at lower mole fractions of EtOH. This may account for negative deviations in log-linear behavior of the solubility of PCE at lower EtOH fractions (Morris et al. 1988). Thus, it takes higher concentrations of EtOH molecules to form their own network of hydrogen bonded polymers, that consist of a larger area of hydrophobic properties, to which PCE can intermolecularly bond.

PCE (C_2Cl_4) is a symmetric molecule, therefore non-polar. However, the four C-Cl bonds are locally very polar, and can thus lead to dipole-dipole intermolecular bonding with other molecules. This can explain why PCE has a solubility in water (150 mg/l; (Lide

1996)) higher than a non-polar molecule with lower localized polarity, like hexane (11 mg/l; (Lide 1996)). However, water, having all polar characteristics within the molecule, is not a similar environment for a non-polar solute to enter. The hydrogen-bonding network decreases this possibility further. Hence, the relatively low solubility. PCE is completely miscible with EtOH, due to decreased hydrogen bonding (as compared to water) and the presence of a hydrophobic portion of the EtOH molecule, which leads to strong dispersion forces between the two. Additionally, dipole-dipole forces are present between these two compounds.

Solubility of Hydrocarbons into Water/alcohol Mixtures and its Relationship to Amount of Cosolvent

An ideal solution can be defined as one that does not deviate from Raoult's Law (Atkins 1994):

$$p_a = x_a p_a^* \quad (2-1)$$

where p_a [$\text{ML}^{-1}\text{T}^{-2}$] is the vapor pressure of a in the liquid (binary for our purposes), x_a is the mole fraction of a in the liquid, and p_a^* is the vapor pressure of the pure liquid a .

Using Raoult's Law, for an ideal solution:

$$\mu_a = \mu_a^* + RT \ln x_a \quad (2-2)$$

where μ_a [$\text{ML}^2\text{T}^{-2}\text{moles}^{-1}$] is the chemical potential of a in the liquid, μ_a^* is the chemical potential of the pure liquid a at standard state, R [$\text{ML}^2\text{T}^{-2}\text{moles}^{-1}\text{degrees}^{-1}$] is the universal gas constant, and T [K] is the absolute temperature. The chemical potential of substance a expresses how the free energy of the system changes as a is added (Atkins 1994). As can be seen from Equation (2-2), how this potential changes depends on the composition of

the system (x_a). The chemical potential, hence the free energy of the system, is held to this relationship for an ideal solution. Physical properties like solubilization and IFT that depend upon the free energy of the system are therefore strongly linked to this relationship, often exhibiting log-linear behavior with composition, especially in more dilute solutions (Chen and Delfino 1997; Morris et al. 1988). Adding alcohols to water to enhance the solubility of contaminants during remediation processes is one example of where this miscibility relationship is beneficial. However, volume fractions of cosolvents used are generally high (70-90%) (Annable et al. 1996) and deviations from ideal solution behavior are often observed.

Solubility estimation methods most commonly used ("mixed solvent solubility estimation methods") assume that the solvent molecules are randomly mixed. Therefore, deviations from these models (in a positive sense) indicate that in organic/solvent water systems the solvent molecules are not randomly mixed. Increased deviations from random mixing with water occur as cosolvent molecular size increases and hydrogen bonding capability decreases (Dickhut et al. 1991). This is due to cosolvent self-interaction increasing, providing a more desirable environment for hydrophobic solutes in aqueous solution, and decreased hydrogen bond "networking" allowing the solute to move more freely and find more desirable zones.

Non-ideal binary monohydric alcohol and water mixtures have been studied for quite some time. Use of alcohols as industrial solvents has also prompted more detailed studies. Solubility relationships of various hydrocarbons in these mixtures to the amount of alcohol present have been determined (Dickhut et al. 1989; Groves 1988; Pinal et al. 1990). The most prevalent relationship used is log-linear.

It has been shown that a 70% ethanol/18% water/12% n-pentanol mixture can be used to solubilize various hydrocarbons from contaminated media (Annable et al. 1996; Rao et al. 1997). Binary methanol, ethanol and isopropyl alcohol/water mixtures have also been used (Augustijn et al. 1994; Brandes 1992; Imhoff et al. 1995). Typically, high volume fractions (>80% v/v) of alcohol are used. Specific studies on the superiority of these mixtures in cosolvent flushing applications could not be found. However, as the fraction of cosolvent increases, the aqueous solubility of NAPL constituents increases (Brandes and Farley 1993). However, monohydric alcohols, like ethanol, and water binary mixtures have been shown to behave non-ideally. Simple relationships like the log-linear model (Li et al. 1996; Yalkowsky et al. 1976) may not be applicable over the large volume fraction range possible for the use of cosolvents.

Log-linear relationship

The log-linear model is used quite frequently when describing cosolvent systems. Yalkowsky (Banerjee and Yalkowsky 1988) and others have shown that in solutions of appreciable (>10% v/v) cosolvent, the molar solubility of a non-polar solute can be approximated by:

$$\log S_m = f_c \log S_c + (1-f_c) \log S_w, \quad (2-3)$$

where S_m , S_c , and S_w are the solubilities of the non-polar solute in the mixture, pure cosolvent, and pure water, respectively, and f_c is the cosolvent volume fraction. This equation neglects solute-solvent interactions and is based upon the accepted linear relationship between the free energy of solution and the solute surface area (Valvani et al. 1976). The model is exactly obeyed only as the solvent components become identical (Li

and Andren 1995). The log-linear model assumes the water and cosolvent behave as two distinct entities and neglects the interaction between them. This model fails when interactions between solvent components are strong and differ from interactions among molecules of individual pure components and when the solute strongly prefers one solvent component over the other (Li and Andren 1995). Over the total volume fraction spectrum, deviations obviously occur mostly at both extremes, where one of the solvents is present at very low concentrations and cannot avoid interaction with the other solvent. At very low cosolvent volume fractions, the solute solubilized will only be influenced by one cosolvent molecule at a time. Any solubility enhancement will therefore be proportional to the number of cosolvent molecules present. This cosolvent will be hydrated in solution, and consequently, it will disrupt the water network structure (Grunwald 1986). In these situations, one would expect the log-linear relationship that applies at higher cosolvent fractions to become linear, due to a change in the mechanism of solubilization (Banerjee and Yalkowsky 1988). This change usually occurs in the range of $0.1 < f_c < 0.2$. The cosolvent/water mixture behaves as a completely random arrangement of molecules with no tendency to segregate (i.e., an ideal mixture) (Dickhut et al. 1991). At these low volume fractions, cosolvents are more like cosolutes in behavior and do not influence the solution in an appreciable way.

For a remediation process, cosolvent volume fractions are typically on the order of 80%; so the minor cosolvent is water. Any operation therefore in the 80 to 100% range could possibly be in the linear portion of the solubility relationship discussed above. The primary advantage of the log linear method is its simplicity, which makes it a convenient

tool for estimating solubilities of hydrophobic chemicals in a variety of aqueous mixtures (Li and Andren 1995).

Cosolvency power

The relative solubilization enhancement is usually presented as the “cosolvent power”, σ (Banerjee and Yalkowsky 1988; Yalkowsky et al. 1976). This cosolvency power is defined as the logarithm of the ratio of the solute solubilities in pure cosolvent to pure water, or

$$\sigma = \log S_c - \log S_w. \quad (2-4)$$

In some instances the solute may be completely miscible in the pure cosolvent (i.e., PCE in ethanol) where the use of the “end-to-half- slope” ($\sigma_{0.5}$) is necessary (Li et al. 1996). This is defined as

$$\sigma_{0.5} = (\log S_{0.5} - \log S_w)/0.5, \quad (2-5)$$

where $S_{0.5}$ is the solubility at $f_c = 0.5$. In combination with Equation (2-3), this results in the expression,

$$\log S_m = \sigma_{0.5} f_c + \log S_w. \quad (2-6)$$

Other methods for solubility estimation

To account for deviations from ideal or regular solution theory, other methods have been developed in previous research. These include the Extended Hildebrand (EH) method, the Excess Free Energy (EFE) method, and the Universal Functional Group Activity Coefficient (UNIFAC) method.

Extended Hildebrand (EH) method. Hildebrand and Scott (1950) and Scatchard (1931) introduced regular solution theory to describe solutions that maintain ideal entropy of mixing, but involve heat change during mixing. This can occur only if the random distribution of molecules is maintained even in the presence of specific solute-solvent interactions (Barton 1975). However, solutions of organic compounds in polar solvents are not regular since significant solvation can occur (Li and Andren 1995). To attempt to account for deviations from ideal behavior, Martin et al. (1979; 1982) assumed the binary cosolvent and water mixture is itself ideal, but the ternary (or higher) solution behavior may deviate from the ideal due to solute(s)-solvent interactions. This method is represented by the following expression for the mole fraction solubility:

$$\ln x_{s,mix} = \frac{\Delta S_f}{RT} (T - T_m) - \frac{q_s z_j}{RT} (\delta_{mix}^2 + \delta_s^2 - 2W), \quad (2-7)$$

where

$$(\delta_{mix} = z_1 \delta_1 + z_2 \delta_2 + \dots), \quad (2-8)$$

and $x_{s,j}$ is the mole fraction solubility of solute s in solvent j ($j=1,2,3..$); ΔS_f [$\text{ML}^2\text{T}^{-2} \text{ moles}^{-1} \text{degrees K}^{-1}$] is the molar entropy of fusion; R is the ideal gas constant; T and T_m are the absolute system and melting temperature; q_s [$\text{L}^3 \text{ moles}^{-1}$] is the molar volume of the solute; z_j is the solute free volume fractions of the solvents in the mixture; δ_s , and δ_j are the Hildebrand solubility parameters for the solute and each solvent, respectively; and W [$\text{ML}^{-1}\text{T}^{-2}$] is the interaction energy in those systems with strong solute-solvent interactions. This estimation technique requires the determination of the solute specific interaction

energy, W . The EH method is most useful in situations in which solubility determinations for a specific solute are desired, as in this study (Dickhut et al. 1991).

Excess free energy (EFE) method. The EFE method (Williams and Amidon 1984b) accounts for some deviations from the log-linear prediction. Non-ideal solution behavior is attributed to excess free energy from n -body interactions in the given system. By ignoring four-body and higher order interactions, the model is reduced to a three-suffix equation for the mole fraction solubility of a solute in a mixed solvent. For a ternary system (solvent, cosolvent and solute) this model is given as:

$$\ln x_{s,mix} = z_1 \ln x_{s,1} + z_2 \ln x_{s,2} - A_{1-2} z_1 z_2 (2z_1 - 1)(q_s / q_1) + A_{2-1} 2z_1^2 z_2 (q_s / q_2) + C_s z_1 z_2, \quad (2-9)$$

where A_{1-2} and A_{2-1} are the binary solvent-cosolvent interaction constants; q_i is the molar volume of the species i ; and C_s is the ternary interaction constant. This method requires vapor/liquid equilibrium data (at the system temperature) to derive the solvent-cosolvent interaction constants. However, A_{1-2} and A_{2-1} can also be calculated using UNIFAC data. The ternary interaction constant, C_s , requires, in practice, solute solubility measurements over a range of cosolvent fractions to determine this parameter (Williams and Amidon 1984a). This method is less acceptable because it relies on the experimental solubility data to determine the parameters needed for mixed solvent solubility estimations (Dickhut et al. 1991). Furthermore, specifically for the systems studied herein, the solute (PCE) is completely miscible in one of the solutes (ethanol or isopropyl alcohol). Therefore, the mole fraction solubility of PCE in ethanol is undefined. This eliminates this model as a tool to predict PCE solubility in these systems.

UNIFAC method. The UNIFAC method uses the sizes and shapes of molecules in the solvent mixture and the interactions between the functional groups they contain to account for the non-ideal solution behavior (Fredenslund et al. 1977). Its fundamental assumption is that the chemical behavior of a fluid is due to the sum of contributions made by the molecules' functional groups. This method calculates the activity coefficients (γ_i) based on the functional groups of a molecule of species i and their interactions with other groups in the system. It is given as:

$$\ln x_{s,mix} = \left[\frac{\Delta s_f}{RT} \right] (T - T_m) - \ln \gamma_{s,mix}, \quad (2-10)$$

where

$$\ln \gamma_{s,mix} = \ln \gamma^C + \ln \gamma^R, \quad (2-11)$$

and $\gamma_{s,mix}$ is the UNIFAC activity coefficient of the solute in the solvent mixture, γ^C is the combinatorial fraction and γ^R is the residual fraction. The combinatorial fraction reflects the size and shape of the molecules, and the residual fraction depends on the functional group interactions. Parameters for each functional group, such as volume and area parameters (normalized van der Waals volume and surface areas) and parameters of interaction with other functional groups (obtained from phase equilibrium experimental data) are put into a series of equations to calculate γ^C and γ^R . The UNIFAC method is limited by the experimental data used to determine its parameters in Equation (2-11), some of which have been updated since the inception of this method (Hansen et al. 1991).

Choice of solubility estimation method

Whatever the method finally chosen to best represent PCE/cosolvent/water behavior, some general conclusions have been made in the literature. As the cosolvent molecular size decreases, the hydrogen bonding capability increases. This leads to significant non-ideal behavior. This indicates that in these types of systems (especially ethanol and isopropyl alcohol) the solvent molecules are not randomly mixed. Self-interaction among organic solvent molecules increases and is hydrophobic. This creates a more desirable environment for hydrophobic solutes, increasing solubility higher than expected in ideal solvent mixtures (Dickhut et al. 1991). It is generally accepted that no single model is able to accurately predict hydrophobic species solubility in any system, especially over a wide range of environments, such as increasing cosolvent fractions. Until one such model is developed, use of the best resulting fit to the experimental data produced will have to be sufficient.

If solubilization relationships are characterized, it may be possible to use a lower fraction of alcohol and have similar NAPL solubilities, by selecting a better cosolvent mixture. Given economic, hydraulic, and environmental factors, even a cosolvent that results in NAPL solubility slightly less than a possible competitor could potentially be a viable candidate in the field. This is especially important if mobilization of NAPL is strongly undesirable. Interfacial tension is the key parameter that can determine whether mobilization will occur or not, and is discussed below.

Interfacial Tension of Ternary Alcohol/water/PMOS Mixtures

Solubilities of hydrophobic organic compounds (or Partially Miscible Organic Substances, PMOS) are strongly dependent upon the nature of the interfaces between the

two phases in organic/aqueous phase systems. The cohesive and adhesive forces of the molecules of a liquid-liquid system are the factors that determine the extent to which a given solute is soluble in a given solvent. It is these factors which also determine the magnitude of the interfacial tension (IFT) (Donahue and Bartell 1958). IFT is a critical parameter necessary to characterize this interface and to characterize non-homogeneous liquid systems (Glinski et al. 1994). It is often necessary to know the IFT to predict the fate of organic liquids. IFT is defined as the change in Gibbs free energy per unit change in interfacial area.

$$\left(\frac{\partial G}{\partial A}\right)_{T,P,n} = \gamma \quad (2-12)$$

Accurate estimation of this parameter is critical to predict behavior of liquid phases during field remediation operations. To predict IFT, semi-empirical formulae are used. These include Antonov's Rule (Antonov 1907), and the methods of Girifalco and Good (1957), Donahue and Bartell (1958), and Fu (1986).

Relation to amount of cosolvent

Consider only two dissimilar liquids. The IFT between the two liquids results from an imbalance of forces acting on molecules at the interface. The IFT value is a function of the interaction between not only the molecules of the two different liquids, but also the molecules of the individual liquids themselves. The magnitude of the IFT reflects the relative difference between intermolecular forces within the bulk liquid and the intermolecular forces between the liquids (Demond and Lindner 1993). This can be extended to more than binary systems, with increasing intermolecular interactions to consider.

As a cosolvent is added in increasing proportion to an aqueous mixture the interfacial tension between it and a separate organic phase decreases. This decrease is due to the increasing similarity between the two phases. The cohesive forces within the two phases are high when the phases are dissimilar, resulting in excess free surface energy, or interfacial tension. As cosolvent is added to the aqueous phase, these cohesive forces decrease, decreasing the IFT. At the same time, the increasing similarity between the two phases increases the mutual solubility of the solutes within each phase. The historical literature has recognized this relationship between solubility, IFT, and the amount of cosolvent added. The major estimation techniques are described below.

Different interfacial tension prediction methods

Method of Fu et al. The only method at the present time to estimate IFT for ternary (or quaternary) systems is the one developed by Fu et al. (1986). It is derived from the thermodynamic equation developed by Shain and Prausnitz (1964)

$$\gamma_{OW} = \frac{RT}{\bar{A}_i^s} \ln \left(\frac{\gamma_i^s x_i^s}{\gamma_i x_i} \right), \quad (2-13)$$

where R is the universal gas constant, T is the absolute temperature, γ_i^s and γ_i are the activity coefficients of component i in the interfacial and bulk phases, respectively, x_i^s and x_i are the mole fractions of component i in the interfacial and bulk phases, respectively, and \bar{A}_i^s is the partial molal cross-sectional area of component i in the interfacial phase [$L^2 \text{mole}^{-1}$]. This can be applied to any mixture containing any number of components, as long as values for the thermodynamic parameters are known (or estimated). This method

makes a couple of simplifying assumptions that lead to the final expression for calculating the interfacial tension of a ternary mixture.

$$\gamma_{ow} = \frac{KRTX}{A_{w0} \exp(X)(x_1q_1 + x_2q_2 + x_{3r}q_3)}, \quad (2-14)$$

where K is an empirical constant (relating the number of molecules in the interfacial phase to the ratio of the molecular cross-sectional area to its surface area);

$X = -\ln(x_1 + x_2 + x_{3r})$; A_{w0} is the van der Waals surface area of a standard segment (2.5×10^9 cm²/mol, (Abrams and Prausnitz 1975)); x_i is the mole fraction of the i th component in the phase where that component is a solute, x_{3r} is the mole fraction for the third component in the phase where it is richer; and $q_i = A_{wi}/A_{w0}$, where A_{wi} is the van der Waals surface area for component i (q_i is the pure component area parameter defined by the UNIQUAC model) (Abrams and Prausnitz 1975).

The value of K is suggested by Fu et al. (1986) to be 0.9414, based on a linear regression of 54 binary systems. The average relative deviation from the measured IFT was 23%. However, if only data with IFT greater than 10 dyne/cm are considered, this deviation decreases to 6.3% (Fu et al. 1986). With the value of K taken to be 0.9414, Fu et al. tested 23 ternary systems and the average relative deviations were 17.9% for mixtures with IFT > 5 dyne/cm, and 11.5% if only those data points with and IFT > 10 dyne/cm are considered. However, this may be a significant, especially if trying to predict a value during cosolvent flooding operations when IFTs can decrease well below 10 dyne/cm. Additionally, for some systems either x_{3r} or x_{3p} (mole fraction of the third

component in the richer or poorer phase) can be chosen to obtain a better correlation.

The exact cause of this phenomenon is not clear.

Donahue and Bartell. Donahue and Bartell (1958) relied on the fact that miscibility and IFT reflect the same intermolecular forces. They discovered there was a linear relationship between the IFT of liquid pairs and the log of the sum of mutual solubilities in binary systems.

$$\gamma_{OW} = a - b \ln(S_{O(W)} + S_{W(O)}) \quad (2-15)$$

where a and b are empirical constants (regressed intercept and slope, respectively), $S_{O(W)}$ is the mole fraction solubility of the organic in water, and $S_{W(O)}$ is the mole fraction solubility of the water in the organic. For higher order systems it is obvious that this method cannot be applied directly. However, an additional relationship of the IFT being a function of the mutual solubility of the cosolvent alcohol and the NAPL is still possible.

Others. The oldest method still in use to estimate interfacial tension is Antonov's rule (Antonov 1907). It is stated by the relationship

$$\gamma_{OW} = \gamma_{W(O)} - \gamma_{O(W)}, \quad (2-16)$$

where γ_{OW} is the estimated IFT between the organic liquid and water, $\gamma_{W(O)}$ is the surface tension of water saturated with the organic, and $\gamma_{O(W)}$ is the surface tension of the organic saturated with water. As this is for a binary system only, its applicability to cosolvent systems is unfounded. Furthermore, use of this method for PCE systems has been shown to be inaccurate (Donahue and Bartell 1958).

Girifalco and Good's method is derived on the basis of the work necessary to separate the liquids at their interface. They assumed that the potential energy function for the interaction across the interface was described by the geometric mean of the IFTs (Demond and Lindner 1993). This method states that the IFT of a binary system is:

$$\gamma_{ow} = \gamma_o + \gamma_w = 2\Phi(\gamma_o\gamma_w)^{1/2}, \quad (2-17)$$

where Φ is the interaction parameter describing the similarity of intermolecular force between the two liquids, and γ_o and γ_w are the interfacial tensions between the oil phase and air, and water and air, respectively. The value of Φ ranges from 0.5 to 1.15 for organic liquid water systems, with lower values associated with dissimilar liquids and higher values associated with similar systems (Demond and Lindner 1993). Again, this is a method applicable to only binary systems.

Choice of IFT estimation method

Antonov's rule and Girifalco and Good's method are either too simplistic (lack a theoretical basis) or do not perform well, respectively (Demond and Lindner 1993). Girifalco and Good's method has a theoretical base, but is applicable only to binary systems. The most accurate methods appear to be those of Fu et al. (1986) and Donahue and Bartell (1958) (Demond and Lindner 1993). Donahue and Bartell's method performs better if measured mutual solubility data are available. Fu's method is preferred in cases where the mutual solubility data must be estimated. However, both of these methods have lower accuracy for systems where the IFT is less than 10 dyne/cm (Demond and Lindner 1993). This region of IFTs is where cosolvent flushing schemes will transition from maximizing solubility or mobilization of the contaminant. Furthermore, Fu's method is the

only one to directly apply to ternary systems. This method or a more direct empirical correlation is favored in this study.

Relation of IFT to Solubility of Organic Solute

As mentioned previously, there are various methods that can estimate the relationship between the solubility of a PMOS into a cosolvent/water phase and the amount of cosolvent added. Correspondingly, a relationship exists (Fu's method) between the IFT and the mole fraction solubility of a third solute (cosolvent). Therefore, with proper connection between the two relationships, one should be able to determine the dependence of the solubility of a PMOS with the equilibrated interfacial tension of the system. In a subsurface system, this type of direct relationship between these important parameters will allow quick comparison of enhanced solubility with the predicted IFT. If the remediation technique is designed to solubilize and not mobilize a DNAPL plume, there could be situations where driving to increase the solubilization of the DNAPL would result in significant lowering of IFT, and hydraulically move the system into mobilization regimes. If mobilization is a concern, a lowering of the cosolvent fraction a given amount may safely increase the IFT and only impact solubility by a small factor. This could lead to only a few additional pore volumes of the flushing fluid, or fractions thereof, used to obtain similar mass recovery of the DNAPL, while ensuring less risk of mobilization.

Materials and Methods

All chemicals were obtained from Fischer Scientific and were chromatography grade, with the exception of ethanol (EtOH). 99.9% EtOH was obtained from Ultra-Chem Corporation. Various mixtures of cosolvent and water were made in 40 ml EPA

vials with Teflon-lined screw caps. The resulting mixtures were defined by the volume fraction of cosolvent (f_c) in the aqueous phase, which were calculated from the amounts of water and alcohols that were measured separately and then combined in preparing the solvent mixtures (Li and Andren 1994). Ten milliliters (ml) of PCE and 10 ml of the cosolvent mixture was added to each vial, so that the initial ratio of aqueous to NAPL phases was 1:1. The vial was then placed in a mechanical rotator and rotated at room temperature ($25 \pm 0.5^\circ\text{C}$) for 48 hours, removed and allowed to settle for 24 hours. A 1 to 2 ml sample of the aqueous phase was then taken and placed in GC autosampler vials and crimp sealed with Teflon lined caps. The remaining fluid in each vial was then carefully poured into a straight-walled glass crystallization dish (50 mm diam. \times 35 mm depth), which had been previously cleaned for IFT measurements using the procedure of Wilson et al. (Wilson et al. 1990). After a few minutes of settling, the IFT was measured with a Du Nuoy ring tensiometer, Fisher Scientific Model 21 Tensiomat. The solubility of PCE was determined by injection of 1 μl of the equilibrated aqueous phase into a Perkin-Elmer Autosystems GC. The GC column used for this study was a 30 meter \times 0.530 mm, 3 μm fixed phase, DB-624 column, manufactured by J&W Scientific. Column conditions were set at 35°C for 2.5 minutes, then ramped up 6 degrees per minute to 95°C . The carrier head pressure was set at 4 psig. A flame-ionization detector (FID) was used in the analysis for PCE. Although the detection for PCE is much improved using an electron capture detector (ECD), the concentration range of interest was from 150 ppm to 20,000 ppm. With these higher concentrations and the wide range of possible results, the linearly responding FID was chosen over the ECD. Additionally, simultaneous analysis for other components (non-halogenated) was also possible.

Results and Discussion

Initial data collection has been conducted for various cosolvent/water/PCE mixtures. Results of solubility measurements support the non-ideality of alcohol/water mixtures. The results show a sigmoidal type relationship of solubility to the original volume fraction of cosolvent (Figure 2-2).

Log-linear Solubility Estimation

Ethanol

Using the relationships described in Yalkowsky et al. (1976), a cosolvency power for EtOH was determined to be $\sigma_{0.5} = 3.73$. This “end-to-half-slope” cosolvency power is applicable when the solute (PCE) is completely miscible with the cosolvent (ethanol), and is calculated by Equation (2-5). The cosolvency power is then used as the linear slope in Equation (2-6). The resulting log-linear prediction is shown in Figure 2-2 for reference. Solubility of PCE in low volume fraction EtOH mixtures ($f_c < 0.35$) is below the log-linear predictions. This is possibly due to an insufficient quantity of EtOH to fully influence the mixture as a cosolvent and the strong hydrogen bonding network of water still present, as discussed above. Furthermore, at these low EtOH fractions, the PCE solute molecule may only be influenced by one cosolvent molecule at a time (Li and Andren 1995). Correspondingly, at higher volume fractions ($f_c > 0.5$) PCE solubilities are slightly above those predicted for the log-linear relationship. Ethanol present at high fractions overwhelms the water molecules and the cavity network structure so that hydrogen bonding is no longer a large factor (Franks and Ives 1966). Increases at higher f_c could be due to the self-alignment of the ethyl groups of ethanol molecules, presenting a more

favorable organic “zone” for PCE partitioning, and breaking the three-dimensional hydrogen bond network of water completely. PCE favors solubilization in alcohols much more than water, and this strong preference leads to failure of the log-linear method (Li and Andren 1995).

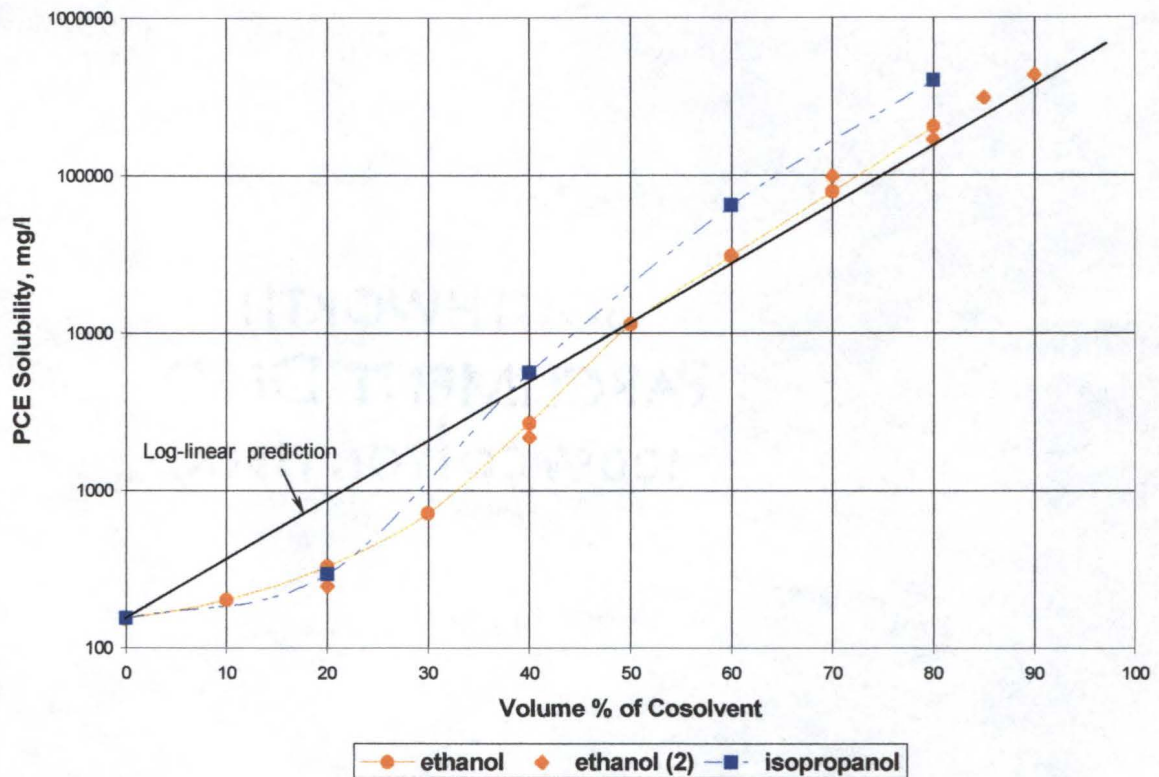


Figure 2-2. Solubility of PCE as a function of cosolvent volume fractions (initial phase volumetric phase ratio 1:1).

Isopropanol (IPA)

IPA shows increased solubility of PCE as compared to EtOH. The decreased polarity of the IPA molecule (relative to EtOH), increase in hydrophobicity, and the decrease in hydrogen bonding due to steric hindrances allows for increased amounts of PCE to solubilize into the cosolvent mixture. The resulting cosolvency power is

approximately 4.13, an average based on the solubilities of PCE at $f_c = 0.4$ and $f_c = 0.6$. The solubility of PCE at $f_{\text{EtOH}} = 0.8$ is approximately the same as that at an IPA fraction $f_c = 0.7$. This example of reduction in cosolvent use can be economically and politically beneficial in some field scenarios. Typical costs for these solvents are \$0.40/lb and \$0.35/lb for ethanol and isopropyl alcohol, respectively (Chemical Marketing Reporter, 1995). Therefore, cost savings can be obvious.

UNIFAC Method

Results of the solubility estimations are plotted with those predicted by the UNIFAC method and are presented in

Figure 2-3. The UNIFAC method appears to be adequate for describing cosolvent effect on the solubility of PCE. Large deviations (under predictions) occur at lower volume fractions for isopropanol, most likely due to the inability of UNIFAC to properly account for solute-cosolvent/solvent interactions at these lower cosolvent fractions. UNIFAC estimations improve quickly at $f_c = 0.2$ and differences between actual and predicted values remain the same as the volume fraction approaches those most likely used in remediation scenarios. Thus, the method may be adequate for quick approximations in these systems.

Extended Hildebrand Method

The solubility parameters for the various components are given below in Table 2-1. It has been reported (Martin et al. 1982) that when the range of solubility parameters of the solvent pair approaches the solubility parameter of the solute, the curve may bow sufficiently that a log-linear expression of solubility on volume fraction of cosolvent no

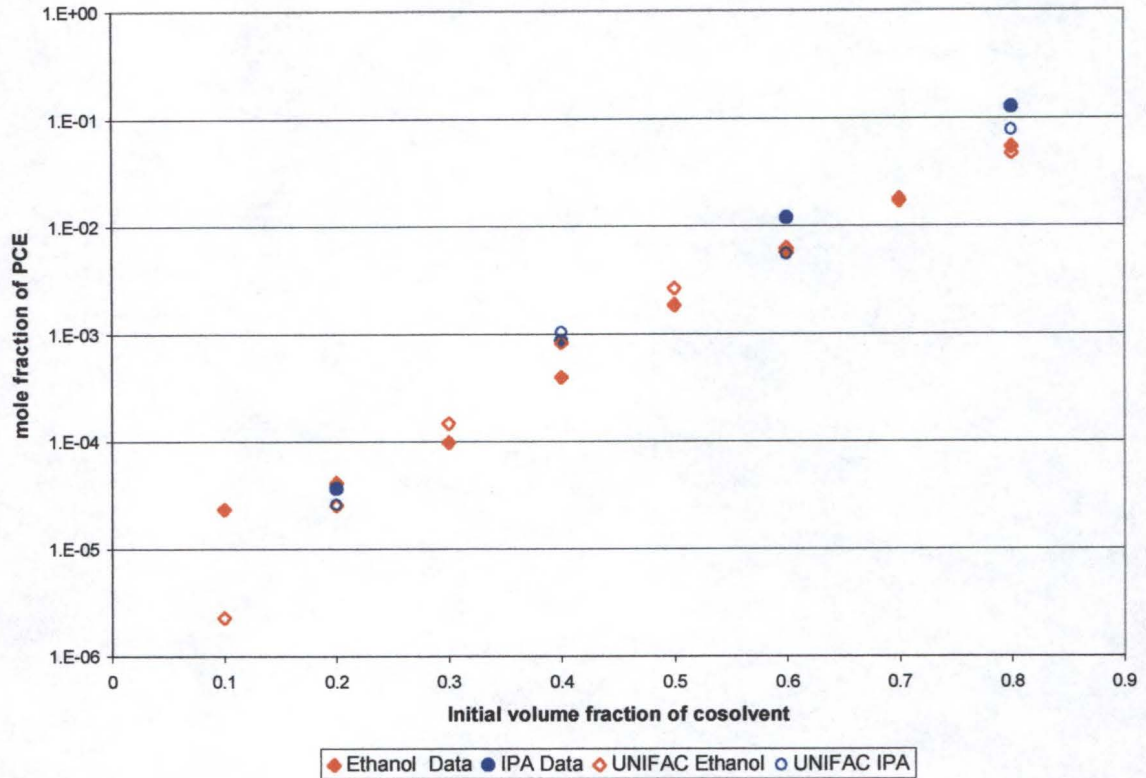


Figure 2-3. Comparison of Measured Solubility Data and those predicted by the UNIFAC Method.

Table 2-1. Solubility parameters for study components (Barton 1975)

Component	Solubility Parameter (cal/cm^3) ^{1/2}
Water	23.4
PCE	9.3
ethanol	12.7
isopropyl alcohol	11.5

longer fits the data satisfactorily. A quadratic or higher polynomial must therefore be used as required by methods such as the extended Hildebrand method. Thus, the log-linear approach, even though it is often useful, should be used with caution over a wide range of

cosolvent volume fractions (Martin et al. 1982). To apply the extended Hildebrand approach takes a little more effort, but it usually reproduces the solubility in mixed solvent systems better over an entire range of solvent compositions.

The log-linear method would seem to apply to such a system as ethanol/water/PCE, since the solubility parameter of the solute is 3 to 4 units below that of the organic solvent (ethanol) (Martin et al. 1982). However, as seen in Figure 2-4 below, the Extended Hildebrand theory predicts the solubility of IPA better than either UNIFAC or the log-linear method. This is due to the inclusion of solute-solvent interaction, which is important when the solute (PCE) is more miscible in one of the solvents (isopropanol) than the other (water). The Hildebrand method is incorrect throughout the entire cosolvent regime, but improves as the solvent-solvent interaction assumption becomes more valid as isopropanol becomes the primary solvent, similar to most cosolvent remediation scenarios.

The main advantage of the extended Hildebrand approach is that it handles solutes in polar and non-polar systems, whether the solute's solubility parameter is greater than, less than, or lies between the solubility parameters for the solvent pair (Martin et al. 1982). Although the extended Hildebrand is widely applicable, some corrections are needed in various situations. These include a correction factor for the entropy of mixing to account for the differences in molecular size (Flory-Huggins correction term) and a term for the additional entropy effects associated with hydrogen bonding substances (Amidon et al. 1974). For water/alcohol solvent systems, this is especially true. Transfers of small hydrocarbons from nonpolar liquids to water are accompanied by large negative entropies

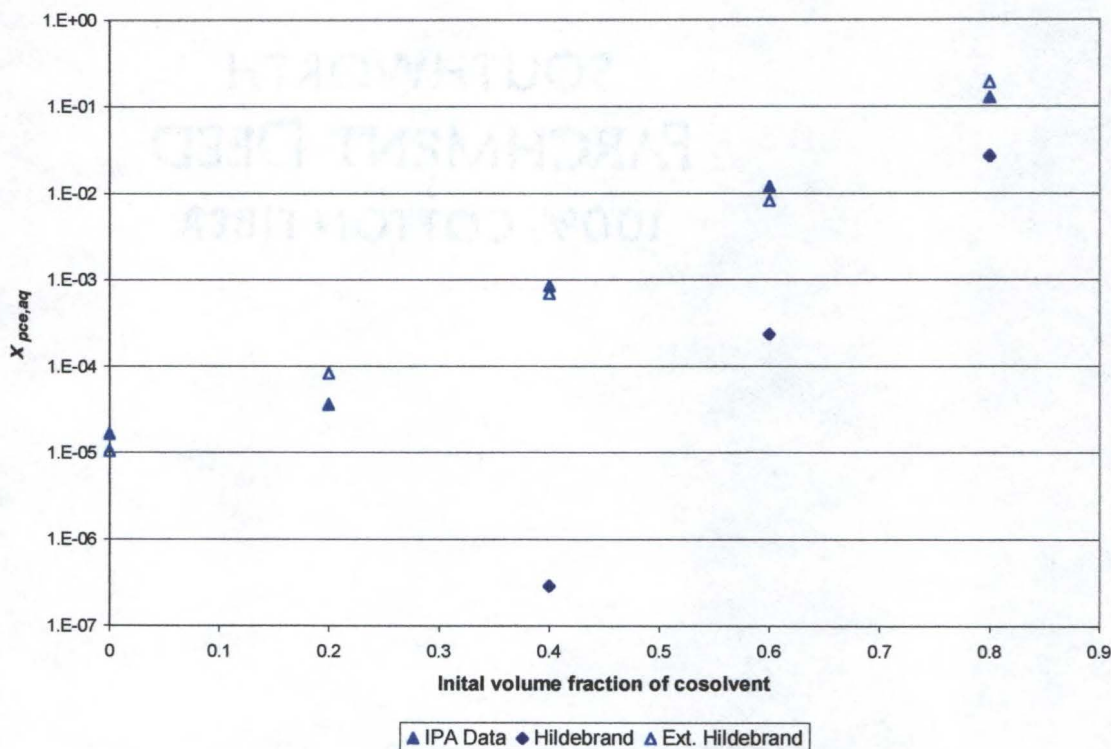


Figure 2-4. PCE Solubility Prediction of the Hildebrand and Extended-Hildebrand Theories for the IPA Cosolvent Mixtures.

and small heat effects (Amidon et al. 1974). Alcohols are known to be associated through hydrogen bonding in the liquid state, with this association decreasing in order of primary, secondary, and tertiary due to steric limitations (Franks and Ives 1966). Other methods to improve the solubility prediction of alcohol systems, such as the Molecular Surface Area approach and the Microscopic Surface Tension (Amidon et al. 1974) have shown only “good” results.

Williams and Amidon (1984b) described the non-ideality of an ethanol-barbital-system at low-volume fractions of ethanol as due to greater solute-solvent interactions than solvent-solvent. This results in solubilities below ideal predictions. Conversely, at

high volume fractions solvent-solvent interactions dominate to result in above ideal solubility predictions (Williams and Amidon 1984b). This is exactly what occurs in ethanol and isopropanol cosolvent systems.

Minor cosolvent addition

Results from addition of other less-polar solvents (in small fractions) to try to increase the solubility of PCE, while decreasing the **total** amount of solvents in the mixture, is presented in Figure 2-5. The benefits of this are little to none at all. For example, the solubility of PCE in a 60% EtOH/30% H₂O/10% isobutyl alcohol mixture is just under 100,000 mg/l. This is a total alcohol content of 70%. A cosolvent mixture of only 70% EtOH/30% H₂O results in a PCE solubility of approximately 90,000 mg/l. Furthermore, the addition of a less-polar solvent may not aid in solubility due to its partitioning into the DNAPL phase. Here, it does little to improve the aqueous solubility, but it can cause density changes if significant amounts of solvent partition into the NAPL phase. This partitioning can also cause swelling of the NAPL, possibly mobilizing DNAPL due to lower IFTs. These lower IFTs are due to the interface of these systems becoming surrounded by like molecules in both phases, reducing the tension between them. Even if there is a slight improvement in the solubility of PCE, the increased environmental risk of the addition of two solvents to the subsurface and the added complexity of phase behavior and mobilization possibilities due to reduced IFT are not sufficiently outweighed.

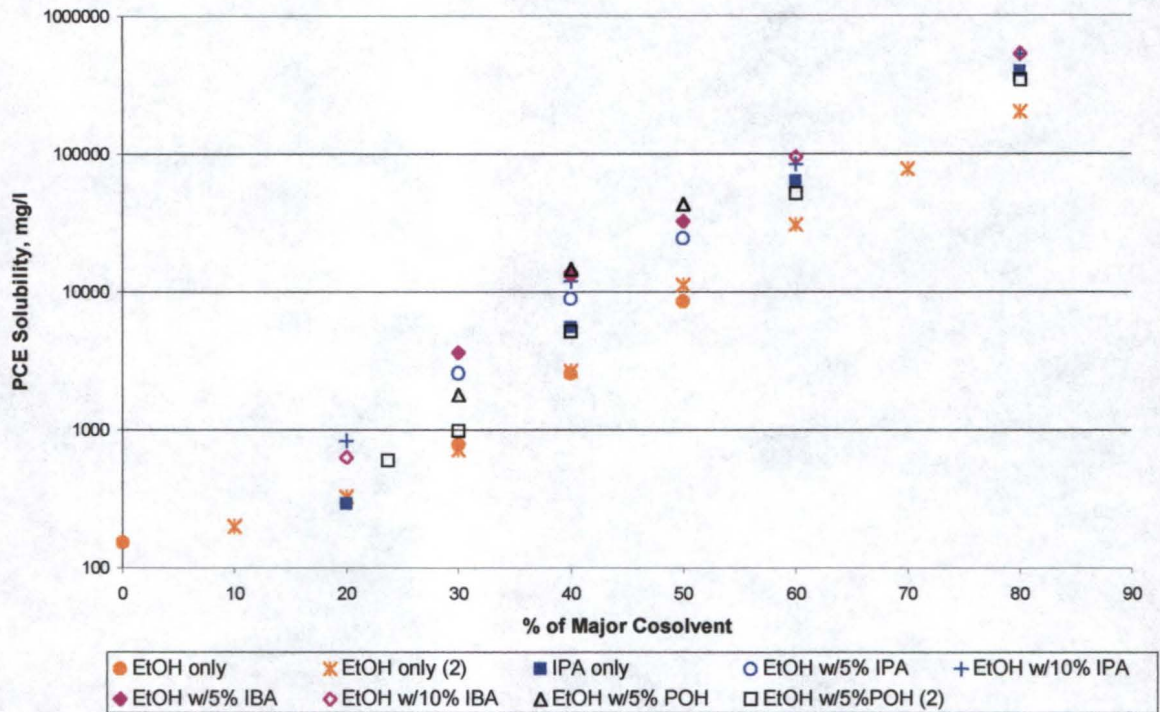


Figure 2-5. Solubility of PCE as a function of various cosolvent volume fractions (initial phase volumetric phase ratio 1:1)

Interfacial Tension Measurements and Predictions

Interfacial tension measurements agree well with literature values (Imhoff et al. 1995; Pennell et al. 1996b). IFT exponentially decreases as a function of cosolvent volume fraction (Figure 2-6). IPA IFT measurements indicate that these mixtures have a stronger response to increases in volume fraction of cosolvent, as compared to the EtOH mixtures. In addition, over the ranges of economical remediation application (>70% for EtOH), IFT is fairly insensitive to additional volume fractions of cosolvent. If mobilization is a concern, then a drastic reduction in IPA fraction may be necessary, with resulting decreases in solubility being the tradeoff for hydraulic stability. Assuming the

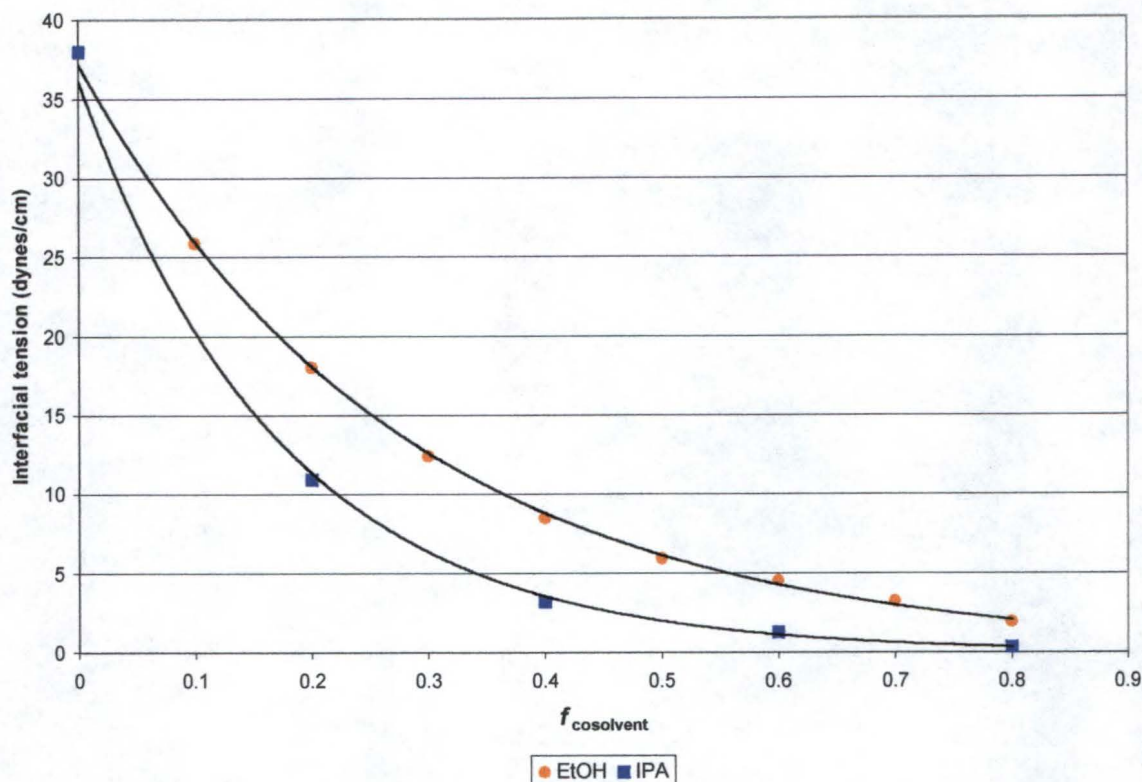


Figure 2-6. Relationship of equilibrated interfacial tension of PCE/alcohol/water ternary systems as a function of initial cosolvent volume fraction.

appropriate regime is considered, a possible benefit of using IPA over EtOH may be that similar levels of solubilization may be achieved for smaller volume fractions of cosolvent (IPA vs. EtOH).

A relationship between the logarithm of IFT and f_c was determined and plotted as Figure 2-7. Data are strongly correlated, with coefficient of determination (R^2) values of 0.9978 and 0.9975 for EtOH and IPA, respectively. It is interesting to note that this correlation involves the volume fraction of cosolvent prior to mixing. This volume fraction is obviously not the same value after equilibrium has been achieved, especially for alcohols that can significantly partition into the NAPL phase, such as IPA. Although this

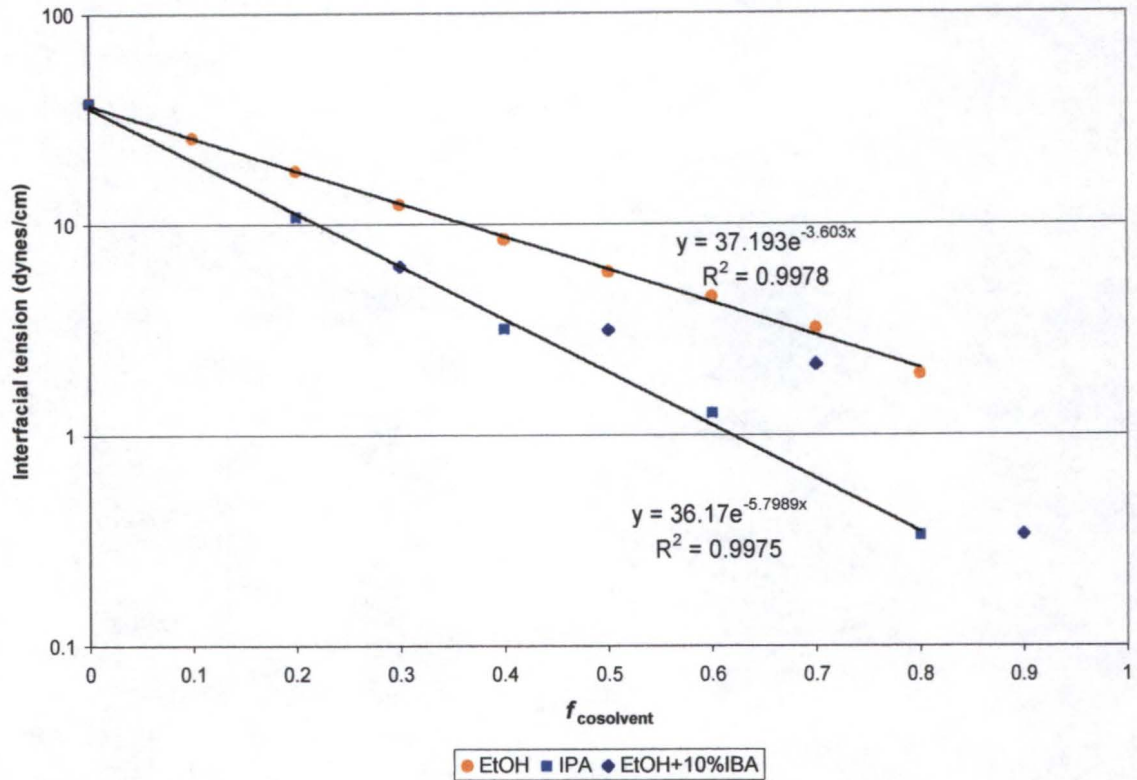


Figure 2-7. Logarithmic plot of the IFT of ternary PCE/cosolvent/water mixtures versus initial volume fraction of cosolvent. Additional data for addition of 10% isobutanol is shown for reference.

relationship may have a weak scientific basis when using the pre-equilibrated volume fractions, the dependence is adequate to use as a predictive tool for field applications. This relationship is similar to the log-linear solubility relationship as represented by:

$$\ln \text{IFT} = \Omega f_c + \ln \text{IFT}_0 \quad (2-18)$$

where Ω is now the “IFT reduction power” of the given cosolvent in aqueous mixtures and IFT_0 is the interfacial tension between pure water and NAPL (PCE). By regression of the data, $\Omega_{\text{EtOH}} = -3.60$ and $\Omega_{\text{IPA}} = -5.80$. This similarity to the log-linear relationship

should not be surprising because IFT is strongly dependent on the mutual solubilities of the two phases' solutes.

Upon correlation of solubility and IFT (a combination of Figure 2-2 and Figure 2-7), the results indicate a possible method for estimation of *in-situ* IFTs based upon solubility of PCE in the cosolvent mixture. This assumes local equilibrium is achieved. Figure 2-8, showing the logarithm of IFT as a function of the logarithm of the solubility of PCE, is the result. The largest deviations from a linear relationship occur at very low solubilities, where remediation technologies are not economically realistic. At higher solubilities, the prediction is quite close to experimental values and IFT predictions are within a few percent. The benefit of using such a plot is the direct estimation of *in-situ* IFT at the flushing front using the aqueous phase concentration of the given contaminant determined from extraction wells. Knowledge of this *in-situ* IFT is critical to determine the amount of mobilization that is likely occurring. This can be determined by using relationships developed by Pennell et al. (1996).

Conclusions

Use of log-linear solubility relationships is not a completely accurate method to predict solubility of PCE in cosolvent mixtures over the entire range of possible volume fractions. Improved predictions are possible at higher volume fractions of cosolvent. These predictions may be adequate for estimations necessary for field studies or remediation efforts. Deviations from the log-linear model are similar to those found in the literature (Dickhut et al. 1991; Li and Andren 1995) and can be explained by fundamental theories described in the literature (Franks and Ives 1966). For improved estimation of

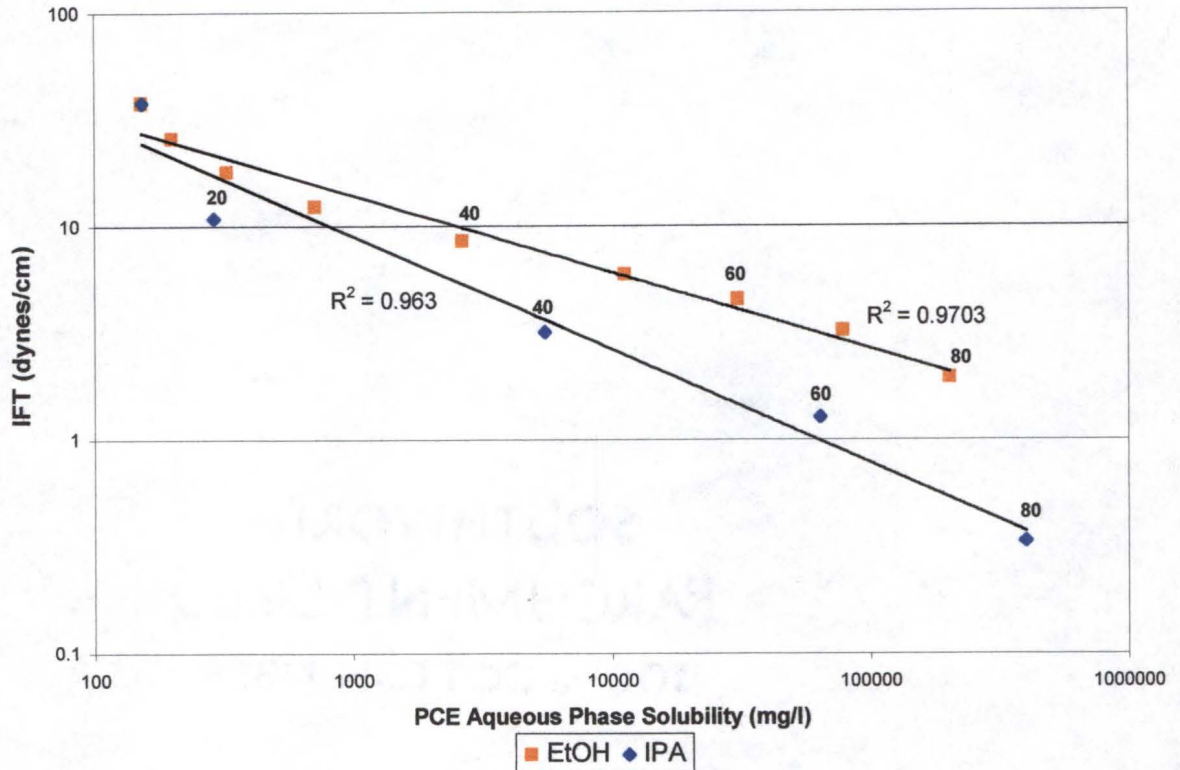


Figure 2-8. Interfacial tension of PCE/cosolvent/water mixtures related to solubility of PCE in the aqueous phase. Numbers above selected data points indicate initial volume fraction of cosolvent.

PCE solubilities, the use of the Extended Hildebrand or the UNIFAC model is recommended. Their added complexity is beneficial to accurate solubility predictions over the entire range of cosolvent fractions.

The interfacial tension resulting from various cosolvent mixtures based on the initial volume fraction of cosolvent leads to an interesting relationship, which is similar to the log-linear model. An “IFT reduction power” can be determined for each cosolvent, which quantitatively describes the ability of the cosolvent to reduce the IFT as it is added

in increasing volume fractions. IFT can also be accurately estimated by PCE aqueous phase solubility, especially in regimes conducive to cosolvent flushing. Due to the dependency of PCE aqueous phase solubility upon the aqueous and DNAPL phase ratio, it should be clarified that this approach is limited. Incorporating this predictive information into a trapping number relationship (Pennell et al. 1996b) will allow better prediction of regimes with solubilization, yet without mobilization of the NAPL/DNAPL phase. This is the topic of the next few chapters.

A historical conclusion remains appropriate:

“The best advice which comes from years of study of liquid mixtures is to use any model in so far as it helps, but not to believe that any moderately simple model corresponds very closely to any real mixture” (Scatchard 1949)

CHAPTER 3 MOBILIZATION OF RESIDUAL PERCHLOROETHYLENE DURING COSOLVENT FLOODING

Introduction

Until recently, remediation technologies for the removal of organic contaminants from subsurface environments focused on the pumping of groundwater and subsequent treatment of these streams. Risk reduction to possible receptors was the driving force behind these actions. However, due to solubility limitations, remedial action time-scales are long and expensive for such treatment. Sources of contamination are very slowly removed due to natural solubilization. In the last few years, research efforts and technology demonstrations have become more focused on source removal. These include surfactant flooding and cosolvent flushing (Annable et al. 1996; Falta et al. 1997; Fortin et al. 1997; Jawitz et al. 1998b; Lunn and Kueper 1997; Pennell and Abriola 1996; Pennell et al. 1994; Pope and Wade 1995; Rao et al. 1997). Although these techniques tend to be more aggressive and have higher initial costs, the removal of a long-term source is beneficial from risk reduction, economic, and legal perspectives.

Of these recent technologies, methods that increase the solubility of the contaminant into a mobile flushing phase have shown promising results (Annable et al. 1996; Fountain et al. 1991). Two general types of chemicals are used to enhance contaminant solubility: surfactants and cosolvents. Both increase the aqueous phase solubility of the contaminant by up to five orders of magnitude, thereby accelerating

remediation efforts. The resulting faster cleanup times are desired to decrease health risks to potential receptors and to reduce project operations and maintenance costs (Sillan 1999).

These processes also reduce the interfacial tension between the aqueous and organic phases. This reduction can drastically change the force balance keeping the organic phase trapped in the soil pores rather than being forced out due to the advective flow of the flushing phase. This possible movement of the organic phase has been labeled 'mobilization'. Correspondingly, the residual NAPL left behind after any flushing action designed to reduce the NAPL saturation is labeled as being 'entrapped'. The process itself is termed 'entrapment'. Literature related to these processes is large, yet incomplete in many aspects, since the mechanisms are complicated by interrelated properties, including complex formation pore structure, fluid properties, and applied conditions. In addition, the variability of the media and fluids is so great that most generalized conclusions have limited applicability (Stegemeier 1977).

Mobilization of oil for the purpose of Enhanced Oil Recovery (EOR) has been studied for a number of years, by several research communities (Lam et al. 1983; Moore and Slobod 1956; Morrow 1987; Morrow et al. 1988; Morrow and Songkran 1981; Patel and Greaves 1987; Ramamohan and Slattery 1984; Taber 1969). This research focused primarily on the use of surfactants to decrease the interfacial tension and mobilize the entrapped oil phase, with efficiency increased by use of a polymer flood behind this bank. In fact, the first patent issued to cover the use of surface-active materials as an aid to the water flooding of petroleum reservoirs was awarded in 1927 (Atkinson 1927). This concept and the conclusions resulting from the associated research has been more recently

applied to the field of surfactant and cosolvent flushing (Annable et al. 1996; Augustijn et al. 1997; Pennell et al. 1996b). Taber (1981) recognized the tendencies of the research and oil recovery communities to use high quantities of alcohols as "cosurfactants" in flushing formulations. He noted that although alcohols are expensive, "the potential advantages for oil [or NAPL] recovery are so great that future research may continue to examine the possibility of using alcohols as the main slug material for some processes." Earlier research applied to EOR focused on the relationships between viscous forces of the flushing fluid and the capillary pressures associated with holding residual oil in the pore structure (Stegemeier 1977; Taber 1969; Taber 1981). Later research amended these relationships to include not only viscous and capillary forces, but forces associated with buoyancy effects (Morrow et al. 1988; Morrow and Songkran 1981; Ng et al. 1978). In most historical research on this topic, buoyancy forces were neglected, or the phases chosen so that their phase densities were nearly identical (Pennell et al. 1996b). These buoyancy effects can become significant as density differences between phases become large, especially when applied to chlorinated hydrocarbon contaminant systems. These mobilization and entrapment relationships developed will be defined below.

Attempts to change the balance of forces and permit an aqueous flushing phase to release or displace a NAPL effectively may be classed into three broad and often overlapping categories. These are attempts to (1) change wettability, (2) change oil-water interfacial tension, or (3) remove the interface completely via miscible flooding (Taber 1981). The interplay of each of these processes is so great during cosolvent flooding that this operation cannot be put solely into one or the other category. However, any cosolvent remediation scheme employed today can be classified via the main NAPL

displacement process desired. These are either complete solubilization or mobilization of the contaminant. This is not to say that the secondary process is avoided at all times.

Again, the forces that are in action during these operations do not allow such segregation.

For the sake of discussion purposes, these two categories are used below.

Solubilization vs. Mobilization

Increased solubilization of contaminants occurs when the aqueous phase becomes more similar in polarity to the organic phase. When two phases are dissimilar in polarity, a tension develops at the interface causing the two phases to remain separate. As modifiers (such as cosolvents) are added to the system, the two phases become more similar, solubilization is increased, and the interfacial tension (IFT) is reduced. If enough modifier is added, the IFT can be decreased to very low values, and ultimately to zero, at which point the two phases are miscible. It is very low IFT regimes where mobilization of the organic phase can result (Pennell et al. 1996b). This is because the rate of solubilization may not keep pace with the lowering of IFT, resulting in high, mobile DNAPL saturations. The excess free phase organic can now move as a separate phase under the reduced IFT. If the organic contaminant is denser than water (DNAPL), such as perchloroethylene (PCE), mobilization can lead to movement of contaminants to deeper aquifers. Hydraulic controls during remediation may reduce the chance of downward mobilization.

In some instances, mobilization of the NAPL is favored, especially for an LNAPL. However, a question developing in the field of *in-situ* flushing of DNAPLs, is the whether to flush under cosolvent (or surfactant) conditions which encourage mobilization of the DNAPL plume or simply to enhance solubilization of the DNAPL contaminant into the flushing mixture. In some situations, one may be more favored over the other. Predictive

capabilities allowing engineers to better understand the regime in which they desire to remediate would be beneficial. An improved understanding of what occurs at the transition between solubilization and mobilization regimes is desired.

Remediation of residual NAPL by contact with a flushing alcohol-rich solution is a complex process. During cosolvent flooding both solubilization and mobilization of the NAPL can occur. Mobilization occurs due to a variety of hydrologic and physical parameters. A NAPL globule is displaced when the IFT is reduced to an extent that the forces created by the presence and motion of the continuous aqueous phase and buoyancy is sufficient to overcome capillary forces holding the NAPL globule in place (Lam et al. 1983). In studying the process of mobilization, complexities arise because the trapped NAPL phase and the cosolvent containing aqueous phase are not in chemical equilibrium and mass transfer occurs from one phase to the other. Hirasaki (1980) has discussed some of the many non-equilibrium phenomena that can contribute to the mobilization process (Lam et al. 1983). To isolate the effects of reduction of IFT on mobilization of PCE, soil column experiments were conducted with the influent cosolvent phase equilibrated and not equilibrated with PCE. Furthermore, solubilization of a partitioning cosolvent such as t-butyl alcohol (TBA) into the NAPL can cause density reduction; hence, a volumetric swelling of the NAPL. Severe swelling in itself may cause mobilization (Lam et al. 1983). This will specifically be addressed in a later chapter.

While interfacial tension (IFT) is critical, it is not the only parameter governing mobilization. Relationships have been established and applied to surfactant use in porous media (Pennell et al. 1996b). These relationships describe the amount of NAPL removed (or remaining NAPL saturation) from a given media via mobilization as a function of a

dimensionless “trapping number”, which includes contributions from viscous, capillary, and buoyancy forces, as described below.

The Trapping Number Relationship

To illustrate the interplay of viscous and buoyancy forces on the displacement of an organic liquid in two-dimensional domains, the relationship of the trapping number developed by Pennell et al. (1996b) can be used. Other authors have arrived at similar relationships, which linearly combine a “capillary number” and a “bond number” (Dawson and Roberts 1997). The Pennell study investigated the influences of forces on the mobilization of residual PCE during surfactant flushing. The balance of forces was in terms of two dimensionless numbers – the capillary and Bond numbers.

The capillary number is defined in terms of aqueous flow within a pore, and relates the viscous to the capillary forces:

$$N_{Ca} = \frac{q_w \mu_w}{\gamma_{ow} \cos \theta} \quad (3-1)$$

where q_w [LT^{-1}] is the Darcy velocity of the aqueous phase, μ_w [$ML^{-1}T^{-1}$] is the dynamic viscosity of the aqueous phase, γ_{ow} [MT^{-2}] is the IFT between the organic liquid and water, and θ is the contact angle between the NAPL globule and the pore wall (usually assumed to be zero for low IFTs situations).

The bond number represents the ratio of buoyancy to capillary forces. It is represented by

$$N_B = \frac{\Delta\rho g k k_{rw}}{\gamma_{ow} \cos \theta} \quad (3-2)$$

where $\Delta\rho$ is the density difference between the two liquids [$M L^{-3}$], g is the gravitational constant [LT^{-2}], k is the intrinsic permeability of the porous medium [L^2], and k_{rw} is the relative permeability for the aqueous phase.

A total trapping number (N_T) was developed that relates viscous and buoyancy forces to the capillary forces acting to retain organic liquids within a porous medium (Pennell et al. 1996b). For vertical flow, N_T is the sum of the two dimensionless numbers, the capillary number (N_{Ca}) and the bond number (N_B):

$$N_T = N_{Ca} + N_B \quad (3-3)$$

In the case of horizontal flow the trapping number is:

$$N_T = \sqrt{N_{Ca}^2 + N_B^2} \quad (3-4)$$

When the trapping number is exceeded, the combination of viscous and buoyancy forces exceeds the capillary forces holding the NAPL globule within a given pore. This excess force will cause the globule to physically move through that pore. In Pennell's (1996b) laboratory studies, there is not a sharp point when mobilization begins, but rather a sloping curve when PCE saturation is plotted against the logarithm of the trapping number. This is due to small anisotropies within the "homogenous" sand columns used (Pennell et al. 1996b). Researchers have observed that small-scale heterogeneities might lead to locally high residual DNAPL saturations that are more easily mobilized than DNAPL residuals in homogenous media (Imhoff et al. 1995; Padgett and Hayden 1999).

As demonstrated by Pennell et al. (1996b), these relationships can be used to predict the soil, hydraulic and IFT conditions required for the onset of PCE mobilization. Their study using surfactants indicated that ultra-low IFTs (<0.001 dyne/cm) are not required to induce mobilization of PCE in unconsolidated porous media. Therefore, predictive capabilities in low IFT ranges (0.1 to 10 dyne/cm) would be beneficial, when considering cosolvents. Their results indicate that the value of N_T should be less than 2×10^{-5} to minimize the potential for NAPL mobilization. They also concluded that NAPL mobilization is a more efficient recovery process than micellar solubilization. Finally, comparison of data from Pennell et al. (1996b) and historical data showed that the trapping number is applicable to systems with or without significant buoyancy effects. As mentioned previously, the Pennell study was conducted using surfactant solutions. To date, no reference has been found in the literature that has generated complete mobilization curves using cosolvents in simulated porous media. Padgett and Hayden (1999) used the same mobilization relationship. However, their focus was the onset of mobilization of PCE via ethanol flushing in varying heterogeneous media. It is critical to use the total trapping number analysis when selecting surfactant formulations to minimize NAPL mobilization (Pennell et al. 1996b), but it is proposed this can be extended to cosolvents as well.

Study Objective

The objective of this study was to conduct soil column experiments similar to Pennell et al. (1996b) using cosolvent mixtures typically used in the remediation field and predict mobilization characteristics of PCE using the trapping number relationship.

Comparison of mobilization curves to historical data is desired, as well as possible differences in surfactant versus alcohol systems, and finally, differences in cosolvents used.

Materials and Methods

HPLC grade PCE (CAS 127-18-4) and isopropyl alcohol (CAS 67-63-0) was obtained from Fisher Scientific, Fair Lawn NJ. The absolute ethanol (>99.5 %; CAS 64-17-5) used in these studies was purchased through Spectrum Quality Products, Inc., Gardena CA. The water used for the cosolvent solutions and for soil column flushing was purified through a Nanopure™ filtration process, and brought to an ionic strength of 10^{-2} M (350 ppm) with calcium chloride. This is published as an average groundwater ionic strength value (Stumm and Morgan 1981). Stock solutions of cosolvent/water mixtures were made with varying volume fractions of cosolvent. These solutions were made in 1-liter quantities using standard volumetric glassware.

GC Analysis

Component solution concentrations were determined via gas chromatography (GC) analysis. GC analysis was performed on a 30 m × 0.530 mm, 3 μm fixed phase, DB-624 column, manufactured by J&W Scientific, using a flame ionization detector (FID). Although the detection limit for PCE is much lower for an electron capture detector (ECD), ultra-low (ppb) detection was not required for this study as the lowest expected value was the solubility of PCE in pure water (150 ppm). Additionally, the strongly linear response of the FID over several orders of response magnitudes made it the desired choice.

Physical Measurements

Density measurements were performed gravimetrically. Two milliliters of solution were measured in a gas-tight volumetric syringe and weighed on a precision Mettler Balance ($\pm 0.0001\text{g}$). A sample's density measurements were repeated at three times to ensure accuracy and precision of this technique. Viscosities of solutions were determined by a Cannon-Fenske Routine Viscometer (Cannon Instrument Company, State College, PA). A du Nuoy ring tensiometer (Fisher Tensiomat Model 11) was used to determine the equilibrium interfacial tension of all samples. The lower limit of this instrument is approximately 0.1 dyne/cm , although IFTs below 1.0 dynes/cm are subject to visual and experimental error. These values were used in all trapping number calculations, assuming equilibrium is quickly achieved within the soil column. For strongly partitioning alcohols, this assumption becomes less valid. This method will tend to underestimate the IFT and therefore overestimate both the capillary and trapping numbers, since the nonequilibrium IFT is greater than the equilibrium value (Lam et al. 1983).

Sand Column Preparation

A small-scale glass column ($4.8\text{ cm} \times 15\text{ cm}$, chromatography column from Kontes Corporation) was used for this study. All end materials shipped with the column were removed except for the 30-40 mesh nylon screen. The soil column was incrementally packed with well-sorted Number 30-40 sand. This sand size was chosen so that the pore size would be approximately equal to the screen mesh size to avoid entrapment of NAPL, yet the sand still contained within the column. Vibration of the soil increments was also performed to improve packing characteristics. Once the column was packed it was weighed with all necessary column parts attached. The soil mass was weighed by

difference and the internal volume of the column used to calculate the bulk density. Using the density of silica sand (2.65 g/cm^3) and the mass of sand added to the column, the volume of sand (V_s) can be calculated. The porosity of the soil column is then easily calculated from the total volume of the column as: $\eta = (1 - V_s)/V_t$. Approximately 15 pore volumes of de-aired water (via vacuum) were then pumped through the column and the pore volume determined.

PCE Saturation

“Pure” PCE (dyed with $5 \times 10^{-5} \text{ M}$ oil-red-o dye, Fisher Scientific, CAS 1320-06-5) was introduced to the column to establish residual saturations. This dye concentration has been shown not to significantly affect solubilization and IFT properties (Pennell et al. 1996b; Young 1999). The PCE was introduced in an up flow mode to achieve stable displacement of water. When PCE appeared at the top of the column, the flow rate was increased 5 fold to increase PCE saturation (Dawson and Roberts 1997). The flow was then reversed and 3 pore volumes of water pumped through in a down flow mode to displace free product PCE, at a flow rate of 5.0 ml/min . The flow was again reversed and a few milliliters of water pumped into the column to remove PCE held at the influent screen due to end effects. The resulting PCE saturation ($\%S_{PCE}$) was determined gravimetrically.

Hydrodynamic Parameters

The intrinsic permeability (k) of the porous media was determined by measuring inlet and outlet pressures during aqueous phase flow. Resistance due to column end effects and tubing were measured independently using an empty soil column of the same

construction and identical tubing and fitting (Morrow et al. 1988). This resistance was subtracted from pressure drop measurement over the filled column to determine pressure drop across the media only. A differential pressure transducer (Cole-Palmer Instrument Company, Niles IL, 0-5 inches H₂O differential transducer) was used to monitor this pressure difference at various times during an experimental run.

Relative permeability (k_r) values were determined again by differential pressure measurements at various DNAPL saturations. However, these measurements during initial runs were inconsistent. Subsequently, all relative permeability values were estimated using van Genuchten parameters (van Genuchten 1980) for the sand medium, found from Tempe cell testing.

Sand Column Mobilization Studies

Experiments were conducted, similar to Pennell's (1996b), to develop a mobilization curve for PCE and cosolvent mixtures. The column was sequentially flushed with increasing volume fractions of cosolvent, continuously. Gradually increasing inlet cosolvent fractions avoided front instabilities due to the density differences. At the front, due to dilution, PCE may come out of the flushing phase, creating a macroemulsion. This emulsion may resolubilize as it is exposed to the higher cosolvent fractions, or elute from the column as a macroemulsion. This is not desired, as this quantity of PCE is more difficult to quantify. Gradient elution was performed, also in part, to help minimize macroemulsion formation.

To determine the amount of PCE solubilized compared to the amount mobilized, one of the phenomena must be eliminated to quantify both. The trapping number curve was first constructed using aqueous streams (water plus cosolvent) equilibrated with PCE.

This eliminated solubilization and allowed visual volumetric determination of mobilization (from purely IFT reduction) based on the PCE phase generated from the column. Similar experiments were then conducted on the same sand column using non-equilibrated ethanol mixtures (without any PCE added). PCE saturations and trapping numbers were determined and results between the two methods compared. Equilibrated cosolvent runs were then repeated using IPA and t-butyl alcohol as cosolvents and compared to those of ethanol to investigate swelling impacts.

For each cosolvent fraction, the run was continued for at least one pore volume, generally two, to ensure the resident fluid was characteristic of the injected fluid, yet minimize any possibility of local solubilization. Gradient elution improves the efficiency of this process. The remaining NAPL saturation percentage ($\%S_{PCE}$) was then determined both gravimetrically and volumetrically (based on visual measurement in a graduated cylinder). This was done for various cosolvent volume fractions ranging from 20% to 90% v/v cosolvent/water mixtures.

Results and Discussion

Equilibrated Gradient Column Studies

For each run, a series of trapping numbers (Pennell et al. 1996b) was determined, using the predicted IFTs from the batch equilibrium experiments. A plot of $\%S_{PCE}$ versus trapping number, N_T , was then generated. Results from gradient soil column displacement experiments are shown in Figure 3-1 through Figure 3-3. Figure 3-1 is the effluent PCE concentration as a function of pore volumes (PV; 1 PV is approximately 100 ml) of saturated EtOH/H₂O/PCE cosolvent mixtures flushed through the column. Note

that the volume percentages of ethanol shown are pre-equilibrated volume fractions, which differ from equilibrium volume fractions, especially at higher percentages of ethanol. It can be seen that effluent PCE concentrations, after 1 PV of each fluid has passed, approach equilibrium conditions. Significant mobilization begins to occur when the 85% EtOH solution is resident within the column. Reduction in DNAPL saturation at earlier pore volumes (0-4 PVs) is thought to be artificial, caused by small amounts of PCE being removed from the effluent end of the column apparatus due to possibly lower capillary forces, under moderate IFT reductions.

Blank Equilibrated Gradient Study

A gradient experiment was conducted virtually identical in procedure to the one described above, except no PCE was loaded into the column. Each flushing phase was pre-equilibrated with PCE. This was done to determine if any of the free-phase PCE generated from the column during any experiments could arise from simply the dilution of solubilized PCE at each of the gradient fronts. After completion of the entire gradient, less than 0.2 ml of PCE was collected. This volume was decided to be insignificant to our studies. The possibility of frontal dilution contributing to the mobilized DNAPL volume was discarded.

Non Equilibrated Column Studies

Results from a non-equilibrated gradient elution are presented in Figure 3-2. Effluent concentrations show that these mixtures at study flow regimes quickly reach equilibrium conditions. Mobilization does occur as shown, but it represents a very small percentage (< 0.7%) of the total DNAPL saturation. Under this gradient regime, essentially all DNAPL was removed via solubilization prior to introduction of the 90%

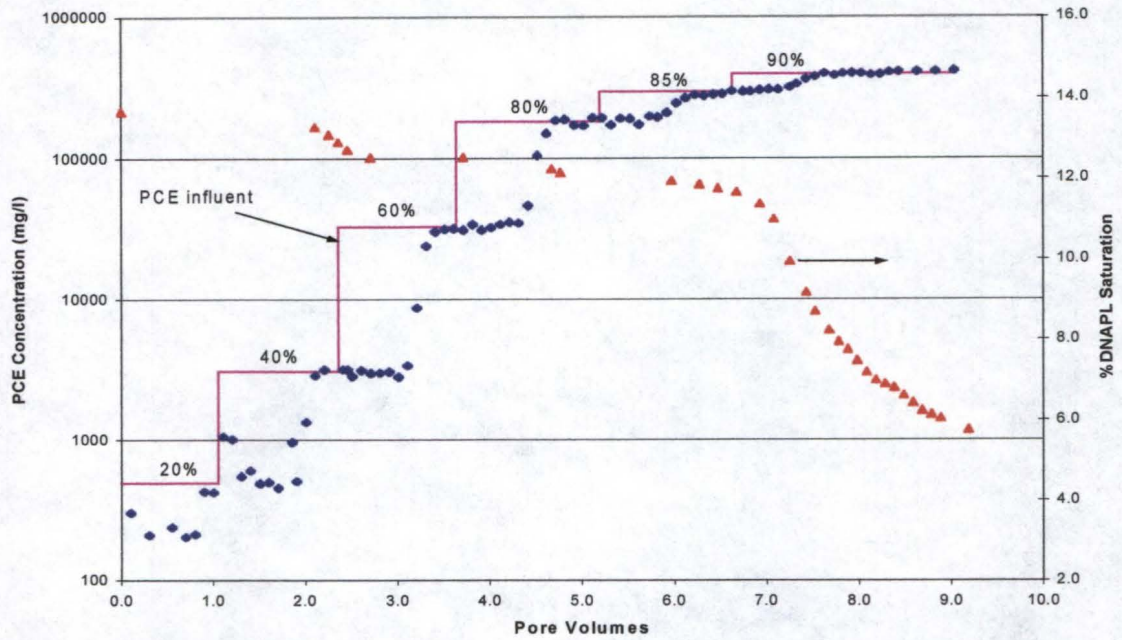


Figure 3-1. Gradient effluent profile for saturated PCE run (influent %'s shown are ethanol volume fractions prior to saturation).

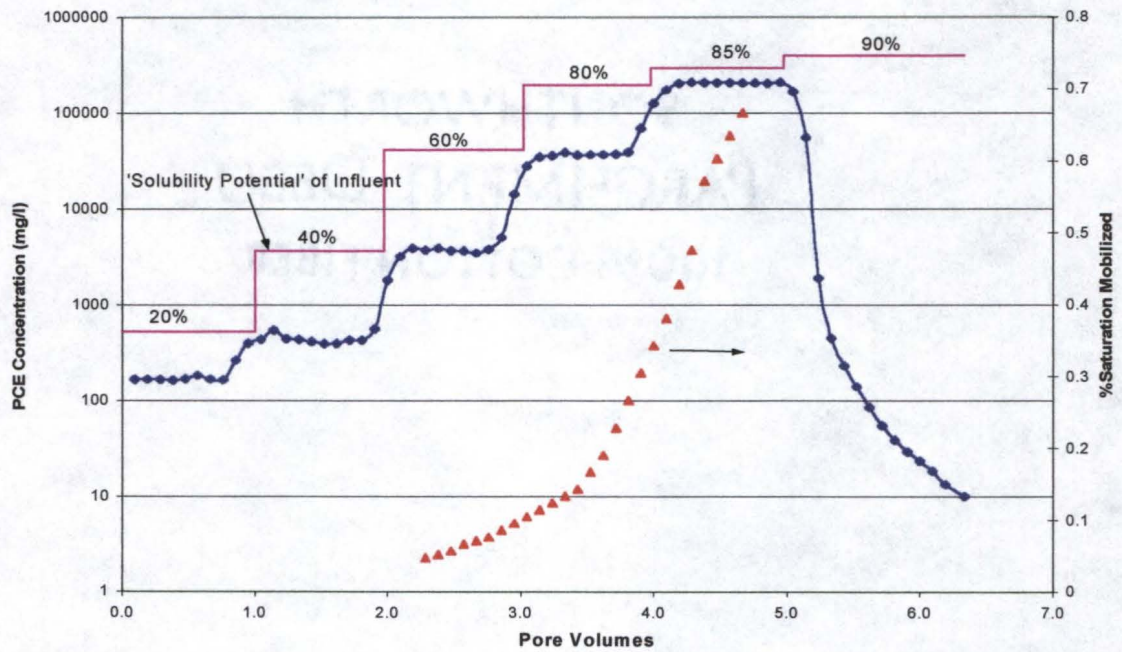


Figure 3-2. Gradient effluent profile using unsaturated ethanol mixtures - percent of mobilization shown.

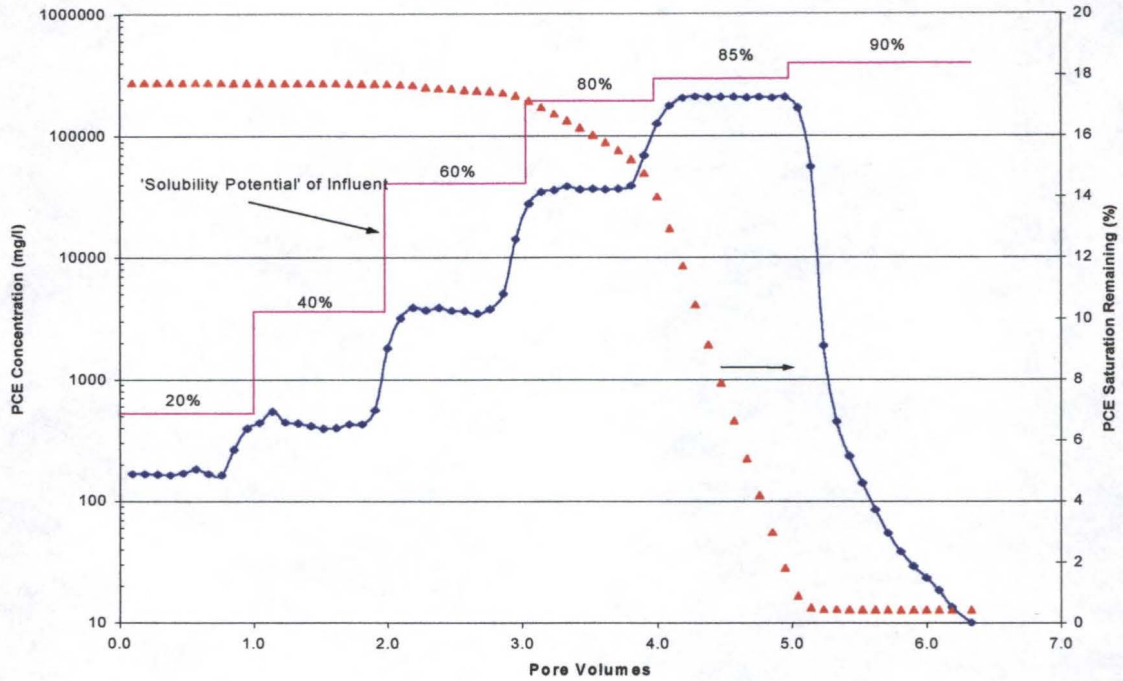


Figure 3-3. Gradient effluent profile using unsaturated ethanol cosolvent mixtures with PCE saturation reduction shown.

EtOH cosolvent. Significant reductions in PCE saturations occur during the injection of the 80% EtOH mixture. This can be seen in Figure 3-3. Calculations to determine the trapping number were conducted using physical measurements shown in Table 3-1.

Table 3-1. Physical Measurements of PCE Saturated Cosolvent Solutions

EtOH v/v %	IFT dyne/cm	ρ_{cs} g/cm ³	Kinematic	Dynamic
			Viscosity cSt	viscosity cP
0	37	1.002	0.92	0.922
20	15.85	0.9752	1.586	1.547
40	7.74	0.9444	2.42	2.285
60	4.25	0.9107	2.542	2.315
80	1.91	0.9303	1.945	1.809
85	1.14	0.9689	1.661	1.609
90	0.55	1.0765	1.285	1.383

Generation of Mobilization Curves

Relative permeabilities (k_r) calculated from pressure measurements made during a run were inconsistent due to probable variability in column conditions, including strong buoyancy effects. Therefore, permeabilities during the run were estimated using van Genuchten parameters (van Genuchten 1980) for the sand medium, found from Tempe cell testing. Although these values are calculated, they are reasonably close to actual values. Furthermore, small differences in k_r will not introduce significant error into the trapping number. The contact angle (θ) for the relationship was assumed to be zero. Although this is probably not valid at higher IFT values, it becomes more appropriate as IFT decreases, and subsequently in areas where mobilization occurs. Data points to construct these curves were based on properties of the displacing fluid and relative permeability of the media being flooded. As can be seen in Figure 3-4, mobilization for PCE begins at a trapping number of approximately 2×10^{-4} . This is different by an order of magnitude from that of Pennell (1996b). For surfactants, it was predicted that mobilization of PCE would begin at a trapping number of approximately 2×10^{-5} to 5×10^{-5} .

Also shown in Figure 3-4 is the PCE desaturation curve for the non-equilibrated run. This clearly shows the non-equilibrated experiment never reaches the critical trapping number required for mobilization. On a column average basis, the saturation decreases due to solubilization before the mobilization trapping number is reached. Therefore, significant mobilization in the column effluent is not observed. Additionally, the gradient profile could have been stopped, and the injected concentration fixed at any one of the alcohol fractions (60, 80 or 85%) and saturations reduced to zero without

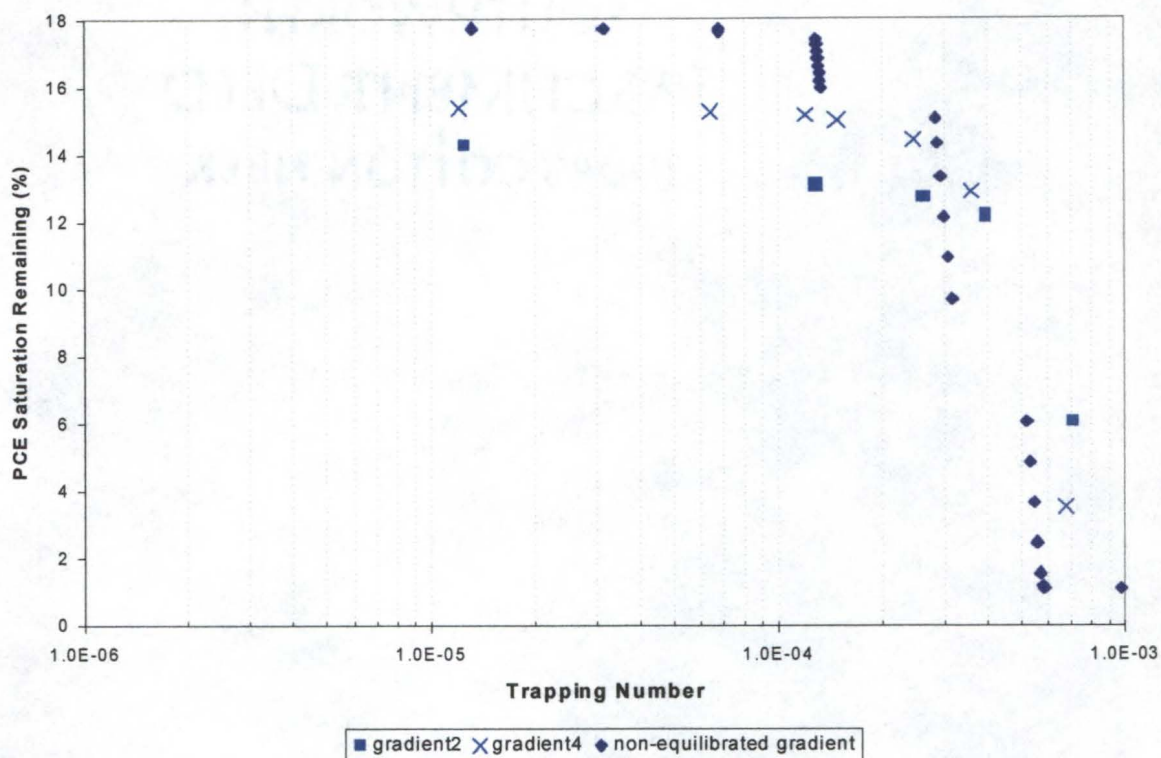


Figure 3-4. Mobilization curves showing effect of a cosolvent (ethanol) flushing phase which is pre-equilibrated with PCE (gradient 2 and 4) and a flushing phase with full solubilization potential (non-equilibrated). All are gradient runs.

mobilization. This can be seen if one extrapolates the portions of the desaturation curve where significant reduction in saturation occurs. Thus, if flooding regimes are controlled, the removal process of NAPL may never cross the mobilization envelope.

Resulting mobilization curves for the ethanol system are shown in Figure 3-5 with Pennell et al. (1996b) data shown for reference. The data indicate that mobilization of PCE begins at a trapping number of approximately 2×10^{-4} . Three gradient runs are shown in addition to three runs that were conducted independently, without any gradient. These were conducted to verify that the desaturation curve for PCE residual was not dependent on mode of flushing or previous exposure to lower cosolvent volume fractions. As can be seen, the trapping relationship is independent of the mode of flushing.

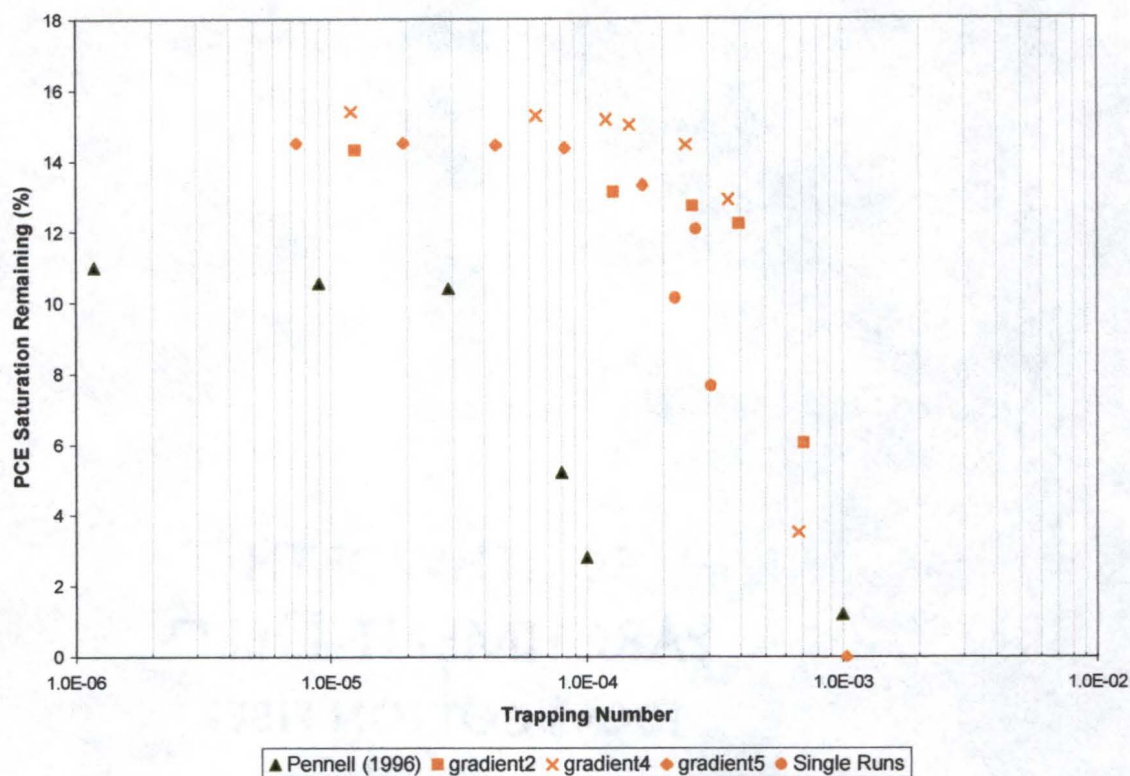


Figure 3-5. PCE Desaturation Curves – PCE saturated ethanol cosolvent runs compared with data from Pennell et al. (1996).

From initial results, it appears that there is a difference between this study's data and those from the surfactant work of Pennell et al. (1996b). Taber (1969) noticed a difference between displacements of residual oil with surfactants and water/alcohol systems. Although the Taber's initial critical value of the capillary number only was approximately the same in each case, the surfactant tended to desaturate more oil for the same capillary numbers, i.e., more oil was recovered at a lower capillary number. Taber explained this difference by the adsorption of surfactant on the media surfaces, causing earlier mobilization due to lower interfacial forces. Pennell et al. (1993) noted, that critical trapping number values derived from the capillary and Bond numbers is system

specific and can vary over an order of magnitude depending on the properties of the organic phase, matrix, and experimental design. To determine the possible reasoning for this difference, surfactant solutions similar to Pennell et al. (1996b) were made and their methods repeated. The results are shown in Figure 3-6. Physical data of each surfactant solution were assumed to be those published in Pennell et al. (1996b). Spot checks of solution properties matched those in their work reasonably well, but values of IFT were getting too low (<1 dyne/cm) to be reproducible with the du Nuoy ring tensiometer used for this work. The data from the surfactant series falls essentially on top of the cosolvent grouping. This suggests that the difference between the data sets is not due to differences between surfactant and cosolvents, but rather those related to media or experimental specifics.

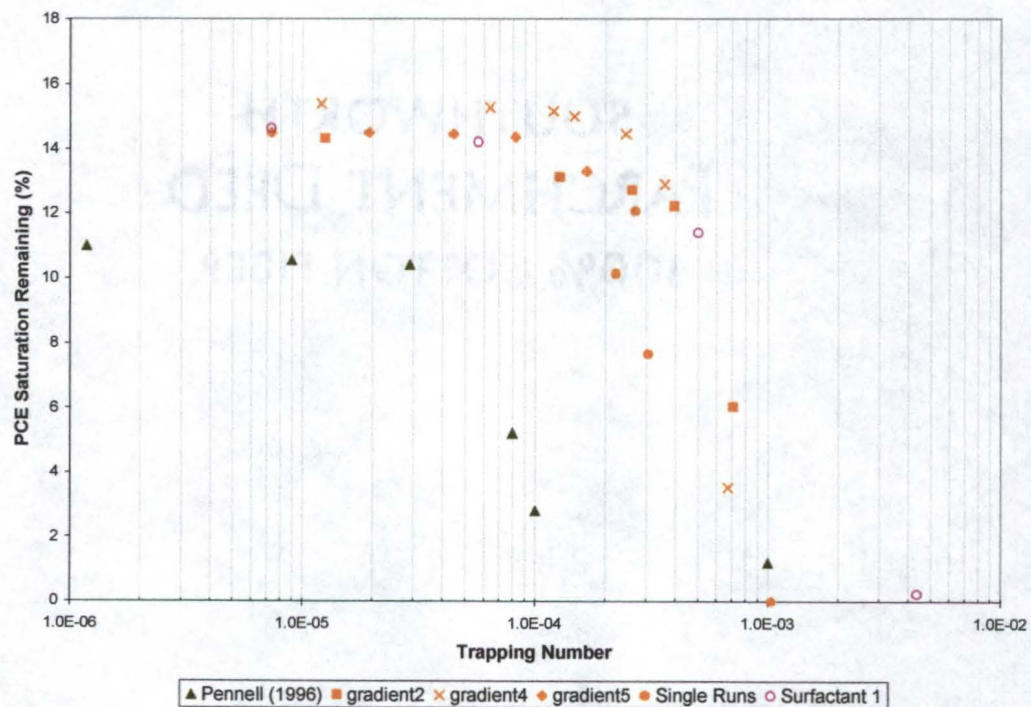


Figure 3-6 Ethanol mobilization curves with surfactant run superimposed.

To further understand possible differences between NAPL removal due to solubilization and mobilization, runs were conducted with all phases in equilibrium with each other. The only column loading and flushing method possible to achieve this was to first load the column with the desired cosolvent that had been pre-equilibrated with PCE. The corresponding equilibrated PCE phase was then loaded into the column (up flow) at 5 ml/min until PCE was eluting from the top of the column, then flow was increased to 25 ml/min until a total of one pore volume of DNAPL had been introduced. Equilibrated cosolvent then was flushed downward through the column (down flow) at 5 ml/min to bring the DNAPL phase to a new residual. This method and the results are described in the next chapter.

Swelling Effects of Cosolvents

Results from similar experiments conducted for ethanol are shown in Figure 3-7 and Figure 3-8 below for isopropyl alcohol (IPA) and t-butyl alcohol (TBA), respectively. Physical properties of these solutions are in Table 3-2. Swelling of the DNAPL due to IPA partitioning is slight. The impact of this swelling is not significant on the outcome of the onset of mobilization, as shown on the trapping number curve. Note that the volume of DNAPL remaining behind after each gradient increase in cosolvent volume fraction had to be corrected back to a pre-flushing volume for comparison purposes. Swelling of the PCE due to TBA was great, making mass balance calculations subject to probable error. Swelling correction factors were based on batch studies using a 1:1 aqueous to PCE initial phase ratio.

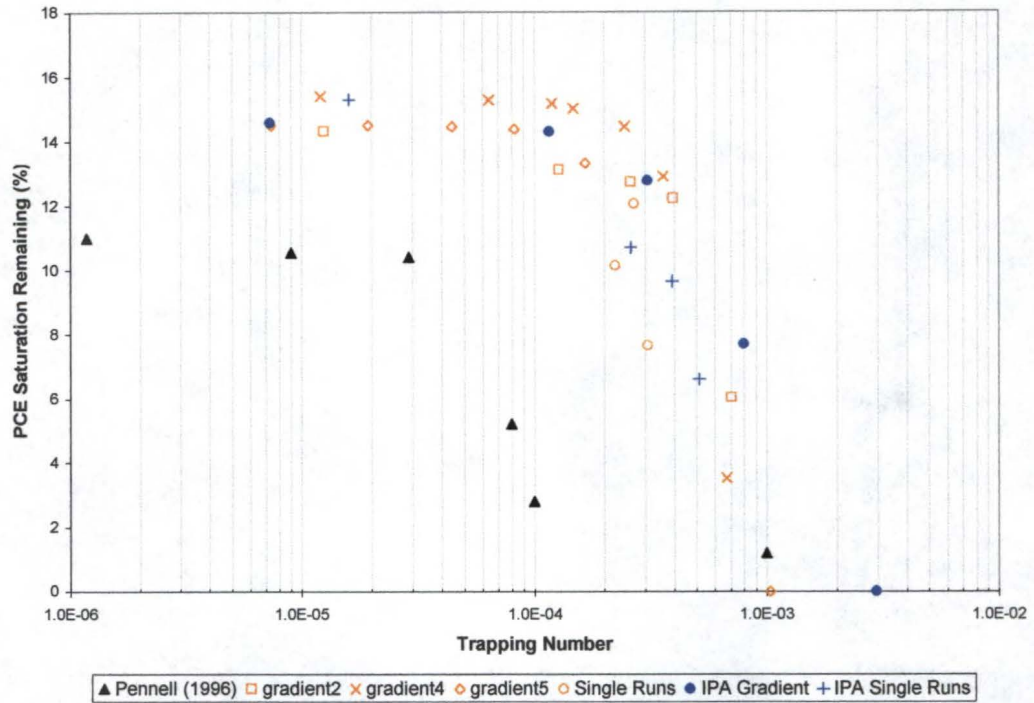


Figure 3-7. Results from mobilization studies using pre-equilibrated IPA solutions, superimposed on the ethanol study results.

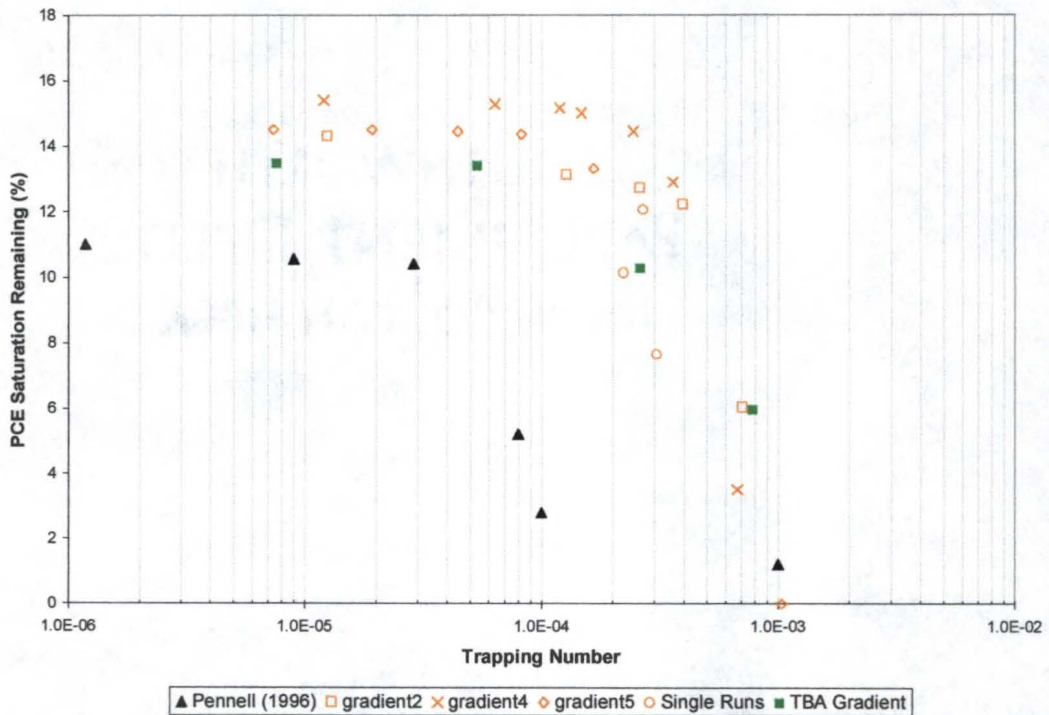


Figure 3-8. Results of mobilization of PCE during gradient TBA column flushing; TBA pre-equilibrated with PCE.

Table 3-2. Physical properties of solutions used in swelling mobilization studies.

<i>Cosolvent</i>	f_c v/v %	IFT dyne/cm	ρ_{cos} g/cm ³	Kinematic Viscosity cSt	Dynamic Viscosity cP
-	100 %H ₂ O	37.00	1.002	0.929	0.930
IPA	40	3.01	0.947	3.08	2.91
IPA	60	1.17	0.931	3.57	3.32
IPA	75	0.42	0.975	2.89	2.82
IPA	85	0.08	1.087	1.99	2.16
TBA	19.2	5.69	0.978	2.09	2.05
TBA	32.1	1.28	0.969	2.69	2.60
TBA	49.6	0.36	0.960	3.21	3.08

Conclusions

The trapping number is an effective parameter to help predict mobilization of non-aqueous phase liquids in subsurface environments. Trapping number results and onset of PCE mobilization were found similar, although slightly greater, to those of Pennell et al. (1996b) for both surfactant and cosolvents. Ethanol used as a cosolvent (at volume fractions less than 85%) enhanced solubilization of PCE to the point where this process is dominant and mobilization of PCE can be avoided for the media studied. However, under severe conditions, mobilization using cosolvents can occur. This includes large step inputs to high cosolvent fractions, where DNAPL saturation is still great enough for immediate IFT reduction to cause mobilization, at least in a local sense. This of course could be important if, within that locality, DNAPL moves out of the zone of hydraulic control. These issues are further addressed in two-dimensional box studies.

As should be expected, differences between surfactant and cosolvent systems are not apparent on a mobilization curve. Mobilization curves appear to be independent of

alcohol type. Swelling effects, when DNAPL volumes are adjusted to pre-equilibrated values did not appear to affect onset of mobilization. However, as partitioning of the alcohol into the NAPL increased, the volume of NAPL increases and becomes difficult to quantify. Further research into this area is needed.

CHAPTER 4
ENTRAPMENT VERSUS MOBILIZATION OF RESIDUAL
PERCHLOROETHYLENE DURING COSOLVENT FLOODING

Introduction

Enhanced Oil Recovery (EOR) has been practiced for quite some time and approaches have been “refined” to improve the collection efficiency of oil. In the oil recovery industry, quick and efficient removal of oil from subsurface environments is obviously desired. EOR is achieved under immiscible conditions either by reducing the amount of oil entrapped or by mobilization of some of the trapped oil. Under strongly water wetting conditions, which is assumed throughout this research, trapped NAPL is held as discrete blobs. The processes of entrapment and mobilization are associated with displacement of continuous and discontinuous oil, respectively (Morrow et al. 1988). Therefore, maximizing mobilization of free-phase NAPL and minimizing the amount entrapped behind the flooding front is desired. For the remediation of contaminant plume sources, minimization of contaminant left behind is an obvious goal from a risk management standpoint, but if mobilization of banks of NAPL is the desired scheme, maintaining this bank by minimizing entrapment is also desired for process efficiency. Many studies have been conducted focusing on these processes relating to EOR (Moore and Slobod 1956; Morrow 1987; Morrow et al. 1988; Stegemeier 1977; Taber 1969). With the recent increase in application of this technology to remediation of contaminants, additional information relating to these processes

specifically focused on NAPL contaminants is needed. Until recently, remediation technologies for the removal of organic contaminants from subsurface environments focused on pumping of groundwater and subsequent treatment of this stream. Risk reduction to possible receptors was the driving force behind these actions. However, due to the solubility limitations of these types of treatment, remedial action time-scales are long and expensive. The source of contamination is very slowly removed due to natural solubilization. In the last few years, research efforts and technology demonstrations have become more focused on source removal. These include surfactant flooding and cosolvent flushing (Chaudhry 1994; Fortin et al. 1997; Pennell and Abriola 1996). Although these techniques tend to be more aggressive and have high initial costs, the removal of a possible long-term source is beneficial from risk reduction, economic, and legal perspectives.

Of these recent technologies, methods that increase the solubility of the contaminant into a mobile flushing phase have shown promising results (Annable et al. 1996; Falta et al. 1997; Fountain et al. 1991; Jawitz et al. 1998b; Rao et al. 1997; Sillan 1999). Two general types of chemicals are used to enhance contaminant solubility: surfactants and cosolvents. Both increase the aqueous phase solubility of the contaminant accelerating remediation efforts by two to five orders of magnitude. The resulting faster cleanup times are desired to decrease health risks to potential receptors and to reduce project operations and maintenance costs.

These processes also reduce the interfacial tension between the aqueous and organic phases. This reduction can drastically change the force balance keeping the organic phase trapped in the soil pores or being force out due to the advective flow of the

flushing phase or density contrasts. This possible movement of the organic phase has been labeled 'mobilization'.

Solubilization, Mobilization and the Trapping Number Relationship

Prior discussion and literature review of solubilization and mobilization of NAPLs via cosolvent and surfactant flushing can be found in chapters 2 and 3 and is not repeated here for brevity. The reader is encouraged to review those sections, if necessary.

Mobilization and Entrapment of Residual Non-Aqueous Phase Liquid

Differences between the processes of entrapment and mobilization have been documented previously in EOR research (Morrow et al. 1988; Morrow and Songkran 1981). During their entrapment experiments, saturations appeared uniform throughout the column and relative permeabilities at reduced residuals were not functions of time and flow rate. Morrow and Songkran (1981) estimated that mobilization of trapped NAPL blobs is about five times more difficult to achieve than prevention of trapping. In their efforts to mobilize a trapped gas, severe *solution effects* (due to pressure gradients and gas solubilities) were encountered in an attempt to mobilize by increasing the capillary number. These were in distinct contrast to trapping behavior, where solution effects proved to be insignificant (Morrow and Songkran 1981). During the entrapment process, local changes in interfacial shapes within individual pores are small and not likely to account for the large changes in residual saturation that were measured under different capillary numbers. The mechanism of entrapment, they believed, is due to change in imbibition mechanism caused by small hydrostatic pressure differences across a NAPL blob. This is due to either a change in Bond number from density contrast changes. When capillary forces dominate, NAPL blobs become isolated from the main body of continuous

fluid once an imbibition event occurs. Each NAPL blob will have a few to several pore openings across which an imbibition capillary pressure is maintained. With an increase in the trapping number, specifically the Bond number, the tendency for imbibition to occur into the upper (for a DNAPL) region of a vertical pore increases since the hydrostatic pressure between the region increases. If this additional hydrostatic pressure is sufficient to allow imbibition into the upper region first, the blob is mobilized. A similar mechanism can apply to reduction of DNAPL saturation by increasing viscous forces except that the required supplemental pressure at the leading edge of the blob is provided by the viscous pressure gradient.

Movement of a trapped NAPL globule involves drainage at its leading edge and imbibition at the rear. Assuming a completely water wetted random sphere pack, the pressure drop required for mobilization (ΔP_m , $[ML^{-1}T^{-2}]$) is given by the difference between drainage and imbibition displacement pressures. At 70% water saturation, this difference is $2.8\sigma/r_p$ (σ , is the interfacial tension $[MT^{-2}]$ and r_p , particle radius $[L]$) (Morrow and Songkran 1981). The value of the supplementary hydrostatic pressure component due to buoyancy effects is:

$$\Delta P_s = 0.546\sigma / r_p \quad (4-1)$$

Therefore the ratio of $\Delta P_s/\Delta P_m$ is 0.2, and thus it is approximately five times more difficult to mobilize entrapped fluid than to prevent entrapment (Morrow and Songkran 1981).

Another main conclusion of Morrow and Songkran (1981) is that the space occupied by residual oil saturations after trapping will generally be a subset of the space occupied by the residual saturation prior to any flooding and possible mobilization. This is

under conditions where capillary forces are dominant. This seems to indicate that whatever information on pore size distribution that can be produced from pores filled with residual oil, would be indicative of the distribution for the entire media.

It was also noted that permeabilities (for a given saturation), obtained when residuals are reduced by change in entrapment mechanism, do not necessarily correspond to those resulting when residual saturations are decreased by mobilization of trapped fluid (Morrow et al. 1988). Although this difference could be present during this study, it would not be large enough to effect the entire trapping number significantly.

Study Objective

The objective of this study was to conduct two types of soil column experiments. The first was to generate mobilization curves similar to Pennell et al. (1996b) using a cosolvent mixture typically used in remediation. The second was to generate "entrapment curves" for the same media, using similar fluids. Finally, a comparison was then made between the desaturation curves for the mobilization and entrapment studies.

Materials and Methods

HPLC grade PCE (CAS 127-18-4) was obtained from Fisher Scientific, Fair Lawn NJ. The absolute ethanol (>99.5 %; CAS 64-17-5) used in these studies was purchased through Spectrum Quality Products, Inc., Gardena CA. Due to large difference in cost and small difference in physical properties, reagent alcohol (Fisher Scientific; 90.4 vol. % ethanol, 4.6% methanol, 5.0% isopropanol) was also used when absolute ethanol was not necessary. This included column final washings. The water used for the cosolvent solutions and for soil column flushing was purified through a Nanopure filtration process,

and brought to an ionic strength of 10^{-2} M (350 ppm) with calcium chloride, as done in the previous chapter (Stumm and Morgan, 1981).

Stock solutions of ethanol/water mixtures were made in 1 liter quantities using standard volumetric glassware. Volume percentages were based on volumes of water and ethanol prior to mixing. Although the final total volume is less upon mixing (thus the volume percentages are no longer exact), the difference is minimal (1-2%). Furthermore, labeling of these solutions by using these pre-mixed volume fractions is for convenience only and exact physical parameters used in calculations are determined later.

Physical Measurements

Density measurements were performed gravimetrically. Two milliliters of solution were measured in a gas-tight volumetric syringe and weighed on a precision Mettler Balance (± 0.0001 g). A sample's density measurements were repeated no less than three times to ensure accuracy and precision of this technique. Viscosities of solutions were determined by a Cannon-Fenske Routine Viscometer (Cannon Instrument Company, State College PA). A du Nuoy ring tensiometer (Fisher Tensiomat Model 11) was used to determine the interfacial tension of all samples. The lower limit of this instrument is approximately 0.1 dyne/cm. Laboratory temperature was well controlled and was $23 \pm 0.5^{\circ}\text{C}$.

Sand Column Preparation

A small-scale glass column (4.8 cm X 15 cm, chromatography column from Kontes Corporation) was used for this study. All end materials shipped with the column were removed except for the 40 mesh nylon screen. The soil column was incrementally packed with well-sorted Number 30-40 sand. This sand size was chosen so that the pore

size would be approximately equal to the screen mesh size to avoid entrapment of NAPL, yet still contain the sand within the column. Vibration of the soil increments was also performed to improve packing characteristics. Once the column was packed it was weighed with all necessary column parts attached. The soil mass was weighed by difference and the internal volume of the column used to calculate the bulk density. Using the particle density of silica sand (2.65 g/cm^3) and the mass of sand added to the column, the volume of sand (V_s) can be calculated. The porosity of the soil column is then easily calculated from the total volume of the column as: $\eta = (1 - V_s)/V_t$. Approximately 15 pore volumes of de-aired water (via vacuum) were then pumped through the column and the pore volume determined.

PCE Saturation and Generation of Trapping Curves

Mobilization studies

Experiments were conducted, similar to Pennell's (1996b), to develop a trapping number curve for PCE and the ethanol cosolvent mixtures. "Pure" PCE (dyed with $<5 \times 10^{-5} \text{ M}$ oil-red-o dye, Fisher Scientific, CAS 1320-06-5) was introduced to the column to establish residual saturations. This dye concentration range has been shown not to significantly affect solubilization and IFT properties (Pennell et al. 1996b; Young 1999). The PCE was introduced in a up flow mode to achieve stable displacement of water. When PCE appeared at the top of the column, the flow rate was increased 5 fold to increase PCE saturation (Dawson and Roberts 1997). The flow was then reversed and 3 pore volumes of water pumped through in a down flow mode to displace free product

PCE, at a flow rate of 5.0 ml/min. The resulting PCE saturation ($\%S_{PCE}$) was determined gravimetrically, based on density difference between water and PCE.

The column was then sequentially flushed with increasing volume fractions of cosolvent, without stoppage. Gradually increasing inlet cosolvent fractions avoided front instabilities due to the density differences. At the front, due to dilution, PCE may come of solution, creating a macroemulsion. This emulsion may eventually resolubilize as it moves through the column, exposed to the higher cosolvent fraction, or elute from the column as a macroemulsion. This is not desired, as this quantity of PCE is more difficult to quantify. Gradient elution was performed to help avoid macroemulsion formation.

To determine the amount of PCE solubilized compared to the amount mobilized, one of the phenomena must be eliminated to quantify both. The trapping number curve was first constructed using aqueous streams (water plus cosolvent) pre-equilibrated with PCE. This eliminated solubilization and allowed visual determination of mobilization (from purely IFT reduction) based on the PCE phase generated from the column. Similar experiments were then conducted on the same sand column using unsaturated ethanol mixtures (without any PCE added). PCE saturations and trapping numbers were determined and results between the two methods compared.

For each cosolvent fraction, the run was continued for at least one pore volume to ensure the resident fluid was characteristic of the injected fluid. The remaining $\%S_{PCE}$ was then determined by visual volumetric measurement of mobilized DNAPL. This was done for cosolvent volume fractions 20%, 40%, 60%, 80%, 85%, and 90% EtOH/water mixtures. For each run, a series of trapping numbers (Pennell et al. 1996b) was

determined, using the predicted IFTs from the batch equilibrium experiments. A plot of % S_{PCE} versus trapping number, N_T was then generated.

Entrapment studies

To maintain equilibrium between all fluids for the entrapment experiments, independent runs using cosolvent and DNAPL phases which had been previously contacted and brought to equilibrium was necessary. Three PV's of a reagent alcohol mixture were flushed through the column at a flow rate of 25 ml/min. The cosolvent phase (with solubilized PCE) from the desired batch solution was then flushed through the column in the upflow mode. Only one PV of this fluid was necessary, as the front of this displacement was very efficient and stable, i.e., no fingering occurred. Subsequently, the corresponding equilibrated DNAPL phase (mostly dyed PCE) was introduced into the column at 5 ml/min in the upflow direction until production of DNAPL appeared in the effluent tubing. Then the flowrate was increased to 25 ml/min until a total of one PV was used. Finally, the DNAPL was brought to residual saturation with the same pre-equilibrated cosolvent phase. All fluids were introduced into the column at a flow rate of 5 ml/min, unless specifically noted otherwise.

Porous Medium Parameters

The intrinsic permeability (k) of the porous media and hence, the effective permeability ($k_e = kk_{rw}$), was determined following PCE addition by use of inlet and outlet pressure difference measurements. Resistance due to the column was measured in the absence of packing to allow correction for the resistance due to inlets and outlet screens, connections and tubing (Morrow et al. 1988). This resistance was subtracted from pressure drop measurements over the filled column to determine pressure drops

across the media only. A differential pressure transducer (Cole-Palmer Instrument Company, Niles, Illinois, 0-5 inches H₂O differential transducer) was used to monitor this pressure difference.

Relative permeabilities were estimated based on van Genuchten parameters (van Genuchten 1980) determined by Tempe cell (Soil Moisture Equipment Co., Santa Barbara, CA) measurements (Figure 4-1). These were compared to the data from Morrow and Songkran (1981) and found to match closely with actual data measured in porous media (glass beads). This data is reproduced in Figure 4-2.

Thus, the relative permeabilities determined via the van Genuchten parameters based upon the Mualem (1976) method were determined to be adequate for the soil column. Measurement of the relative permeability with the pressure transducers was initially attempted, but fluctuations associated with column resistance effects and

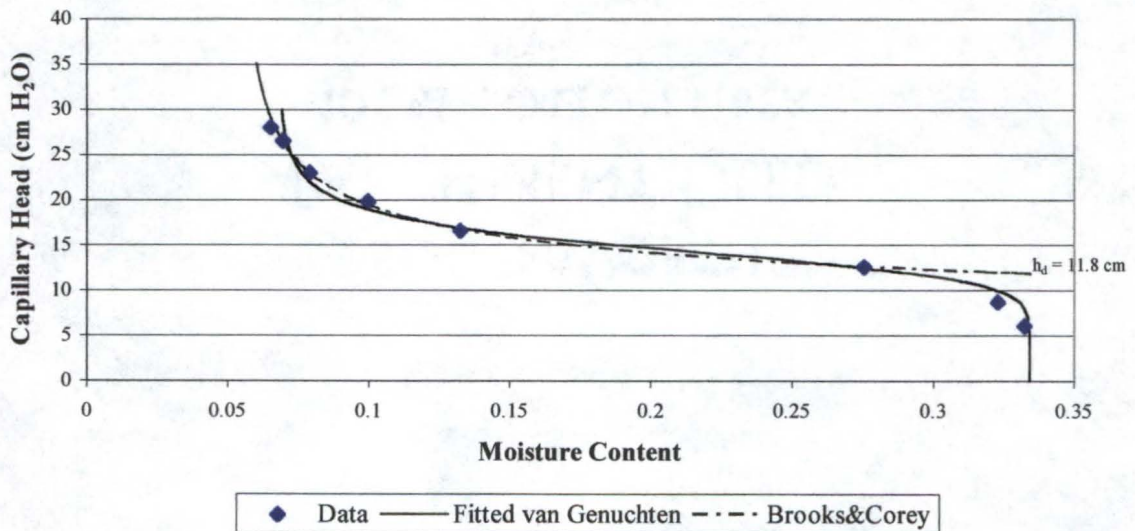


Figure 4-1. Moisture release curve for No. 30-40 silica sand used for these studies, conducted via Tempe cell. van Genuchten (1980) and Brooks & Corey (1964) fits are based on minimizing the sum of squares of the difference between the actual data and the fitted line.

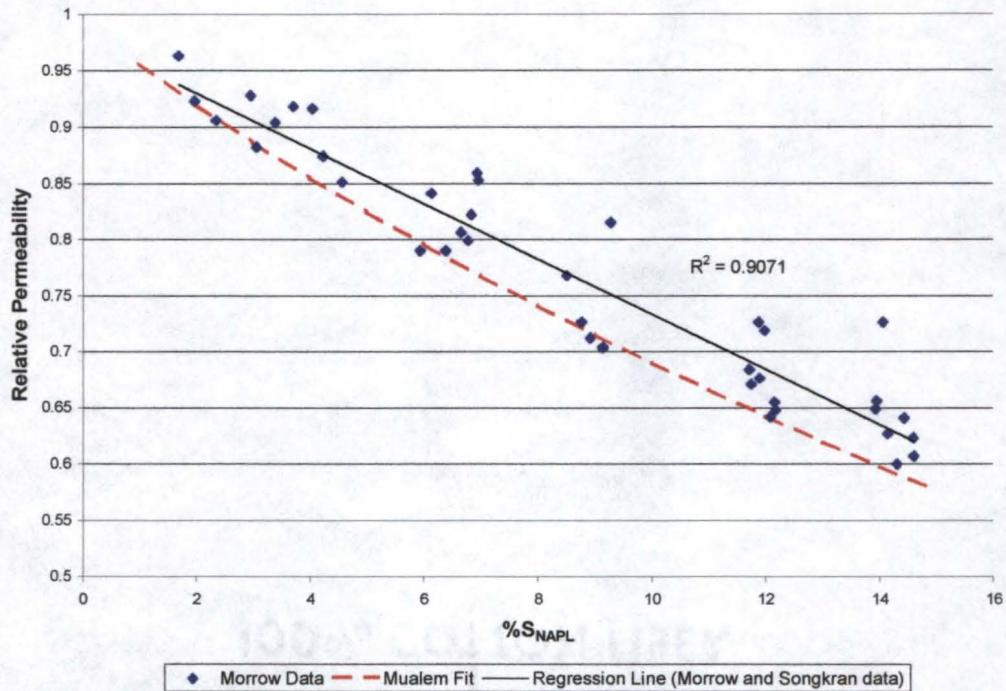


Figure 4-2. Relative permeability to the wetting phase at less than normal nonwetting phase residual saturations: Morrow and Songkran (1982) data shown with regression ($R^2 = 0.907$) and fit of this study's Tempe cell data based on van Genuchten (1980) parameters and the Mualem (1976) method.

buoyancy effects, due to sometimes large density differences, made these measurements erratic. Although this parameter is not directly measured for this study, this should not provide significant error, as differences in relative permeability estimates are minor.

Results and Discussion

Entrapment in Homogeneous Sand Column

Curves for the soil column mobilization experiments relating PCE (DNAPL) saturation to the total trapping number are shown in Figure 4-3, with Pennell et al. (1996) data shown for reference. The data indicate that mobilization of PCE begins at a trapping

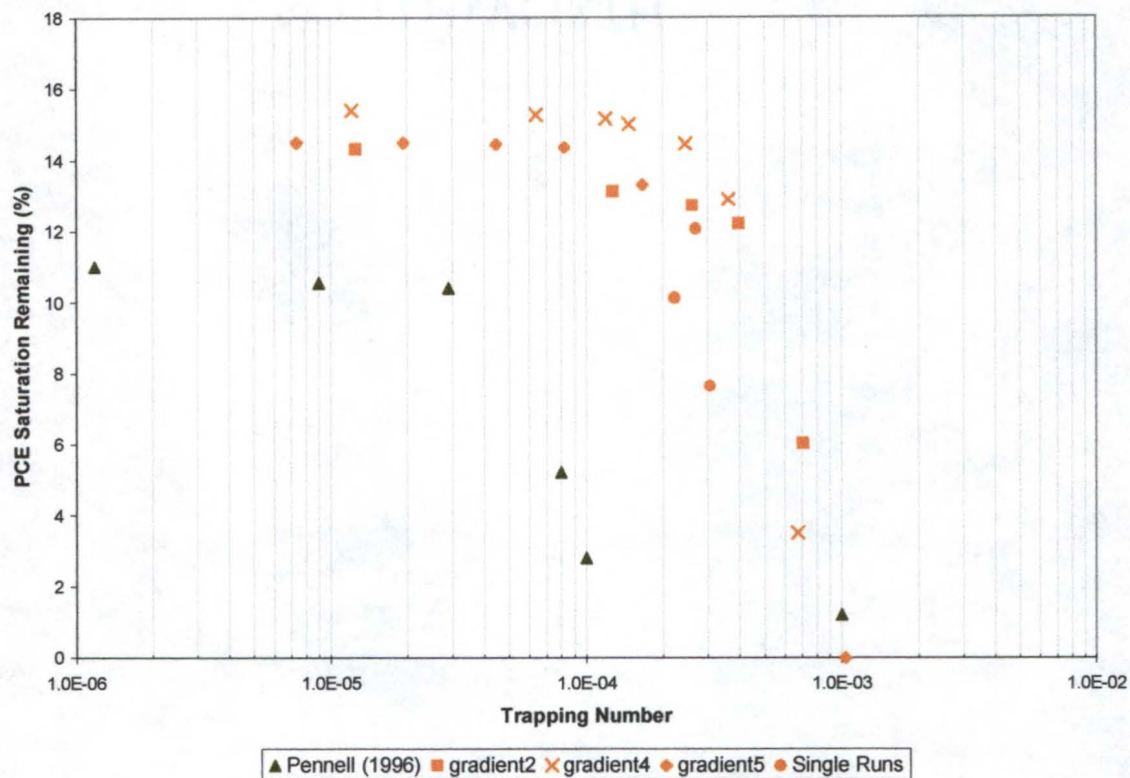


Figure 4-3. PCE Desaturation curve – experimental ethanol data only compared to those of Pennell et al. (1996).

number of approximately 2×10^{-4} . Three gradient runs are shown in addition to three runs that were conducted independently, without any gradient. These were conducted to verify that the desaturation curve for PCE residual was not dependent on mode of flushing or previous exposure to lower cosolvent volume fraction flushing fluids. As can be seen, the trapping relationship is independent of the mode of flushing.

The DNAPL saturation percentages that resulted from the entrapment experiments were plotted against the run's corresponding trapping number and are shown in Figure 4-4. The data from the mobilization experiments and Pennell et al. (1996) data are shown again for reference. There were two different series of entrapment experiments

conducted. The first involved all pre-equilibrated fluids, conducted as described previously in Materials and Methods. However, in an effort to determine the possible causes of the difference shown in the figure between mobilization and entrapment processes, another series of "entrapment studies" was conducted. These were accomplished identically to the previous entrapment method, except that the DNAPL phase loaded into the column was HPLC grade PCE instead of PCE equilibrated with an ethanol cosolvent mixture. This change does not account for much of the difference between the two processes, indicating that mobilization is not heavily dependent on mass transfer limitations of a slightly partitioning cosolvent, like ethanol. As long as the aqueous phase/NAPL interface is amply supplied with components required to keep the interfacial tension to its equilibrium value, proper mobilization or entrapment will occur. This is obviously more critical during mobilization, as fresh NAPL interfaces are constantly being met with the flushing cosolvent phase.

The slight shift between the two entrapment runs (all phases equilibrated versus only the cosolvent phase equilibrated) can be possibly attributed to slight differences in actual interfacial tensions. The use of equilibrated IFT in the trapping number calculation is presumably close to the actual IFT in the sand medium. The use of equilibrated IFTs for the cosolvent-equilibrated run may underestimate the actual IFT, and therefore overestimate the trapping number. This difference is likely small and lead to the small shift of the two trapping relationships shown in Figure 4-4. One of the remarkable features of these studies is the extreme linearity of the relationship between the DNAPL saturation and the trapping number. Table 4-1 shows the results of a linear regression performed through both sets of data.

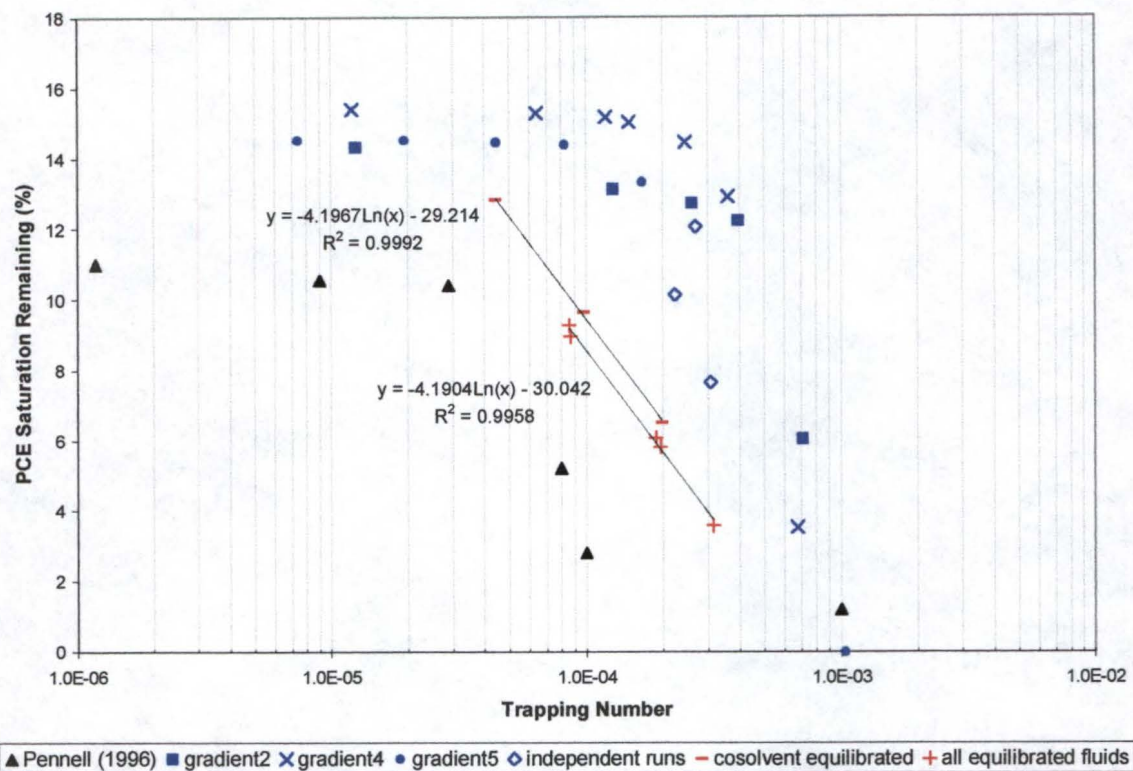


Figure 4-4. PCE desaturation curves for both mobilization and entrapment studies, with linear regressions shown for the entrapment experiments

Table 4-1. Results of linear regression of entrapment studies

Data Series	Slope	y-intercept	R^2
Entrapment (all pre-equilibrated)	-4.1904	-30.042	0.9958
Entrapment (PCE not pre-equilibrated)	-4.1967	-29.214	0.9992

It is worth repeating that each data point is done independently from the others. The slopes of the regression of both data sets are nearly identical. Therefore, the slope appears to be independent of phase equilibrium. As the x-axis is representative of the capillary pressure through the capillary number, it appears the slope represents a factor

relating to the pore size distribution of the media. Taber (1969) stated the similarity between curves of capillary number and percent saturation and standard capillary pressure curves was "obvious". He further stated this similarity should be expected since both processes represent the displacement of a fluid from capillaries of various sizes by a different and immiscible fluid. Thus, the pore size distribution of the porous medium should affect both processes in a similar way (Taber 1969). Of all the factors included in the Trapping Number, the effect of alcohol addition on trapping and mobilization phenomena in these type of studies is due to change in IFT, and not changes in other fluid properties (Ryan and Dhir 1996). If this is the case, trapping number curves should provide us with similar information as capillary pressure curves, which are heavily dependent on IFT. Separate air-water desaturation studies conducted on the same sand using a Tempe cell resulted in a Brooks-Corey lambda of approximately 3.65 (see Figure 4-5). Previous researchers have stated the space occupied by residual oil saturations will generally be a sub-set of the space occupied by the normal residual saturation (Morrow and Songkran 1981). This method of obtaining pore-size information has not been found to date in previous literature.

Effect of Pore Size Heterogeneity on the Entrapment of PCE

Similar to the totally equilibrated entrapment studies discussed above, another series of experiments was conducted on the one-dimensional sand column filled with a widely graded sand mixture. This sand medium consisted of equal weight fractions of #20-30, #30-40, #40-50, #50-60, #70-80, and #80-100 sands. The drainage curve and the pore size distribution of this mixture are shown in Appendix A.

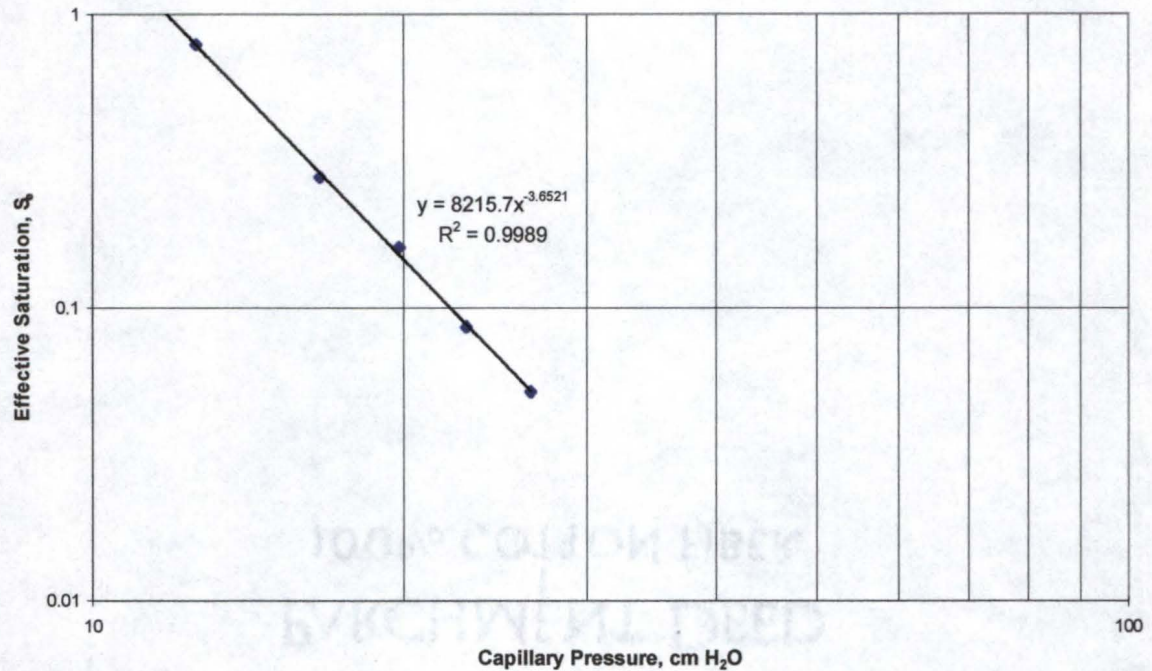


Figure 4-5. Effective saturation of study 30-40 mesh sand as a function of capillary pressure, resulting slope of regressed line is the Brooks and Corey lambda, $\lambda = 3.65$.

Two methods of packing the column were attempted – wet and dry, both with subsequent vibration. The wet packing was accomplished in 3 cm layer with only about 1-2 cm of water above to keep it fully saturated. This was done to minimize the distance of travel for the different particle sizes with varying settling velocities. However, after completion, significant heterogeneity (layering) was observable. This packing was still used for study and results are shown below.

To minimize the layering, a quick fill of the sand mixture under dry conditions was also done. Subsequent vibration necessitated the addition of a small layer of new sand at the top of the column. The column was then saturated with water from below via vacuum aspiration.

The results of the wide distribution packing are added to the desaturation curves presented above and this is shown in Figure 4-6 below. As shown in Figure 4-6, the wide distribution and the homogeneous entrapment studies do not behave similarly. It was expected that the slope of the entrapment curve for the wider pore distribution would be less, resulting in a more gradual desaturation curve. However, it appears that the behavior is exactly the opposite. The data reveal that the saturation generally increases with higher trapping numbers (lower interfacial tensions). This may be due to PCE being able to enter smaller and smaller pores as the interfacial tension between it and the equilibrated cosolvent decreases. Additionally, small layered zones of finer media in the column may allow fluids with lower IFT to enter and never be able to come out. As previously

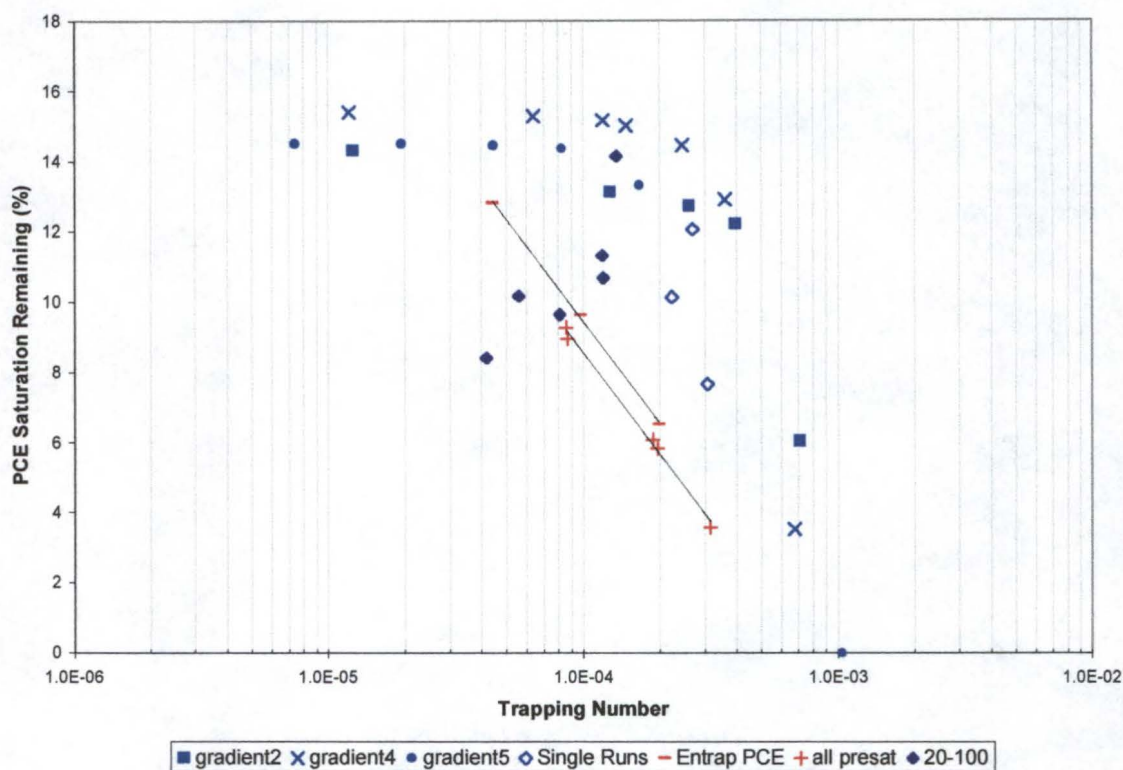


Figure 4-6. Results of entrapment experiments on the heterogeneous packing (#20-100 sand), shown with homogeneous entrapment and mobilization results for reference.

mentioned, Morrow and Songkran (1981) concluded that it is approximately five times more difficult to mobilize than to prevent the entrapment of a NAPL. Therefore, it is possible for the DNAPL to enter more pores at lower IFTs and subsequently not be able to as easily be mobilized back out. This behavior was not observed in the homogeneous packing since relatively all pore sizes are similar in size.

Conclusions

Entrapment and mobilization of residual NAPL are separate and distinct processes. This difference can be seen if both processes are plotted on a trapping number curve. The entrapment process, represented by the percent of remaining DNAPL saturation (S_{NAPL}), appears to be log-linearly related to the trapping number. The exact interpretation of this relationship is not clear now, but it is believed to be associated with the log-linear dependence of saturation with capillary pressure. This is similar to the Brooks-Corey relationship shown in Figure 4-5.

Dependence of the entrapment process on media heterogeneity is not clearly shown. It was expected that the slope of the entrapment curve for the heterogeneous media would be less than that of the homogeneous sand, indicating a more gradual release of NAPL throughout the wider range of pore sizes. Difficulty in truly reproducing isotropic heterogeneous packing may have contributed to the scatter of data for the wide pore size distribution packing. However, it is plausible that due to lower permeability zones in the packing, the reducing IFT allows additional PCE/DNAPL to remain in these smaller pores, increasing saturation. This may be a negative factor in choosing to use

gradient elution of DNAPLs, as reduced IFTs ahead of any mobilized DNAPL could entrap contaminant in smaller pores, leading to longer removal times and possible lower removal efficiencies.

CHAPTER 5
MOBILIZATION AND ENTRY OF DNAPL POOLS INTO FINER SAND MEDIA:
TWO-DIMENSIONAL BOX STUDIES

Introduction

In-situ flushing remediation is quickly becoming a popular method to remove source-zone contamination. Whether using surfactants, alcohols, or oxidants as injection fluids to accelerate the displacement, dissolution, or chemical transformation of contaminants, control of contaminant movement is critical. Control is critical not only during the flushing process to improve recovery and to minimize environmental impact, but consideration of contaminant control is vital during the planning and proposal stages as well. Proposals to property owners, local, state and federal government agencies are more likely to gain approval after sound recommendations and strategies for contaminant control have been outlined. The basis for these a priori strategies often include theoretical chemical and hydrologic calculations or modeling, but the most valuable input arises from field experience. Test cells constructed to study flushing technologies, including one at Hill Air Force Base (AFB), Utah (Annable et al. 1996) and one currently being used at Dover AFB, Delaware provide excellent opportunities from which to draw conclusions and apply them to the "open-field" real remediation situation. However, an important experimental method that lies between these two study options in scale, is the use of a 2-Dimensional (2-D) box or chamber to study the movement and remediation processes of these flushing chemicals. A good review of 2-D laboratory experiments can be found in

Chevalier and Peterson (1999). 2-D boxes provide not only the horizontal dimension to simulate the hydrologic flushing process involving injection and extraction wells, but the added vertical dimension. This vertical dimension becomes important when studying non-aqueous phase liquids (NAPLs) that are much lighter or heavier than water or the flushing fluid. In the case of dense non-aqueous phase liquids (DNAPLs), movement downward and out of the hydrologic control of the remediation flow paths, is undesired.

NAPL migration in subsurface environments is affected by: (1) volume of NAPL released; (2) area of infiltration; (3) time duration of release; (4) properties of NAPL; (5) properties of the media; and subsurface flow conditions (Feenstra and Cherry 1988). A cross-sectional schematic of the distribution of organic chemicals resulting from a release of a DNAPL is depicted in Figure 5-1. DNAPLs percolate through the unsaturated (vadose) zone due to gravity effects leaving behind trapped DNAPL globules and volatilized constituents in the gaseous phase. Some lateral spreading occurs due to the effect of capillary forces (Schwille 1988) and due to slight media heterogeneity in the vertical dimension (layering). Similarly, as enough DNAPL is introduced to the medium it can move through saturated zones leaving behind trapped globules (residual saturation). This entrapment process is due to interfacial tension effects and thus capillary forces. The residual DNAPL can solubilize into water moving through the saturated zone forming a contaminant plume downstream, and due to their low water solubility can serve as a long-term source. Eventually, large DNAPL volumes migrate down to a zone that has much lower permeability than the zone in which it resides. Therefore, it spreads horizontally on top of this finer medium until equilibrium conditions are achieved. This resulting zone of contamination consists of high saturations of DNAPL (approximately 50% of the pore

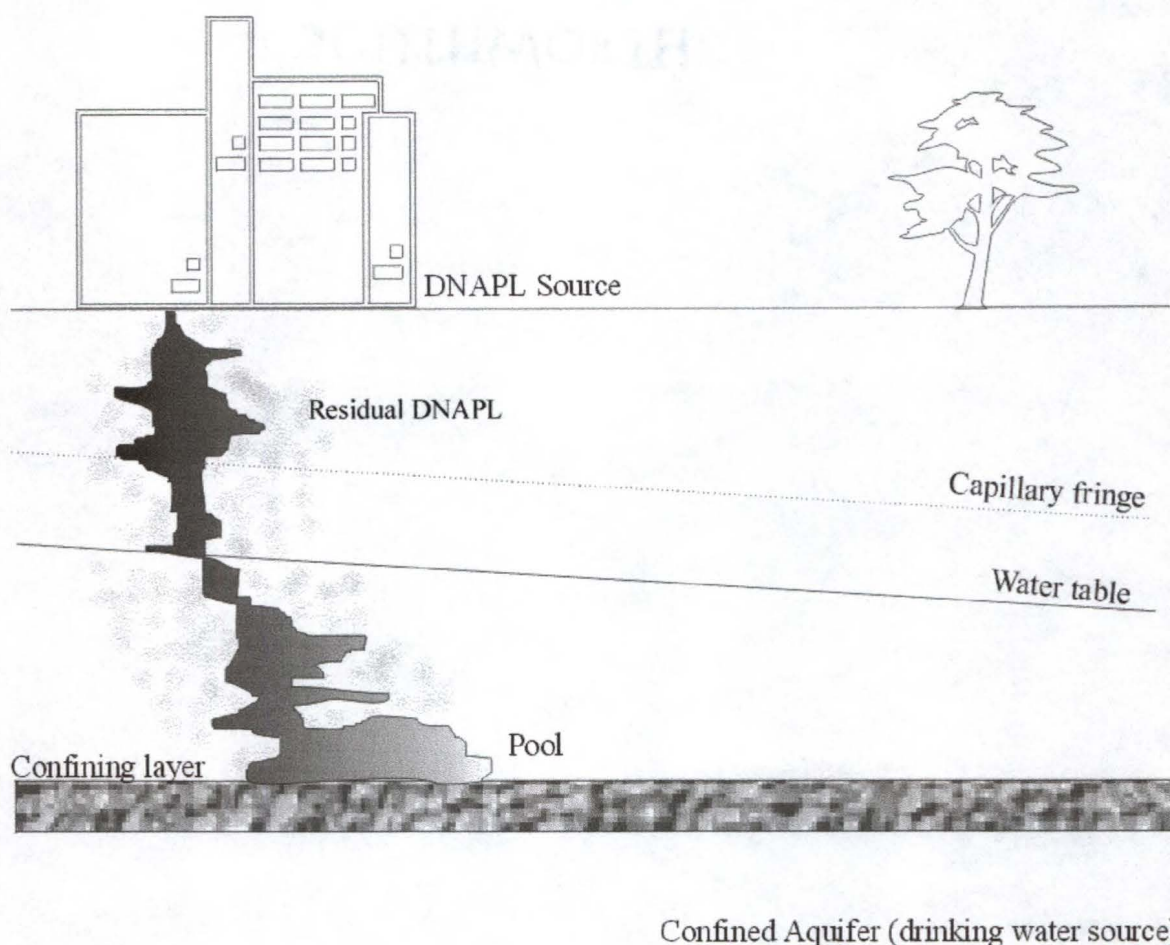


Figure 5-1. Schematic of DNAPL contamination of subsurface aquifer systems, showing free phase and residual DNAPL.

volume), high enough to be considered “pooled” on top of the finer, NAPL capillary barrier.

This process is understood very well conceptually. A good discussion is found in McWhorter and Kueper (1996). It is clear that the maximum capillary pressure occurs at the base of a DNAPL pool. This pressure is directly proportional to both the pool thickness and the density difference of the two fluids. The DNAPL accumulates above the finer layer since the capillary pressure due to the pool does not exceed the displacement

pressure of the "aquitarde." Entry of the DNAPL into the less permeable finer layer is given by (McWhorter and Kueper 1996),

$$\Delta\rho g t = p_d \quad (5-1)$$

where $\Delta\rho$ [ML^{-3}] is the density difference between the DNAPL and the fluid resident in the smaller pores below, t is the pool thickness [L], g is acceleration of gravity [LT^{-2}], and p_d is the displacement pressure of the finer layer [$\text{ML}^{-1}\text{T}^{-2}$]. Converting pressures to head leads to the following equation,

$$\frac{\Delta\rho t}{\rho_{dnapl}} = h_d^{cs/dnapl} \quad (5-2)$$

where ρ_{dnapl} is the density of the DNAPL upon entering the finer layer and $h_{d,cs/dnapl}$ is the displacement head of the finer layer when DNAPL is displacing cosolvent filled pores.

This value, $h_{d,cs/dnapl}$, can be determined via,

$$h_d^{a/w} \frac{\gamma_{cs/dnapl} \cos\theta_{cs/dnapl}}{\gamma_{a/w} \cos\theta_{a/w}} = h_d^{cs} \quad (5-3)$$

where $h_d^{a/w}$ is the air-water displacement head and θ is the contact angle of the fluid pair.

Note that the ratio of contact angles is approximately unity. This is thought to not contribute significantly for these estimations and is therefore excluded. However, as complexity is introduced by in-situ flooding chemicals and their associated chemical and physical properties, the movement of contaminant becomes more difficult to predict. This is especially true when dealing with extremely heterogeneous media, or even a simple one-layered system.

Prediction of DNAPL mobilization into and through an underlying finer medium is desired before a specific flushing strategy is proposed, or even employed at a remediation site. Cosolvents, such as ethanol, are used to increase the rate of dissolution of the contaminant pool and associated residual zones into the flushing alcohol mixture. However, concurrent interfacial tension reduction can become severe, especially at high alcohol volume fractions, allowing DNAPL to mobilize out of pores it was previously entrapped in and enter smaller pores. If the IFT and buoyancy forces are severe enough, this may allow the DNAPL to enter the smaller pores of the underlying "less-permeable" layer upon which it originally was pooled. Predictions of the difference in permeability (pore size) required to prevent entry into a finer layer, under specific flushing regimes would be beneficial. Thus, a systematic approach of determining DNAPL entry into an underlying finer layer, using a 2-D box setup with known media sizes, is warranted. Basic force balance calculations exist to mathematically predict whether entry into smaller pores is possible. Visualization and thus verification of this is not possible in the field, so use of 2-D setup is justified further.

Two-dimensional studies of removal of NAPL from porous media have been published. Numerous studies exist which focus on the flow instabilities resulting from density and viscosity differences, especially in historic petroleum recovery journals (Morrow and Songkran 1981). More recently and more applicable to this study, Jawitz et al. (1998a) examined the flow instabilities resulting from density and viscosity contrasts between resident and displacing cosolvent (ethanol). They concluded that the presence of a capillary fringe and subsequent trapping of cosolvent contributed to the its inefficient removal from the aquifer. However, no NAPL was present to determine possible

mobilization or impact on flow paths. Other studies on effects of heterogeneities and instabilities are Kueper and Frind (1988), Held and Illangasekare (1995), and Illangasekare et al. (1995). Additionally, studies on dissolution of residual NAPLs have been published, including Gellar and Hunt (1993), Miller et al. (1990), and Powers et al. (1994). Dissolution of pooled DNAPLs was investigated by Johnson and Pankow (1992). Grubb et al. (1996) investigated the removal of a light NAPL (LNAPL), toluene, using a combined pure and 50/50 (vol. %) ethanol-water flooding strategy. Downward mobilization of the LNAPL below the lighter overriding flushing phase eventually resulted in trapped LNAPL. The use of the heavier 50/50 mixture subsequently removed this zone via solubilization and physical displacement. Pennell et al. (1996a) qualitatively studied the dissolution of PCE and the downward movement of a DNAPL pool in sand and aquifer material while flushing with surfactant solutions. They concluded that mobilization of DNAPLs via surfactant flooding should be avoided and dissolution of DNAPLs should be the primary removal mechanism.

In summary, little research has been published on a systematic experimental approach to predict and verify mathematical relationships describing NAPL (and more specifically DNAPL) entry into finer media under cosolvent flooding regimes. This was the focus and objective of this research. The methods and results are discussed below.

Materials and Methods

A 2-dimensional (2-D) box, previously constructed by Jawitz (1998a), was used for this study. The overall dimensions of this box are 61 cm in width, 39.4 cm tall and 1.4 cm thick. The inlet and outlet wells were square aluminum tubes, with 0.05 mm slots

spaced at 5 mm intervals. The bottom of the box was the same aluminum tubing, without any perforations. Together, this aluminum square tubing made up both sides and the bottom of the 2-D box. Clear glass, matching the dimensions of the tubing layout, was used and was 0.5 cm thick. The 1.4 cm thickness of the 2-D chamber was over 16 times the largest grain size used in these studies. This thickness was chosen by Jawitz et al. to minimize wall effects (1998a). Similar to their studies and the studies of Schincariol and Schwartz (1990), dye traveling only in the first few grain diameters against the glass would appear lighter in dye color than the bulk front.

General Packing Procedure

Nanopure water, adjusted to pH 8, was added to the box and the box leak checked. The pH adjustment was necessary to minimize adsorption of the Brilliant Blue FCF dye (Erioglaucine A, CAS 94082765, Fluka Chemical, Ronkonkoma, New York) to sand used in these studies (Jawitz et al. 1998a). Flury and Fluhler (1995) found that as pH increases Brilliant Blue FCF dissociates to a mono- and eventually to a bivalent anion ($pK_{a1} = 5.83$ and $pK_{a2} = 6.58$). This pH adjustment ensured that the dye would be in the bivalent anionic form, which minimized adsorption to the sand used. Brilliant Blue FCF has low adsorption (K_d of $0.19 \text{ dm}^3/\text{kg}$) in soil with low organic carbon content (0.43%) and a soil pH of 5.8 (Flury and Fluhler 1995). Number 20-30 Ottawa Sand (U.S. Silica) was used as the constant background media for all 2-D experiments. This media was sieved out of the bag and no further treatment was necessary for these investigations. The coefficient of uniformity is estimated to be 1.2 and the manufacturer reported the roundness and sphericity coefficients of 0.8-0.9 for this sand (Grubb et al. 1996). The sand can therefore be classified as rounded-subrounded. This was added to the box in a

layered fashion (each layer approximately 2 cm thick), with vibration applied at the end of each layer addition. Note all packing was done under water wet conditions. The subsequent layer was then added and mixed with the upper portions of the previous layer to minimize layered effects. This was continued to a depth of 3.3 cm from the bottom of the box. Then a 1 cm thick lens of finer media (this media size varied) was added. Application of this finer media within 5 cm of either well screen was avoided due to possible grain loss through the well screen, especially for the finer media. Upon vibration, this settled and spread to a distance of approximately 3 cm from either well. Again, the background No. 20-30 media was added in layers, vibrated, and mixed up to a total depth of 11 cm. This packing procedure was repeated for each scenario to provide as much hydraulic and media consistency possible. This packing method resulted in a pore volume of 325-330 ml, and a porosity of 0.35. These figures were constant over all packing combinations as the finer layer contributes little to the total 2-D box parameters. The following sand sizes were used for the fine media: Nos. 100-140; 60-70; 40-50; and 30-40. The particle sizes of the sands used are shown in

Table 5-1 for reference. A typical box configuration prior to flooding is shown in Figure 5-2.

Table 5-1. Particle size ranges of sands used.

Sand Mixture (Sieve Numbers)	Maximum particle diameter (mm)	Minimum particle diameter (mm)
20-30	0.841	0.595
30-40	0.595	0.420
40-50	0.420	0.297
60-70	0.250	0.210
100-140	0.149	0.105

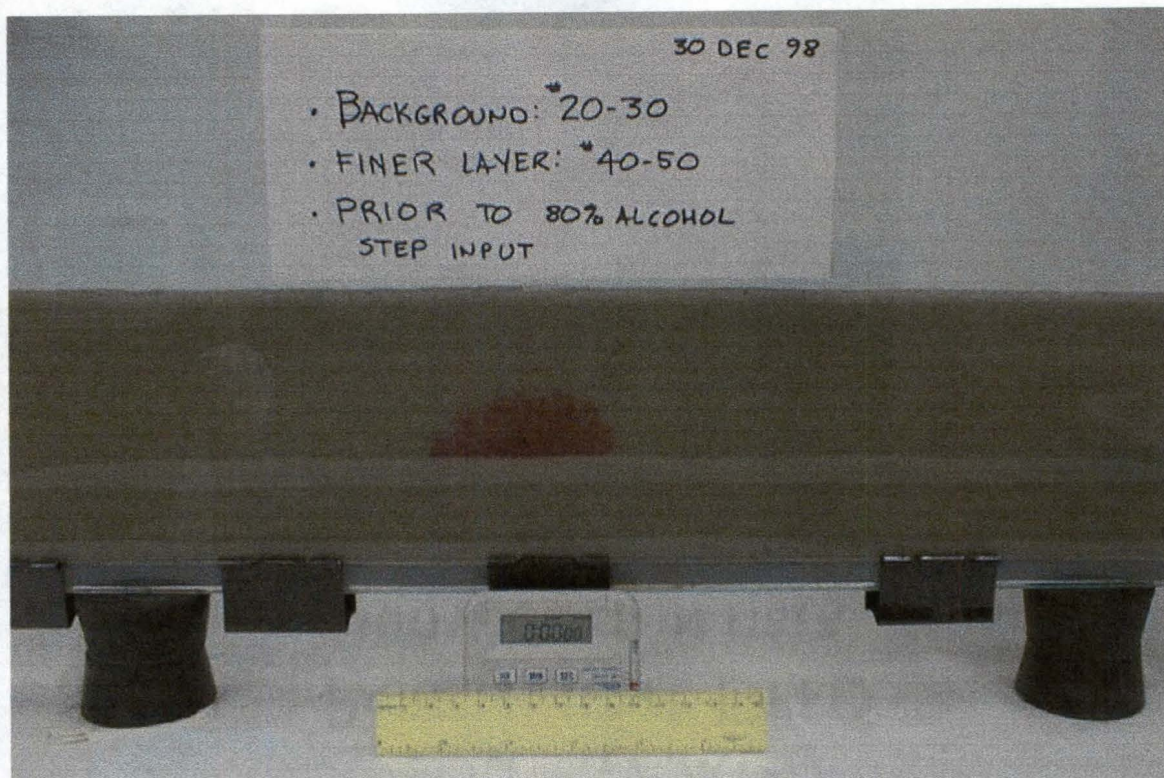


Figure 5-2. Typical 2-D box setup after injection of PCE, prior to any flushing.

Dye Tracer Displacement

To determine the hydrodynamic characteristics of the 2-D flow system, and to qualitatively visualize the baseline flow patterns, 30-50 ml of the Brilliant Blue FCF dyed water (approximately 50 mg/l) was injected into a colorless, water-resident medium at a flowrate of 3.5 ml/min (5.0 ml/min for Runs I and II). This was subsequently flushed through the box with colorless water under controlled hydraulic conditions, similar to those used during actual flushing runs. This concentration of dye results in a density increase of 0.005% (Jawitz et al. 1998a). A flow rate of 3.5 ml/min equates to a horizontal flow velocity of 9.7 m/day (13.9 m/day for Runs I and II). For all experiments, the profile of the dye front was traced at generally 5 minute intervals, as the front moved across the flow chamber. As in Jawitz et al. (1998a), the mixing zone at the interface

between the colorless resident fluid and the dyed displacing fluid was generally less than 1 cm wide. In situations when the mixing zone had a width of more than 1 cm, the location of the front was concluded to be at the center of the visible mixing zone. This was accomplished to determine background flow profiles to eventually compare them to profiles with DNAPL pools present.

DNAPL Introduction

HPLC grade PCE (CAS 127-18-4), colored red with Oil-red-O dye ($\leq 1 \times 10^{-4}$ M, CAS 1320-06-5) was injected into the sand media approximately 1 cm above the fine layer, using a 16 gauge long stainless steel needle, attached to a 20 ml glass syringe. The rate of injection varied due to difficulties with PCE traveling back up the needle to the sand surface. This was minimized by vibration of the media around the needle after insertion. However, DNAPL zone shapes and saturations were reproduced in a visually consistent manner via this method. Generally 2.7 to 3.5 ml of PCE were injected and remained in the media. Any PCE on top of the sand media was removed by suction.

Hydraulic Controls During 2-D Box Experiments

The influent was maintained at constant head with a Marriott Bottle, with the head adjusted to maintain the water table right at the surface of the sand media. The effluent flow was maintained by a Master Flex pump at 3.5-5 cm³/min. The flowrate was determined to avoid total well desaturation, depending on the maximum viscosity expected from the flushing fluid. The influent line was split by a nylon T-valve to provide for easy switching of injection fluids.

At least one pore volume of background water was passed through the media to establish hydraulic equilibrium. 30 to 50 ml of dyed flushing phase was then injected with

a Harvard 22 syringe pump at a flow rate equal to the effluent rate. This was done to provide visual detection of flushing front and override characteristics. Flow was then switched over to non-dyed flushing fluid. The alcohol used as the cosolvent in all flooding studies was reagent grade alcohol (Fisher Scientific; 90.4 vol. % ethanol, 4.6% methanol, 5.0% isopropanol). The reagent alcohol was assumed to have the same properties as pure ethanol (Grubb et al. 1996). Isopropanol and methanol should have minor and compensating effects on mixture equilibria (Sorenson and Arlt 1980).

Results and Discussion

For all floods described below, steady state flow conditions were established prior to injection of tracer or alcohol. All experiments were conducted at a room temperature of $23 \pm 1^\circ\text{C}$. Between each run that used the same 2-D packing, at least five pore volumes of water was flushed to remove all quantities of alcohol from the sand media. Run summaries are presented in Table 5-2.

No. 100-140 Fine Layer

Step input of 100% alcohol

The DNAPL volume was 2.7 ml. The original DNAPL zone shape can be seen in Figure 5-3. 100% reagent alcohol was used as the flushing agent. This was done to provide a worst-case scenario for this media combination. At roughly one-third of a pore volume, collapsing of the DNAPL pool was noticeable, as IFT's were being reduced and mobilization of high saturations was possible.

Table 5-2. Summary of Experimental Runs in 2-Dimensional Box Studies

Run Number	Finer Layer Sieve Size (No.)	Volume PCE Injected (ml)	Flushing Mode	Alcohol Concentration (%v/v)	Entry into finer layer?	Remarks
I	100-140	2.7	Step	100	Yes ⁽¹⁾	(1) along front only
II	100-140	3.2	Step	80	No	
III	60-70	4.8	Step	80	No	
IV	60-70	3.1	Gradient	10 - 90 (1 PV)	No ⁽²⁾	(2) PCE did appear below finer layer
V	40-50	3.3	Step	80	No	
VI	30-40	3.9	Step	80	Yes	
VII	30-40	3.0	Step	70	Yes	
VIII	30-40	3.2	Multi - Step	50; 60; 80 (1 PV ea)	No; No; No ⁽³⁾	(3) Reduced DNAPL Saturation
IX	30-40	3.3	Step	30 TBA	Yes	Movement of PCE more lateral due to lower density
X	100-140	3.2	Step	40 TBA	No	Significant swelling

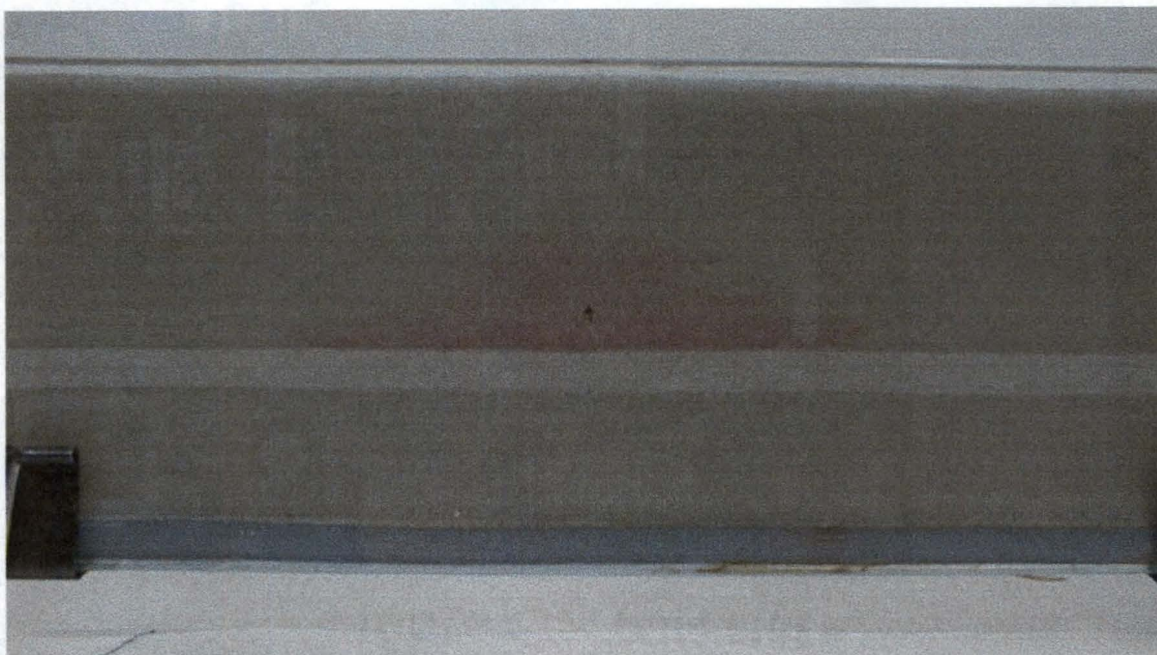


Figure 5-3. Dyed PCE injected into Number 20-30 medium (approximately 2.7 ml) pooled over a 1 cm layer of Number 100-140 medium.

Solubilization diminished the size of this zone and light red 'streams' developed downstream. This reddish color is due to slight partitioning of the Oil-red-O dye into the flushing phase. Partitioning of the dye becomes increasingly possible due to the high amounts of PCE solubilized into the alcohol (>200,000 mg/l). This "banding of dye" has been seen several times in one-dimensional columns and generally occurs when 80 to 85% alcohol is used as the flushing phase. Due to dilution, this rough concentration can occur ahead of the 100% alcohol front. The equilibrated volume fractions resulting from this mixture from bulk studies is approximately 60% alcohol/28% PCE/12 % water.

By 40 minutes into the flush (0.62 PV) further collapse of the pool down onto the finer 100-140 layer resulted in a layer of DNAPL ranging from 0.4 to 0.5 cm in thickness. This pool was most prevalent ahead of the original pool area and spread downstream as a function of time. As the PCE-alcohol IFT was decreasing, DNAPL from upstream

portions of the original pool (above residual saturations) mobilized quickly in the coarse medium, in a direction along the alcohol front and eventually into the finer layer. This phenomenon will be hereafter referred to as "frontal mobilization". This was noticed as early as 31 minutes into the run (~ 0.5 PV). This mobilization occurred in a very thin stream, most likely due to the very sharp interface between the displacing alcohol and the resident water, which is on the order of tenths of centimeters (Grubb et al. 1996). Similar "frontal mobilization" observations have been made by others (Grubb et al. 1996; Pennell et al. 1996b), where DNAPL flows downward due to remaining higher density, yet seeks pores of reduced IFT and thus can flow back against the hydraulic gradient. Further breakthrough of PCE into the finer layer occurred 36-38 cm from the injection well at $t=50$ minutes (0.77 PV). This occurred when the alcohol front had sufficiently passed into the finer layer underneath, allowing mobilization into the finer pores.

One-dimensional horizontal sand column experiments

To better understand flow behavior of residual DNAPLs under the presence of alcohol containing cosolvents, 1-D sand columns were brought to residual saturation with dyed PCE. The procedures and setup for this are explained in Chapter 3. The column was turned horizontal and alcohol injected from left to right (see Figure 5-4). Gradient ethanol injections of 0 to 100 % v/v ethanol over one pore volume were used in an attempt to minimize override. As can be seen in Figure 5-4, this had little impact and override of the cosolvent still occurred. This is due to not only density difference, but also the eventual contrast in relative permeability caused by the downward moving DNAPL. High saturations of PCE developed near the cosolvent interface and globules could be

seen to move diagonally downward along the interface. Eventual pooling developed along the bottom and near the inlet end of the column (Figure 5-4).

This appears to support what occurs when DNAPL saturations are above residual quantities, as the case in the 2-D box experiments. The higher saturation or pooled scenario would be expected to behave similarly, if not in a more dramatic fashion.

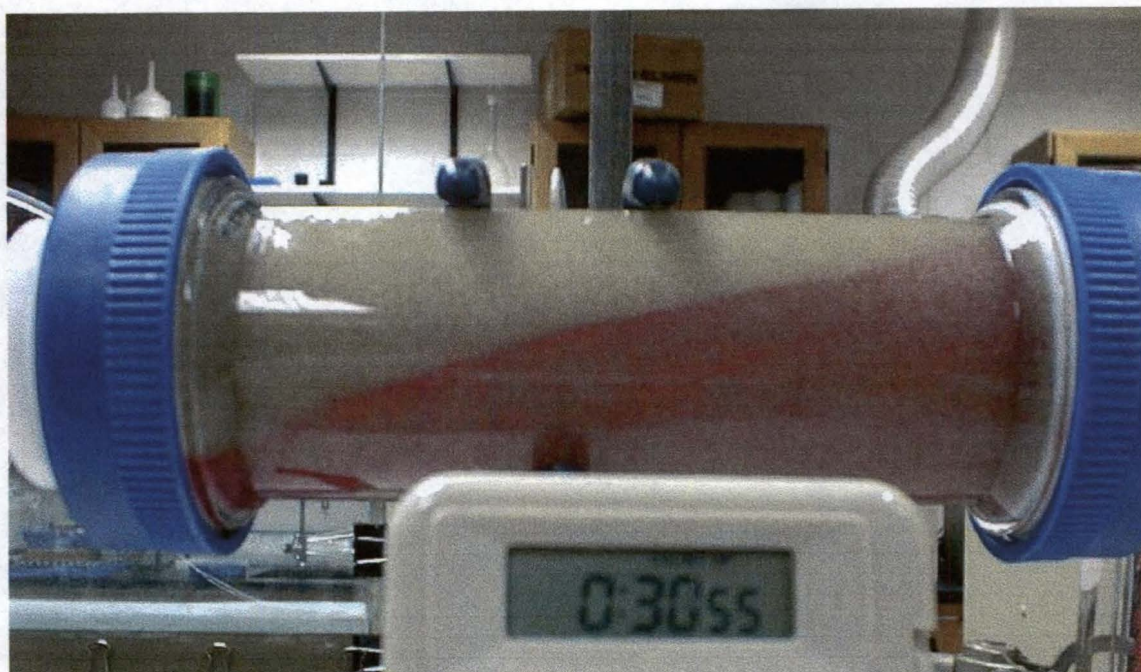


Figure 5-4. Removal of residual dyed PCE by gradient ethanol injection (0-100% v/v) over one pore volume. Darker band at interface is highly saturated PCE which is mobilizing toward the lower left and pooling.

Step input of 80% alcohol

3.2 ml of PCE was injected as described in procedures above. No mobilization of DNAPL was observed during this entire run. Very clear progression of pool collapse occurred as shown in

Figure 5-5, eventually resulting in an extended pool thickness of 0.2

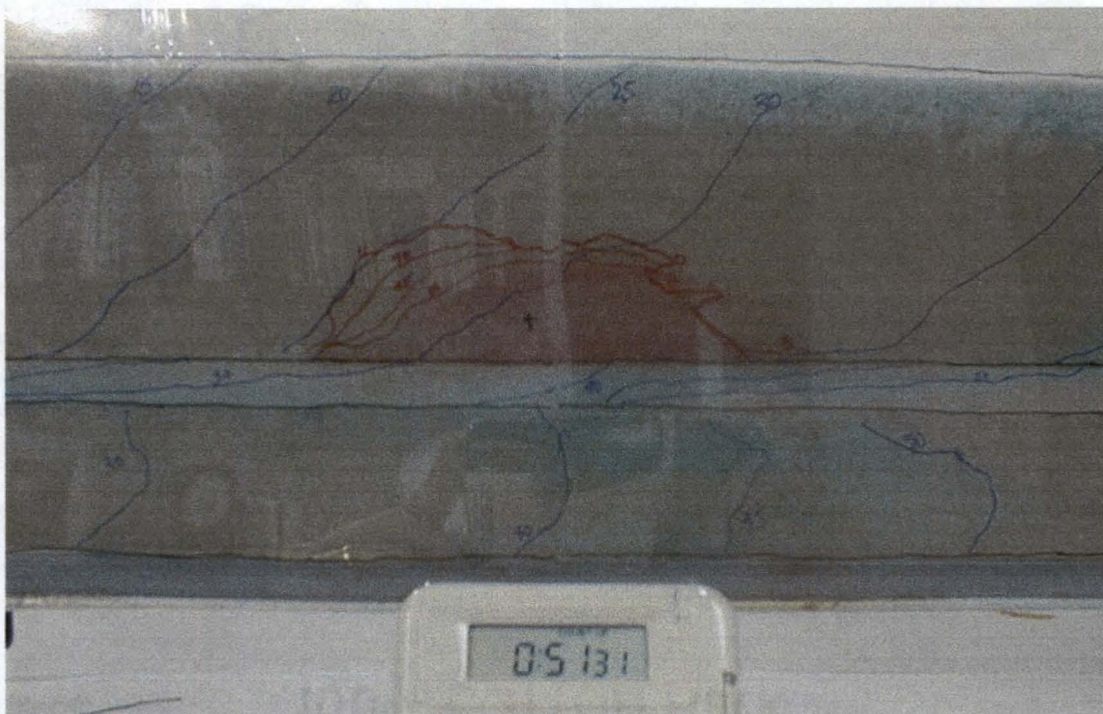


Figure 5-5. Progression of DNAPL pool collapse – Nos. 20-30 background medium, Nos. 100-140 finer layer - after 0.8 PV of 80% v/v ethanol/water step input. Downstream direction is to the right in all pictures.



Figure 5-6. Spreading of DNAPL pool downstream on top of finer Nos 100-140 layer. No breakthrough occurred during this run – 1.1 PV after 80% v/v ethanol/water step input.

to 0.4 mm. The spreading of the pool occurred only downstream of the injection zone (Figure 5-6). No upstream spreading of the DNAPL was observed.

No. 60-70 Fine Layer

Step input of 80% alcohol

Based on the lack of mobilization into the 100-140 layer using an 80% alcohol step input, the next scenario chosen was to flood using the same flushing fluid, but decrease the contrast between the bulk and finer layers from Nos. 20-30 vs. 100-140 to Nos. 20-30 vs. 60-70 mixture. 4.5 ml of PCE was injected for this run. Collapse of the pool occurred with upstream mobilization on top of the finer 60-70 layer. The pool spread approximately 6 cm toward the injection well and 25 cm downstream from the injection zone, eventually draining off the edge and flowing vertically downward due to density differences. This occurred only in this scenario; most likely due to the increased amount of PCE injected (4.5 ml). However, no entry of free phase DNAPL was observed into the finer layer. See schematic of run in Figure 5-7.

Gradient Injection (10-90%) of Alcohol

Initial 2-D box trials were conducted using a similar setup to determine the overall benefits of gradient injection of alcohol over step input to 100% alcohol. However, no finer layer was present, in the bulk 20-30 sand medium. Increased mobilization of DNAPL was observed during the gradient injections than with the step input to 100% alcohol. A conclusion made was that interfacial tension was quickly decreasing during gradient injection, yet the cosolvent's ability to solubilize PCE was not keeping pace

STEP INPUT 80% ALCOHOL
20-30 BACKGROUND
60-70 FINE LAYER

- DUMP
- SHEARING POOL
- ALCOHOL FRONT

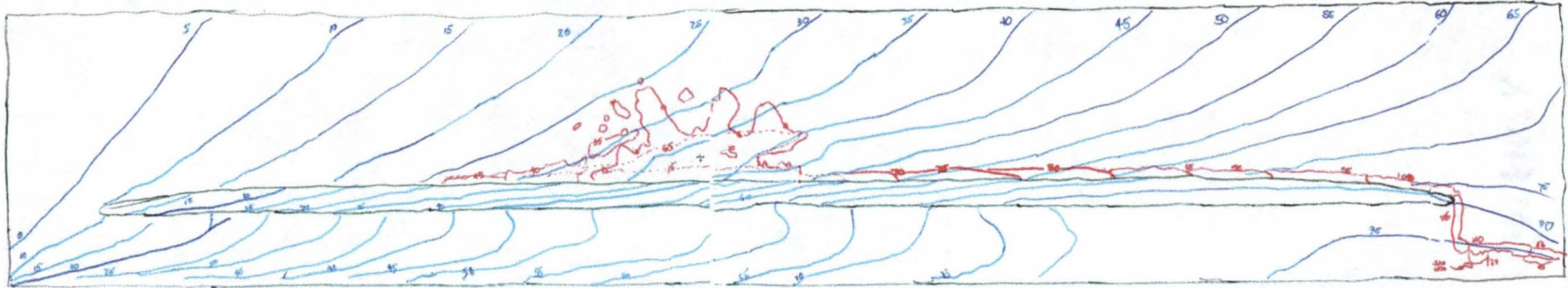


Figure 5-7. Schematic of step input of 80% alcohol - No. 60-70 finer layer.

with the falling IFT. In the case of a step input, although IFTs are very rapidly reduced, the capacity of the pure alcohol solution to solubilize PCE overwhelms the IFT reduction. Essentially the saturation of DNAPL reduces faster due to solubilization, quick enough to prevent mobilization. This preliminary conclusion was tested again with the 2-D box setup described here.

A DNAPL volume of 3.1 ml was injected into the 20-30 medium, resting on a 60-70 medium. A gradient injection from 10% -90% (v/v) alcohol was applied over 1 PV into the 2-D box, using a Shimadzu HPLC pump with a solvent mixer. At 58% alcohol the alcohol influent line was switched over to a Brilliant Blue dyed 100% alcohol reservoir and not removed until 75% alcohol was injected into the 2-D box. The alcohol influent line was then returned to the clear 100% alcohol resulting in a blue band of alcohol phase representing a concentration range from 58 to 75% alcohol. Typical collapsing of the DNAPL zone was observed, with the most significant movement occurring under an alcohol concentration of approximately 50% by volume. Again, horizontal spreading was observed upstream, as well as downstream, from the injection zone as shown in Figure 5-8. Light red bands of PCE-containing alcohol entered into the finer media, moved through the layer and then exited into the coarser media below, where due to density override, lower alcohol concentrations are present (Figure 5-9). This results in PCE coming out of the flushing phase and reestablishment of a separate DNAPL phase (see Figure 5-10). This supports remediation designs that completely flood underneath the contaminant zone and supporting finer layer with 100% alcohol. Pre-established presence of pure alcohol would severely minimize this regeneration of a new DNAPL phase.

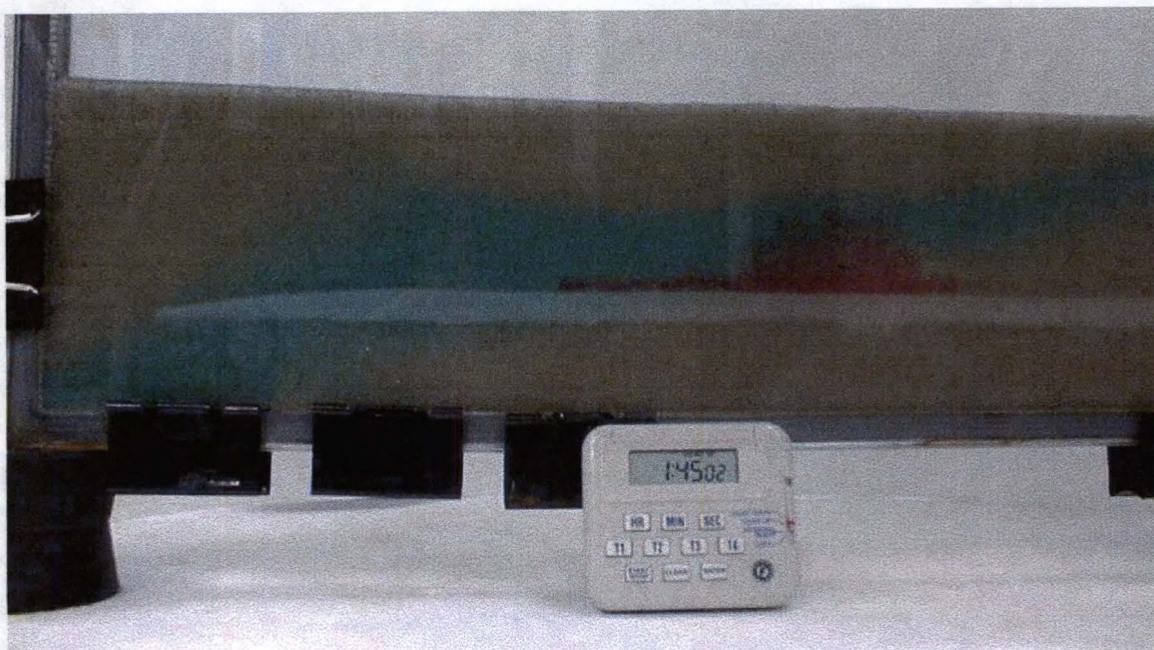


Figure 5-8. Horizontal spreading of PCE pool upstream from injection zone - Nos. 20-30 background media, 60-70 finer layer, 1.1 PV after gradient injection of 10 – 90% v/v ethanol/water over 1PV. Blue band is location of 58% (leading edge) to 76% ethanol

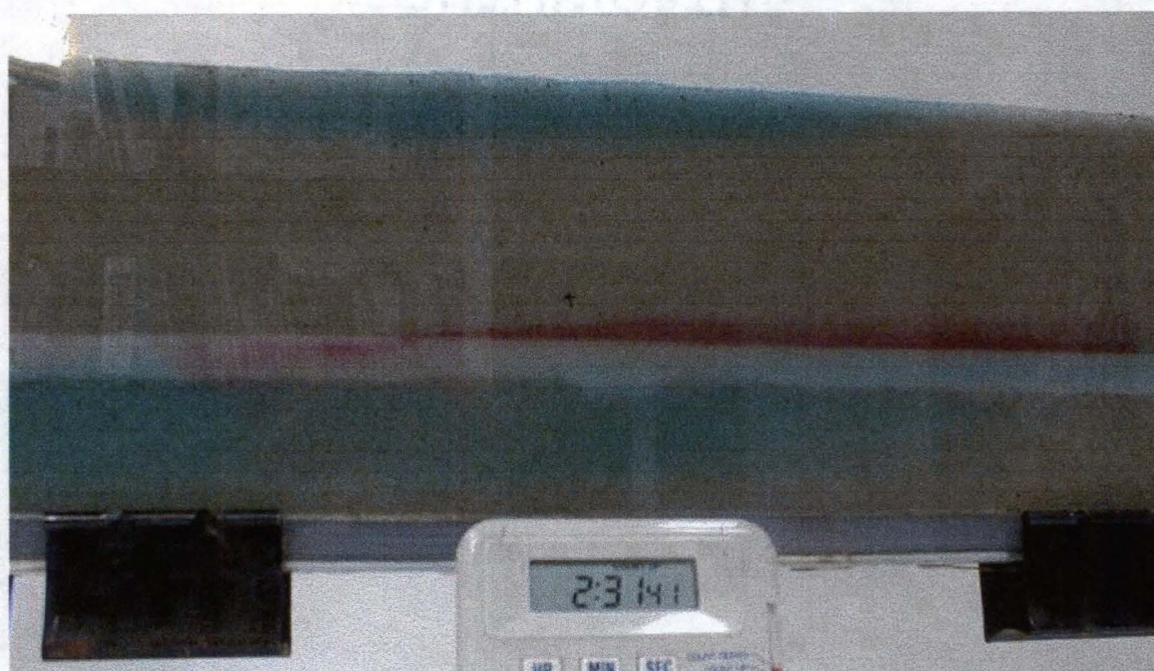


Figure 5-9. Highly concentrated cosolvent phase in which dye has partitioned, entering finer Nos. 60-70 layer. This is not free phase mobilization. Blue band above is from a post gradient step input to 100% reagent alcohol

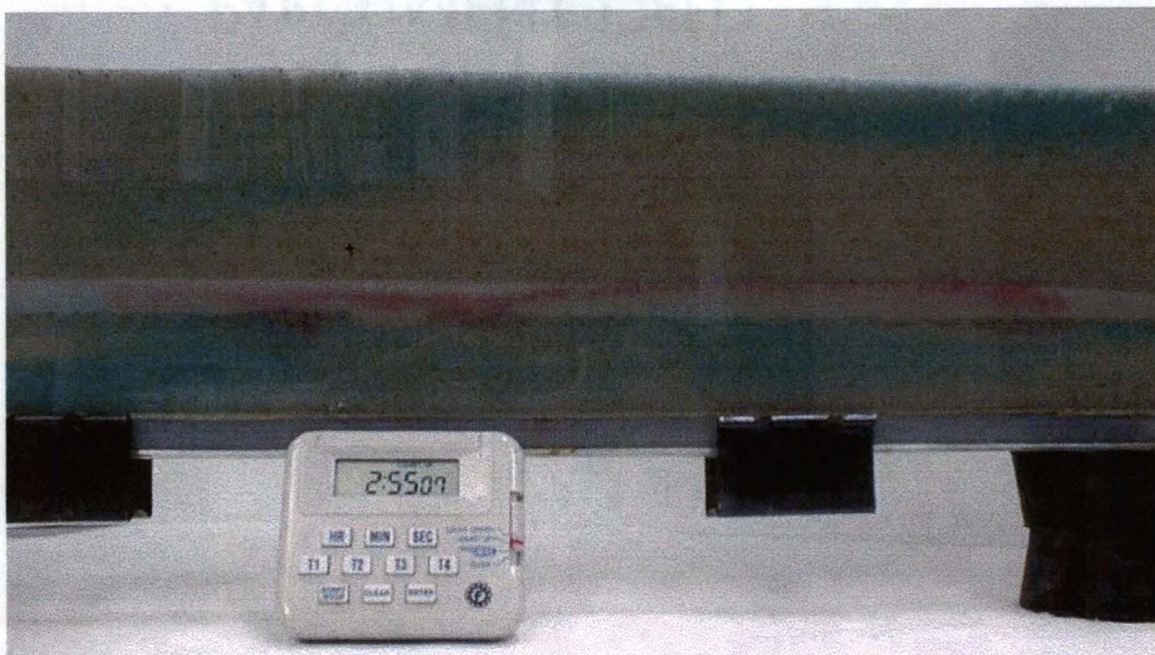


Figure 5-10 – Breakthrough of highly concentrated PCE containing cosolvent phase into finer layer and subsequent reestablishment of DNAPL below the finer layer due to lower alcohol concentrations.

No. 40-50 Fine Layer

Background dye flush after DNAPL injection

A total of 3.3 ml of PCE was injected for this run. Significant flow of flushing phase was observed underneath the DNAPL pool, which was not observed in previous runs. The permeability of the 40-50 layer was greater than the relative permeability of the DNAPL saturated zone. This caused significant flow of dye through the finer layer, underneath the DNAPL pool, instead of override as observed in previous scenarios, with finer, less permeable media (see Figure 5-11). Fronts in the finer layer lagged the front in the 20-30 media only by 10 minutes (0.1 PV).

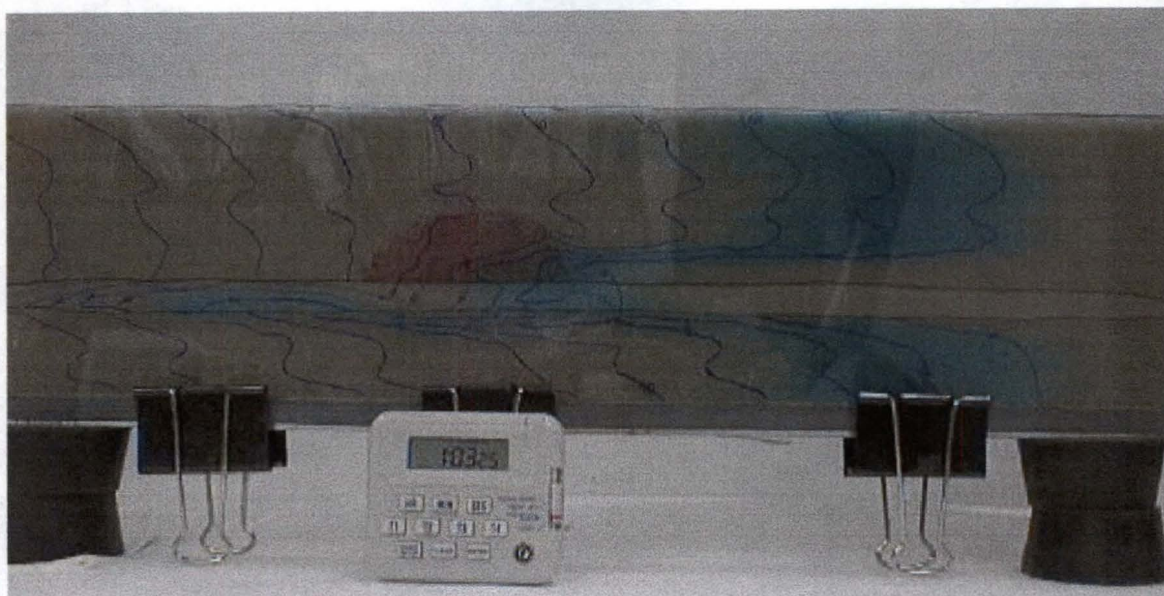


Figure 5-11. Water tracer study for 40-50 finer layer experiment. Note the significant holdup of tracer in lower portions of PCE pool and noticeable progression of dye in finer layer underneath.

Step input of 80% alcohol

Collapsing of the DNAPL pool occurred causing the PCE pool to spread approximately 4.2 cm upstream. The pool spread a total 17.5 cm downstream (see Figure 5-12). No mobilization of a separate phase occurred into the finer layer, although solubilized PCE does breakthrough into the finer layer and into the coarse layer below. However, no free phase PCE was generated below the finer layer.

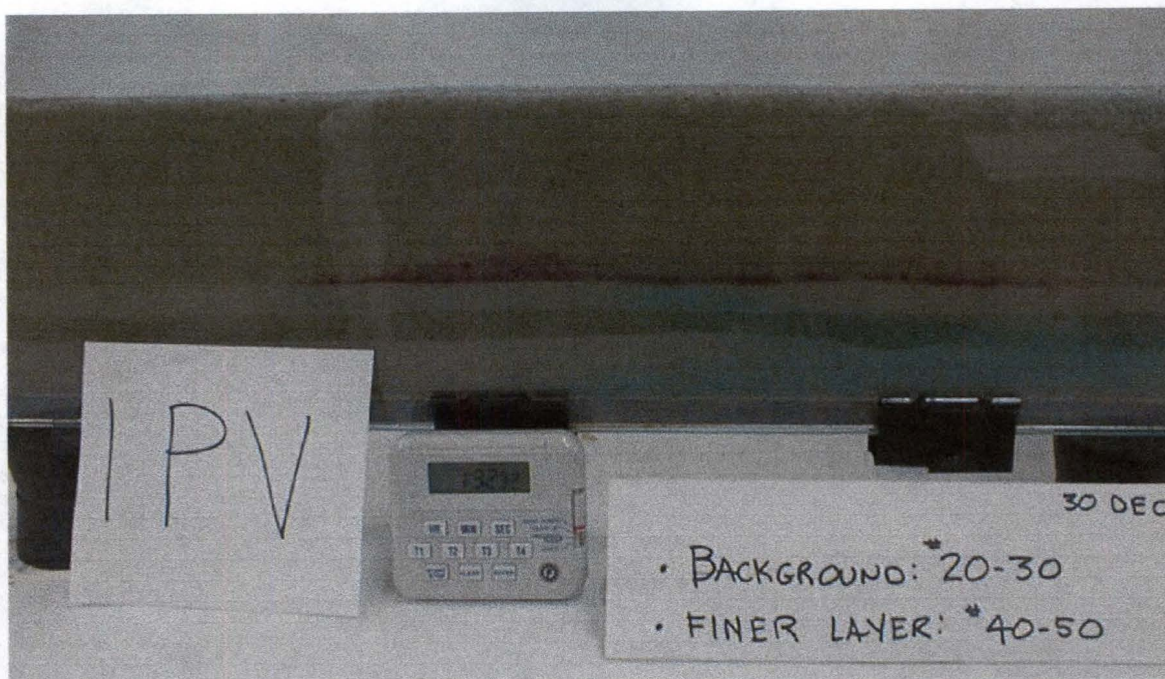


Figure 5-12. Collapsing of PCE pool and spreading of DNAPL along 40-50 layer. No breakthrough of DNAPL observed.

No. 30-40 Fine Layer

Step input of 80% alcohol

Mobilization occurred in three different locations. Two upstream (1.8 cm and 6.5 cm) from the injection zone and one downstream (6.4 cm) (see schematic in Figure 5-13). This movement through the finer layer, based on visual observations, was completely different from the solubilized movement shown above in Figure 5-9. True DNAPL mobilization occurs through one or two pores and networks downward due to gravity differences (see Figure 5-15).

STEP INPUT 80% ALCOHOL
20-30 BACKGROUND
30-40 FINER LAYER

- DWAPL
- SHELVING POOL
- ALCOHOL FRONT

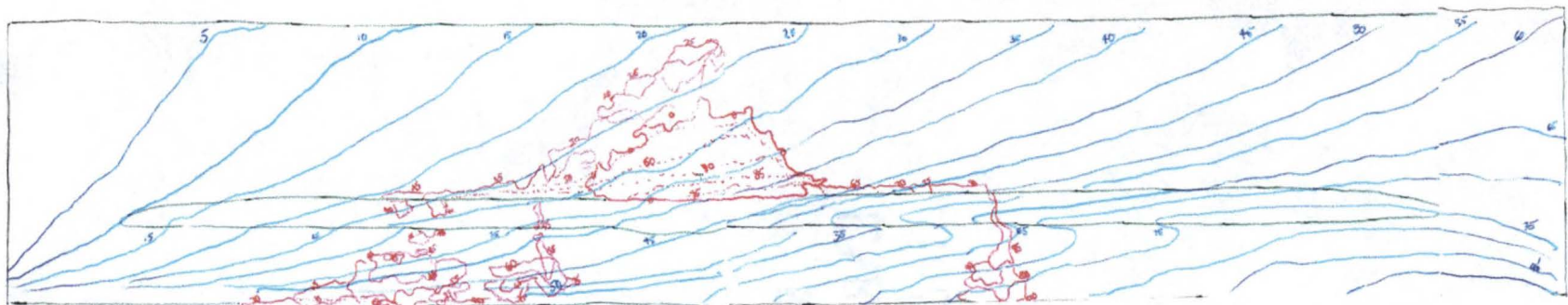


Figure 5-13. Schematic for step input of 80% alcohol – No. 30-40 finer layer.

STEP INPUT 70% ALCOHOL
20-30 BACKGROUND
30-40 FINER LAYER

- DWAPL POOL
- SHELVING POOL
- ALCOHOL FRONT
- BACKSIDE OF TRACER PULSE

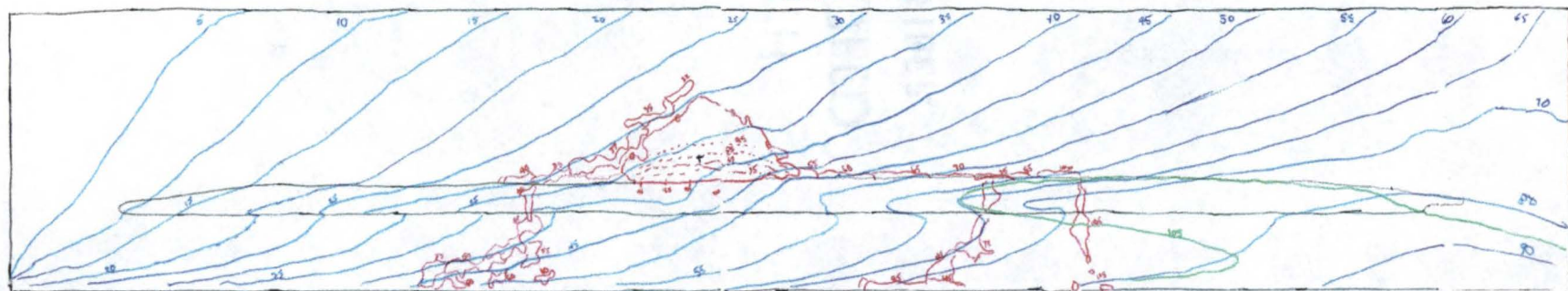


Figure 5-14. Schematic for step input of 70% alcohol – No. 30-40 finer layer.

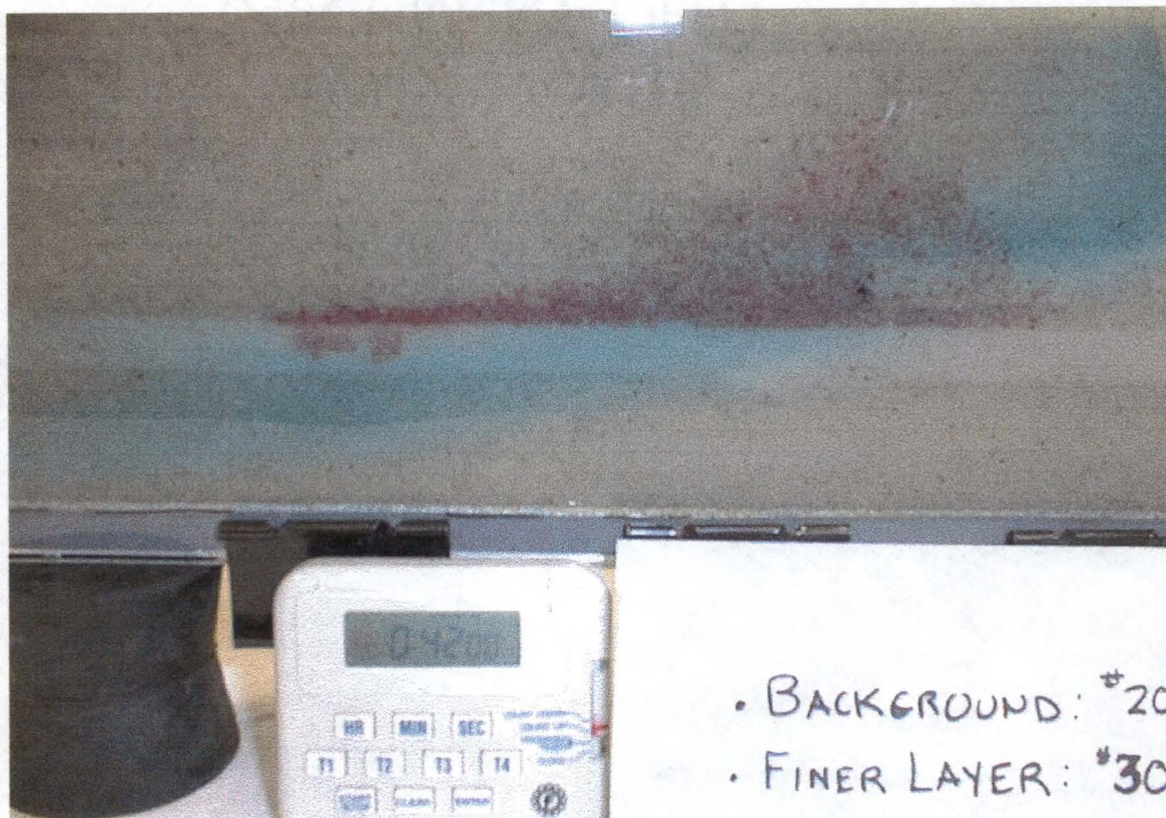


Figure 5-15. Mobilization of DNAPL into finer 30-40 layer at two locations, upstream from injection zone (small + mark in picture) – 0.45 PV after step input of 80% v/v ethanol/water mixture. Mobilization also occurred later at one other location downstream of pool (see text).

Step input of 70% alcohol

Similar to the 80% alcohol run, mobilization occurred in three different locations. However, only one was upstream (3.3 cm) from the injection zone and two downstream (7.4 cm and 10.9 cm). DNAPL globule mobilization was very similar to that of Run 7. One area of breakthrough into the finer layer match exactly with one from the previous run, indicating the possibility of one preferential channel at that location for this packing (see Figure 5-14).

Step input of 50% alcohol

As the injection alcohol concentration decreases, the solubilizing capacity decreases, and longer times are required to remove the DNAPL. However, initial upstream mobilization of DNAPL in the coarser layer, from the upstream side of the injected pool, occurred approximately at the same run times, during both the 80% or 50% alcohol step input. This indicates that the impact of IFT reduction is manifested earlier than the reduction in saturation due to solubilization. However, once immobilized on top of the finer layer, the IFT reduction is not severe enough within the smaller pores, and thus the capillary pressure within these pores is too great for the DNAPL to enter. Similar to previous runs, the lateral spreading of the PCE resulted in a DNAPL layer of 0.4 to 0.5 cm in thickness. After 1 PV of 50% alcohol the flushing concentration was step increased to 60% and flushed for another pore volume. This flushing was continued until this injected fluid saturated the finer layer and thus a similar prediction if mobilization occurred or not made. Mobilization did not occur even for this mixture. This additional pore volume of 60% alcohol reduced DNAPL saturation further due to slow solubilization. Another step increase to 80% alcohol was made to determine if this reduced saturation and thickness of DNAPL on top of the finer layer was still able to mobilize with the new 80% alcohol flushing mixture. No mobilization was seen during this step increase as well.

Two-Dimensional Studies with t-Butyl Alcohol

A swelling cosolvent, t-butyl alcohol (TBA), was chosen to evaluate its effects on DNAPL solubilization, mobilization, and breakthrough behavior in the 2-D environment studied above. Experimental setup, flow rates and head gradients were kept similar to those described above for the reagent alcohol studies.

Step input of 30% TBA: #30-40 finer layer

Dyed PCE (3.3 ml) was injected on top of the finer #30-40 layer. A step input of 30% v/v of TBA was applied to the box, removed at a flow rate of 3.5 ml/min, with the influent head maintained at the top surface of the sand medium. Entry of DNAPL into the finer layer occurred at 44 minutes (0.47 PV) as three fingers slowly progressed into the finer layer. Progression of DNAPL through the finer layer was noticeably different than that observed in the reagent alcohol experiments. Movement of the DNAPL fingers was slower in the downward direction and more lateral spreading occurred, most likely due to the lower density of the DNAPL (approximate equilibrated density of 1.53 g/ml) caused by the partitioning of the TBA cosolvent into the PCE phase. Similar increased lateral spreading was observed with DNAPL mobilization in the background 20-30 layer, both behind (upstream) and in front (downstream) of the original PCE pool.

The volume of the PCE/DNAPL pool did appear to attain a larger volume than in previous reagent alcohol runs. Even at larger runs times when significant solubilization has occurred, the pool volume remained larger than expected or observed in the reagent alcohol experiments. This is again due to the swelling of the PCE from the partitioning of the TBA (approximately 15% based on equilibrium studies).

At 215 minutes (2.3 PV) there still remained a noticeable pink aqueous phase in the upper right portion of the finer layer, indicating not all of the solubilized PCE had been removed.

Step input of 40% TBA: #100-140 finer layer

The 2-D box was repacked with #100-140 sand chosen as the finer layer. This was done to determine swelling effects of a higher percentage of TBA while maintaining

all of the DNAPL above the finer layer. This scenario would more closely represent those experienced in horizontal flooding field situations, where even a more impermeable clay layer is supporting a pooled DNAPL.

Some desaturation due to air bubbles occurred during packing, especially just above the finer layer. Water tracer runs were done (before and after the injection of PCE) to quantify the effects of this desaturation (see traces in Appendix B). The effects were significant enough to warrant overnight flooding of the box with de-aired water (approximately 7 PVs). This removed all visible desaturation except near the extreme downstream portions of the finer layer. This was not seen to cause significant problems to the further use of this packing, since the key observations are observed far upstream from this area.

A volume of 3.2 ml of dyed PCE was injected onto the #100-140 finer layer. The step input of 40% TBA was applied as previously described. Significant differences were observed in pool properties, even compared to the 30% TBA run. No entry of DNAPL into the finer layer was observed during this run. All DNAPL remained above the finer layer as desired. A definite downstream movement of DNAPL was observed, different from that previously observed for the reagent alcohol runs. This movement of DNAPL had more of a horizontal characteristic, due to a lower density contrast, compared to the reagent alcohol studies. The pool appeared to mobilize with large horizontal components until the density contrast became great enough for it to begin to move downward. This was apparently due to there initially being more water diluted pores below the DNAPL, then as the alcohol front entered the pores below the DNAPL at a later time (due to gravity override), the density contrast became great enough for more downward

mobilization. In the process of this “two-step” mobilization of DNAPL, quantities of injected cosolvent became trapped and isolated on top of the finer layer (see Figure 5-16). These pores required significant time to be flushed, due to the relative permeability to the wetting phase being so low around these areas. This can possibly lead to long tailing of PCE concentrations during the removal process. Periodic samples of the extraction well effluent were taken and stored for later analysis by gas chromatography. The results of this analysis were used to construct a breakthrough curve for PCE. This is shown in Figure 5-17.

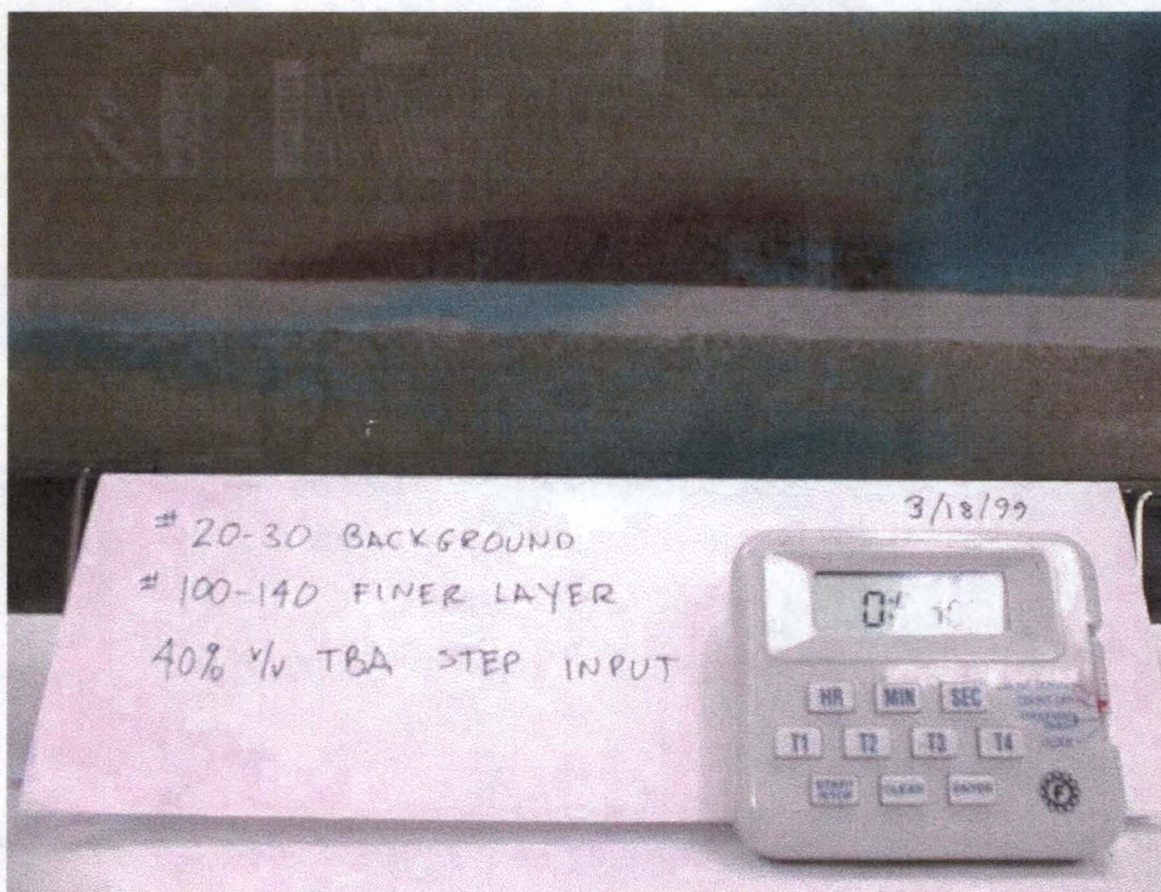


Figure 5-16. Mobilization of the PCE pool by a 40% v/v TBA cosolvent mixture (0.6 PV) resulting in the trapping of a volume of the cosolvent mixture on top of the finer layer.

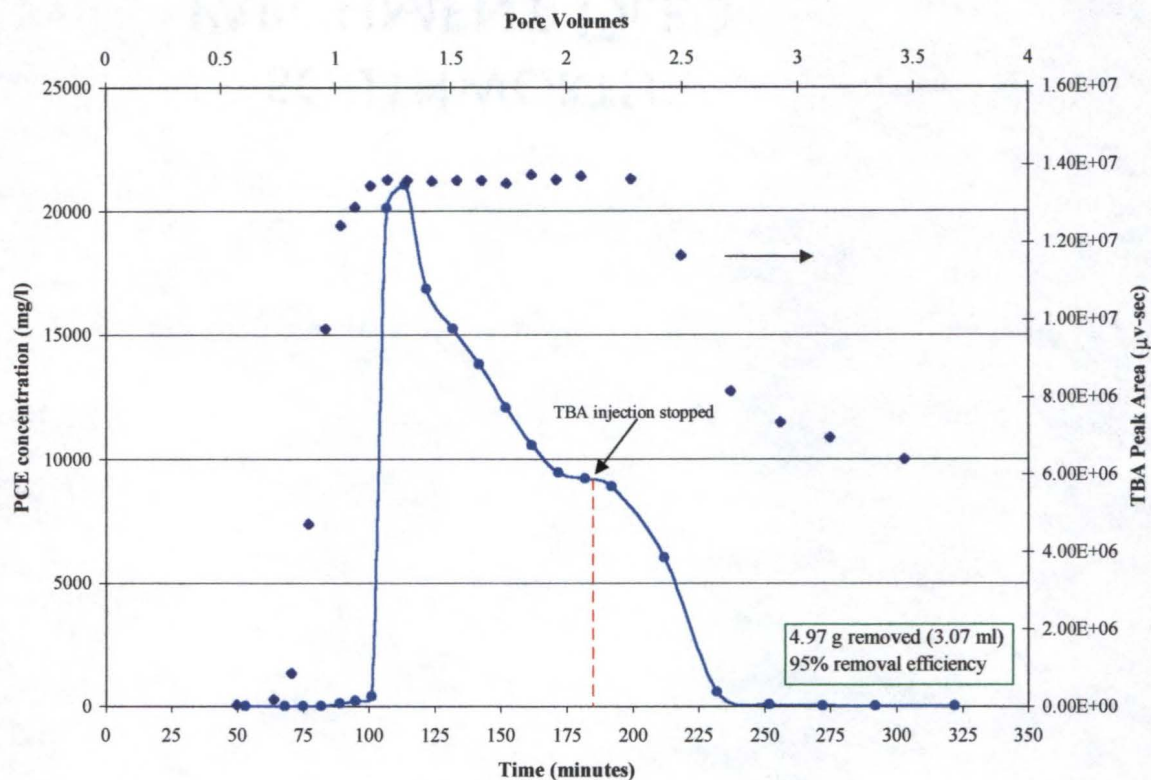


Figure 5-17. PCE and TBA elution profiles from 2D Box after a step input of 40% v/v TBA/H₂O. TBA profile data are shown as GC peak areas for reference.

Approximately 95% of the PCE was removed after just over 2.5 pore volumes of flushing. The linearly decreasing profile from 1.5 to 2 pore volumes is the result of gradual removal (via solubilization) of the swollen pool that has already collapsed and spread on the finer layer. Sequential removal of the upstream portions of the pool was observed. This removal process decreased the surface area of the entire pool available for mass transfer and could explain this gradual, yet consistent profile decrease over this period. PCE concentrations then leveled off for a short time period at about 2.0 pore volumes. This can be due to portions of trapped cosolvent (with high concentrations of solubilized PCE) finally becoming available for removal.

The swelling of the DNAPL pool was definitely observable as shown in Figure 5-18 and when compared to figures above for reagent alcohol experiments. Batch studies with 10 ml of 40% TBA/H₂O and 10 ml of PCE resulted in an equilibrated DNAPL volume of 13.5 ml, indicating a swelling of approximately 35%. Thus, the 3.2 ml originally injected could potentially swell to a volume of 4.3 ml. The volume shown in Figure 5-18 is difficult to estimate due to the variability of DNAPL saturation. However, a rough estimation of the entire bulk volume of the pool is 24 cm³, which assuming a porosity of 0.35, leads to a pore volume of 8.4 cm³. Assuming 50% DNAPL saturation would result in a final estimated DNAPL volume of 4.2 ml.

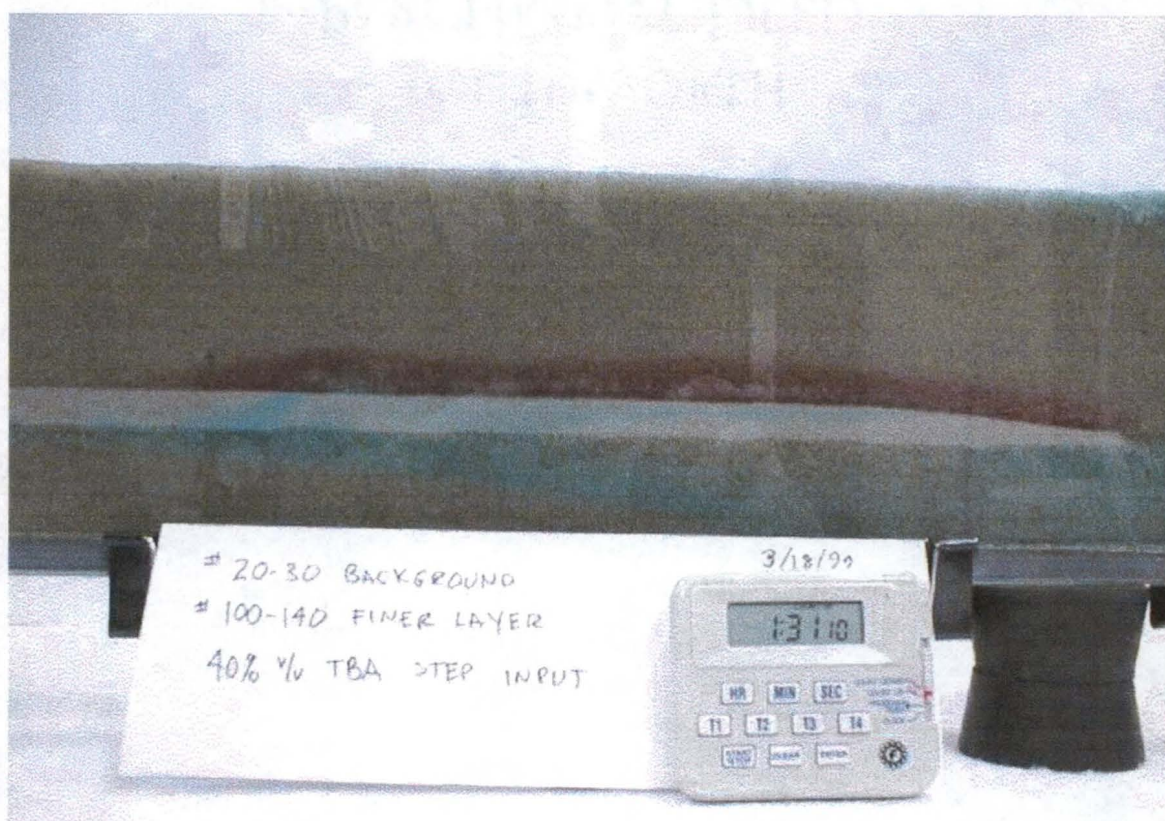


Figure 5-18. DNAPL pool shape after the injection of one pore volume of 40% v/v TBA cosolvent mixture.

The "two-step" mobilization process discussed above appeared to continue as the pool progressed downstream. As a result, a discontinuous thinner layer (0.4-0.7 cm thick) of DNAPL developed. This sub-layer of DNAPL was considered to be in direct contact with the pores of the finer layer, and used in the subsequent entry pressure calculations.

Systematic Quantitative Evaluation and Prediction of Mobilization into Finer Layers

To explain the above results and determine if their qualitative nature matched what can be estimated based on porous media physics and the hydrology of each scenario, calculations based on air entry pressures for each media used were accomplished. Air entry pressures were determined using Tempe Cells (Soil Moisture Equipment Corp., Santa Barbara, California). Total desaturation profiles were produced as a result of these measurements (Appendix A). The desaturation data were fitted with both Brooks and Corey (1964) parameters and those developed by van Genuchten (1980). Curve fitting was accomplished by minimization of the sum of squares of the differences between the data and the fitted prediction. Spreadsheet solver macros were used to iterate and arrive at a minimized error. The parameters resulting from these curve fits are presented in Table 5-3. DNAPL entry values were then calculated for each scenario based on the ratio of IFT of the fluids and the IFT between air and water measured with a du Nuoy ring tensiometer (72.1 dynes/cm). This then incorporates pore size into the calculation based on this entry value. The force balance associated with the entry pressure was presented in the introduction of this chapter. Entry of a DNAPL globule into the finer media can only occur if the head caused by the height of the globule can overcome the capillary head of

Table 5-3 – Summary of desaturation profile curve fitting parameters. Beit Netofa Clay values (α , n , and m) are from van Genuchten (1980). Pore radius for the clay is taken from Wise (1992).

Sand Mixture (Sieve No.)	Brooks-Corey parameters			van Genuchten parameters			
	λ	Air entry head, cm H ₂ O	Average pore radius, mm	α cm ⁻¹	n	m	Average pore radius, mm
20-30	4.67	7.02	0.174	0.11	11.0	0.91	0.166
30-40	3.22	10.6	0.108	0.075	10.2	0.90	0.115
40-50	4.33	18.7	0.0635	0.045	14.0	0.93	0.0659
60-70	9.33	26.9	0.0499	0.034	25.3	0.96	0.0504
100-140	9.99	50.7	0.0270	0.019	16.4	0.94	0.0277
Beit Netofa Clay				0.00152	1.17	0.15	0.00019

the pore below it in the finer layer. Note that densities and IFTs used in these calculations were determined by batch experiments reported previously in Chapter 2. This therefore assumes that these fluids have reached equilibrated values in the 2-D box at the time of possible mobilization. Although these parameters may not be exactly the actual values, differences would be slight and not significant to the decimal place of these predictions. For comparative purposes, the results of these calculations are shown in Table 5-4.

Except for runs V and X, all calculations accurately predict whether mobilization into the finer layer occurred. However, runs V and X cosolvent/DNAPL entry pressures into the finer medium ($h_d^{cs/dnapl} = 0.38$ cm and $h_d^{cs/dnapl} = 0.91$ cm) are well within reasonable errors associated with estimating DNAPL depth (h^{dnapl}) alone. No conclusion, one way or the other, can be convincingly drawn from these runs' estimates. The permeability estimates were made by averaging the results of three repetitions of the falling head technique through a 1-D sand column. Column, tubing, and valve resistances were separated from the media resistance by conducting "blank" falling head tests on the apparatus alone. Table 5-4 results indicate that breakthrough of PCE/DNAPL is not a sole function of permeability of the finer layer below the DNAPL pool. It is also a function of the cosolvent and the properties of the resulting solution that resides in the pores into which the DNAPL can enter, confirming the relationship presented in McWhorter and Kueper (1996). Thus, a more accurate parameter to use to predict PCE entry into lower layers is $h_d^{cs/dnapl}$, the entry pressure of the media by a DNAPL replacing an equilibrated cosolvent mixture. This pressure is that required to allow DNAPL to enter the equilibrated cosolvent resident finer pores below. From the results presented, a

Table 5-4 – Results of globule force balance calculations. Mobilization of globule is predicted if $h_{dnapl} > h_d^{cs/dnapl}$. Permeability of 20-30 medium measured to be $6.35E-7 \text{ cm}^2$. “Clay” scenario based on Beit Netofa clay (van Genuchten 1980) is shown for comparison. Fluid property values shown are approximate and for illustrative purposes.

Run Number	Fine Layer (Sieve #)	Flushing Mode	%v/v Alcohol	$\gamma_{cs/dnapl}$ dynes/cm	ρ_{dnapl} (g/ml)	ρ_{cs} (g/ml)	$\Delta\rho$ (g/ml)	$h_d^{a/w}$ (cm)	$h_d^{cs/dnapl}$, (cm) required	Exp. h_{dnapl} (cm) \approx	Permeability of fine layer k (cm^2)	Did Entry Occur?
I	100-140	Step	100	~0.5	1.55	1.01	0.54	34	0.13	0.4	$1.23E-7$	Y
II	100-140	Step	80	2.1	1.55	1.01	0.54	34	0.53	0.4	$1.23E-7$	N
III	60-70	Step	80	2.1	1.58	0.93	0.65	26.8	0.54	0.4	$2.83E-7$	N
IV	60-70	Gradient	10-90	variable	1.58	0.93	-	26.8	-	0.4	$2.83E-7$	N
V	40-50	Step	80	2.1	1.58	0.93	0.65	18.6	0.38	0.4	$5.45E-7$	N
VI	30-40	Step	80	2.1	1.58	0.93	0.65	10.6	0.21	0.4	$5.00E-7$	Y
VII	30-40	Step	70	3.2	1.59	0.91	0.68	10.6	0.35	0.4	$5.00E-7$	Y
VIIIb	30-40	Step	60	4.5	1.6	0.92	0.68	10.6	0.49	0.4	$5.00E-7$	N
VIIIa	30-40	Step	50	6.3	1.61	0.93	0.68	10.6	0.67	0.4	$5.00E-7$	N
IX	30-40	Step	30 TBA	5.2	1.53	0.99	0.54	10.6	0.41	0.4-0.8	$5.00E-7$	Y
X	100-140	Step	40 TBA	3.9	1.46	0.98	0.48	34	0.91	0.5-1.0	$1.23E-7$	N
-	“clay”	Step	100	~0.5	1.5	1	0.5	7500	51	-	$9.5E-12$	-

guideline to predict entry for a PCE/ethanol system in homogeneous sands is $h_d^{cs/dnapl} < 0.35$ cm. For reference, data taken from van Genuchten (1980) for a Beit Netofa clay is used to calculate a corresponding entry pressure under typical cosolvent flushing conditions to remove a DNAPL like PCE. Based on these assumed conditions (see Table 5-4), approximately a half a meter of DNAPL would be required to enter Beit Netofa clay. This value seems reasonable.

Conclusions

Removal of pooled DNAPL (PCE) on top of finer, less permeable layers during 2-dimensional box cosolvent floods, presents interesting qualitative conclusions. These can be supported semi-quantitatively with pore force-balance calculations.

Pooled DNAPL will collapse under reducing IFT conditions, and if residuals are high enough, can mobilize downward and upstream along overriding cosolvent fronts. This can cause significant build up of DNAPL on the lower confining layer, upstream from a pooled DNAPL system. This allows increased exposure to lower IFT cosolvent solutions that may permeate into the finer layer. Not enough time has passed in the flood to solubilize significant residuals, therefore allowing increased DNAPL heads to exceed entry values of the media below. Downstream mobilization into finer layers can occur as well, only after time has elapsed to allow cosolvent to migrate into the pores of the finer layer. In general, the most significant production of DNAPL through any fine layer in these studies was actually upstream from the source zone.

Gradient injection to remove DNAPLs does not appear to provide significant benefit over step inputs. Override characteristics are not improved upon dramatically.

Furthermore, interfacial tension between injected fluid and DNAPL decreases almost instantaneously compared to removal of DNAPL due to solubilization. Movement of high residuals of DNAPL down onto the finer layer occurs well before significant reduction of saturations due to solubilization. Here, solubilization of DNAPL becomes even less efficient due to essentially only one interface from which to allow mass transfer.

Entry calculations using the physical and hydrogeologic parameters of the chemical phases and media predicted breakthrough of PCE into the finer media in excellent fashion. Breakthrough of PCE under typical ethanol flooding conditions (80% v/v ethanol/water) can generally be assumed to occur in homogeneous sands when $h_d^{cs/dnapl} < 0.35$ cm. Of course, several variables, especially amount of pooled DNAPL present, does not allow an exact prediction for all instances, but a rough prediction based on flooding conditions and media contrasts can be made. It is estimated that for a Beit Netofa clay, approximately one-half a meter of a PCE-like DNAPL would be necessary to enter under extreme cosolvent flooding conditions (IFT = 0.5 dynes/cm; $\Delta\rho = 0.5$ g/cm³, an air entry pressure of 75 meters.)

CHAPTER 6 SUMMARY AND CONCLUSIONS

Batch equilibrium studies were conducted to determine adequate methods to predict physical properties of PCE/cosolvent systems. This included PCE solubility and resulting fluid interfacial tension. Batch studies resulted in cosolvency powers (σ) of 3.73 and 4.13 for ethanol and isopropanol, respectively. Use of the log-linear solubility relationships appears to be not a completely accurate method to predict solubility of PCE in cosolvent mixtures, especially over the entire range of possible volume fractions. The log-linear predictions perform best at higher cosolvent volume fractions. Therefore, these predictions may be adequate for estimations necessary for field studies or remediation efforts. For improved estimation of PCE solubilities over a wider range of cosolvent volume fractions, the use of the Extended Hildebrand or UNIFAC models is recommended. The added complexity of these models is beneficial for accurate solubility predictions over the entire range of cosolvent fractions.

Additionally, the interfacial tension resulting from various cosolvent mixtures and its prediction based on the initial volume fraction of cosolvent leads to an interesting relationship that is similar to the log-linear model. An "IFT reduction power" was determined for ethanol, $\Omega_{\text{EtOH}} = -3.60$, and isopropyl alcohol, $\Omega_{\text{IPA}} = -5.80$, describing the ability of cosolvents to reduce IFT with increasing volume fraction. This parameter quantitatively describes the ability of the cosolvent to reduce the IFT as it is added in

increasing volume fractions. IFT can also be accurately estimated by PCE aqueous phase solubility, especially in regimes conducive to cosolvent flushing. Due to the dependency of PCE aqueous phase solubility upon the aqueous and DNAPL phase ratio and partitioning of cosolvent into the DNAPL phase, it should be noted that this approach is problem specific. Incorporating this property information into a trapping number relationship (Pennell, 1996) allows for improved prediction of remediation schemes remaining within solubilization boundaries, avoiding or minimizing mobilization of the NAPL/DNAPL phase.

The trapping number (N_t) is an effective parameter to help predict mobilization of non-aqueous phase liquids in subsurface environments. Onset of residual PCE mobilization was found to begin at a trapping number (N_t) of 2×10^{-4} . Trapping number results and onset of PCE mobilization were found similar, although slightly greater, to those of Pennell et al.(1996b). Ethanol used as a cosolvent (at volume fractions less than 85%) enhanced solubilization of PCE to the point where this process is dominant and mobilization of PCE can be avoided in homogeneous media similar to #30-40 U.S. silica sand. However, under severe conditions, mobilization using cosolvents can occur. This includes large step inputs to high cosolvent fractions, where DNAPL saturation is still great enough for immediate IFT reduction to cause mobilization, at least in a local sense. This of course could be important if, within that locality, DNAPL moves out of the zone of control. These issues were further addressed in the two-dimensional box studies.

As should be expected, differences between surfactant and cosolvent systems are not apparent on a mobilization curve. Furthermore, mobilization curves appear independent of alcohol type. However, as partitioning of an alcohol, like t-butanol, into

the NAPL occurs, the volume of mobilized NAPL and residual globules of NAPL left behind increase due to swelling and remaining saturation becomes more difficult to quantify. Further research into this area is warranted.

Entrapment and mobilization of residual NAPL are separate and distinct processes. This difference can be seen if both processes are plotted on the same trapping number curve. The entrapment process, represented by the percent of remaining DNAPL saturation ($\% S_{\text{NAPL}}$), appears to be log-linearly related to the trapping number. The exact interpretation of this relationship is not clear presently, but it is believed to be associated with the log-linear dependence of saturation with capillary pressure. However, for heterogeneous media a general trend of increased saturations with decreasing IFTs was observed. This is thought to be caused by the lower IFTs allowing DNAPL access to smaller pores and subsequently not being removed due the increased difficulty of mobilization over entrapment (Morrow et al. 1988). Additional study to confirm this phenomenon and its exact justification is needed.

Removal of pooled DNAPL (PCE) on top of finer, less permeable layers during 2-D box cosolvent floods, presents interesting qualitative conclusions. These can be supported semi-quantitatively with pore force-balance calculations. Pooled DNAPL will collapse under reducing IFT conditions, and if residuals are high enough, can mobilize downward and upstream along overriding cosolvent fronts. This can cause significant build up of DNAPL on the lower confining layer, upstream from a pooled DNAPL system. This allows increased exposure to lower IFT cosolvent solutions that may permeate into the finer layer. If little time has passed since the start of a flood for the flushing phase to solubilize significant residuals, discontinuous globules can pool together

and accumulate on top of the finer layer, resulting in increased DNAPL heads. These DNAPL pressures may exceed entry values of the media below. Downstream, mobilization into finer layers can occur as well, only after significant time has elapsed to allow the cosolvent to migrate into the pores of the finer layer. In general, the most significant production of DNAPL through any fine layer in these studies was actually upstream from the source zone.

Gradient injection to remove DNAPLs does not appear to provide significant benefit over step inputs. Override characteristics are not improved upon dramatically. Furthermore, interfacial tension between injected fluid and DNAPL decreases almost instantaneously compared to removal of DNAPL due to solubilization. Movement of high residuals of DNAPL down onto the finer layer occurs well before significant reduction of saturations due to solubilization. Here, solubilization of DNAPL becomes even less efficient due to essentially only one interface from which to allow mass transfer.

Entry pressure calculations using the physical and hydrogeologic parameters of the chemical phases and media, respectively, predicted breakthrough of PCE into the finer media in excellent fashion. Breakthrough of PCE under typical ethanol flooding conditions (80% v/v) can generally be assumed to occur in homogeneous sand media when $h_d^{cs/dnapl} < 0.35$ cm. Calculations for a Beit Netofa clay estimated that approximately a half a meter worth of equilibrated PCE-type DNAPL would have to accumulate before entry into the clay pores under extreme cosolvent flooding conditions.

Use of the partitioning alcohol t-butanol in the 2-D setup presented interesting qualitative observations. Significant swelling of the PCE resulted, especially for the 40%v/v TBA cosolvent step-input. This swelling, caused by partitioning, and subsequent

delay in downward mobilization due to override, can help in avoiding breakthrough of DNAPL into finer zones, but can also lead to cosolvent becoming trapped on top of finer layers. This volume of cosolvent can produce increased tailing of contaminant removal and increase remediation times. Further study into its avoidance is warranted.

There are quantitative limitations to the theories discussed in this dissertation when one applies them to field situations. However, they are not that serious to prevent them from being used in a more qualitative sense. In design of remediation technologies or strategies, such as cosolvent flushing, scientists or engineers naturally seek to optimize variable parameters. In the case of cosolvent flushing, these include the choice of a cosolvent "recipe" and mode of injection. "Exact" values of key parameters and relationships to other variables can be determined in the laboratory, but we seldom need that accuracy in the field application. Furthermore, addition of heterogeneity, dilution, and dispersion, do not allow exact predictions. The information presented in the previous pages is simply intended to aid in narrowing the many choices an engineer must face when removing a DNAPL from the subsurface with cosolvent mixtures.

APPENDIX A
MOISTURE RELEASE CURVES FOR SAND MEDIA

PARCHMENT DEED
1800/4 OCTOBER 1800

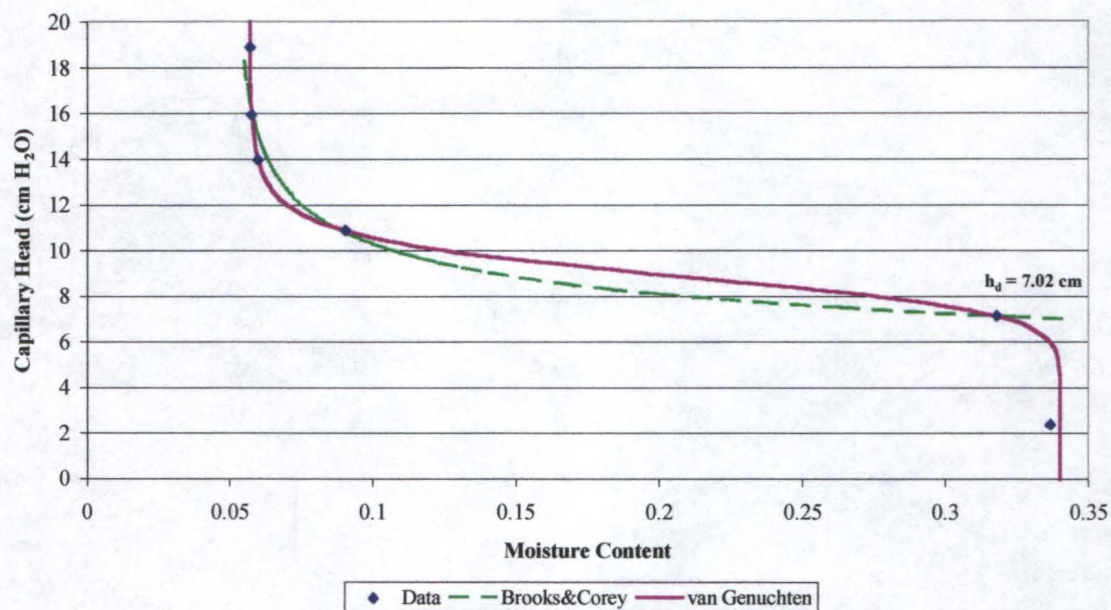


Figure A-1. Moisture release curve for Nos. 20-30 sand.

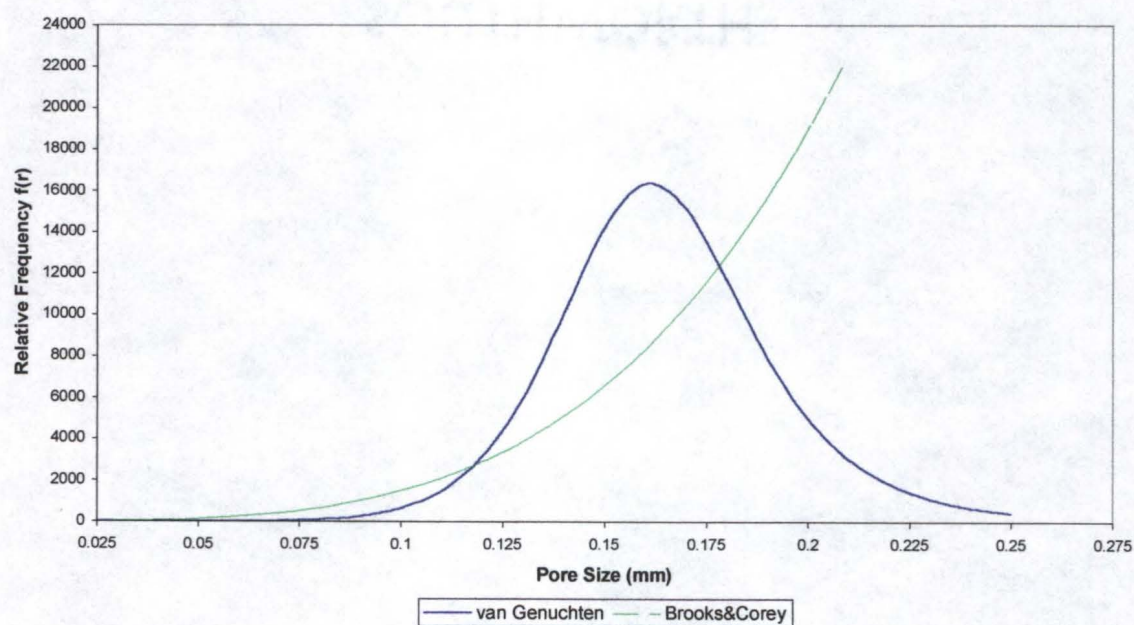


Figure A-2. Pore size frequency distribution of Nos. 20-30 sand.

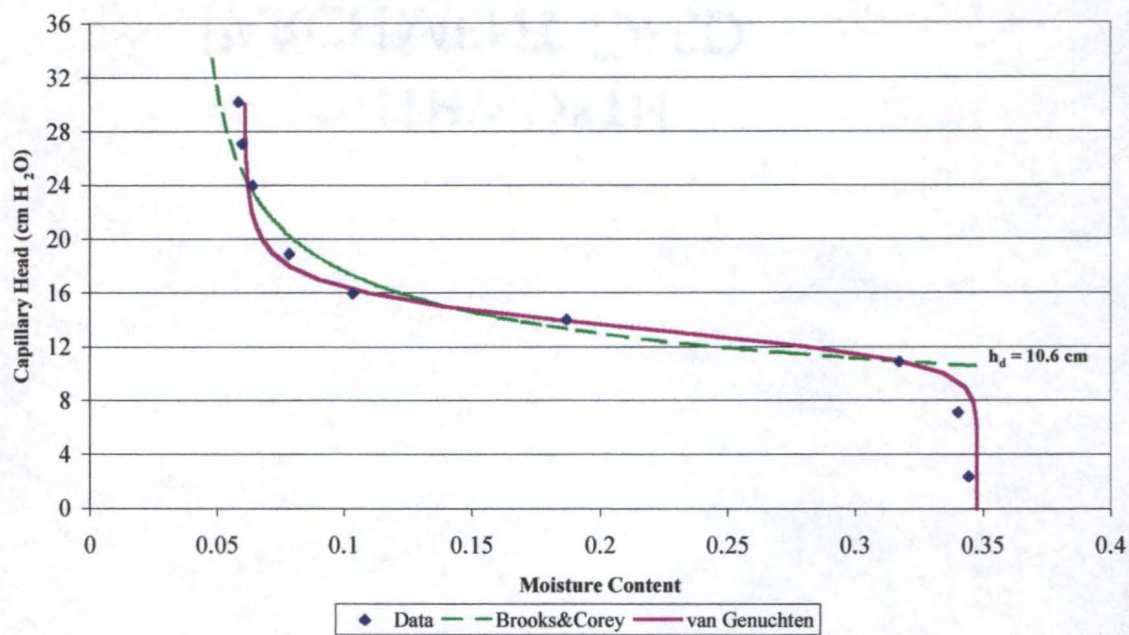


Figure A-3. Moisture release curve for Nos. 30-40 sand

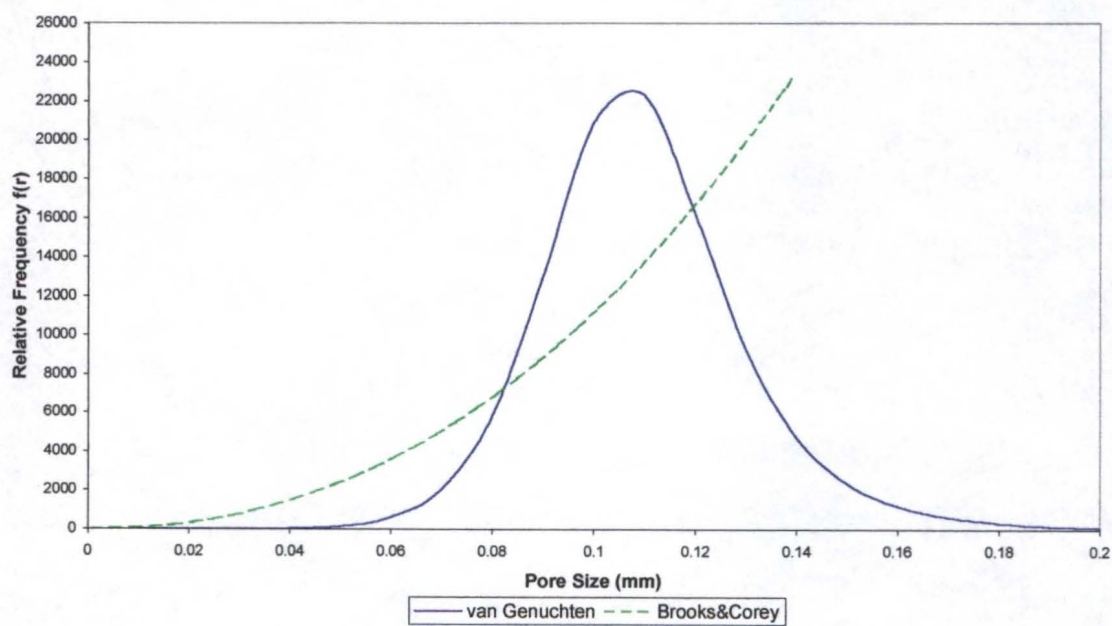


Figure A-4. Pore size frequency distribution of Nos. 30-40 sand

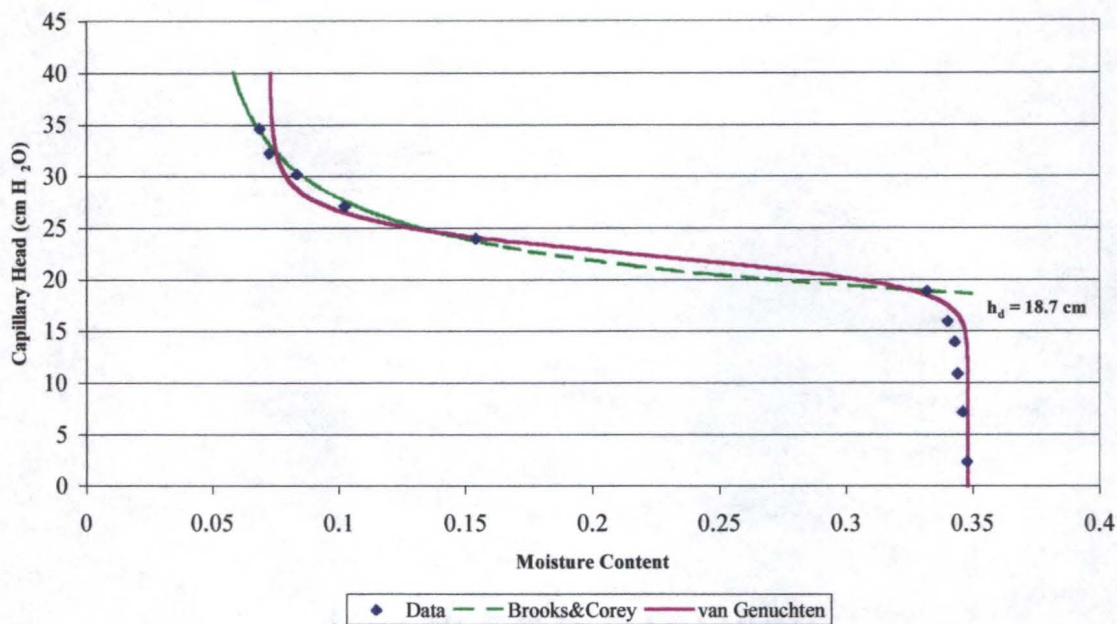


Figure A-5. Moisture release curve for Nos. 40-50 sand.

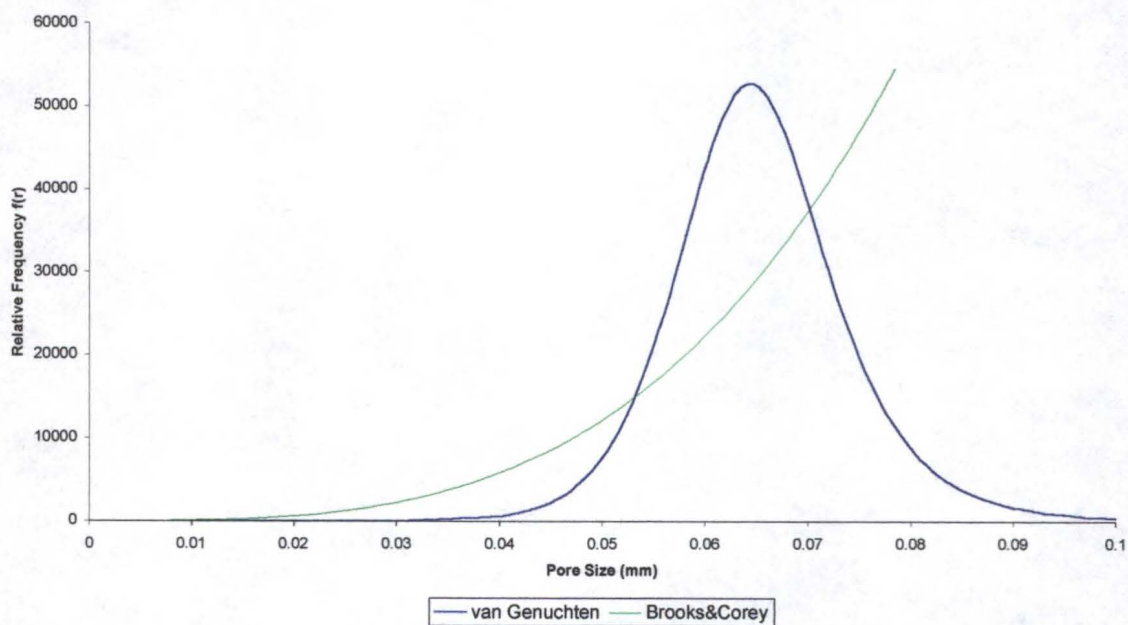


Figure A-6. Pore size frequency distribution of Nos. 40-50 sand.

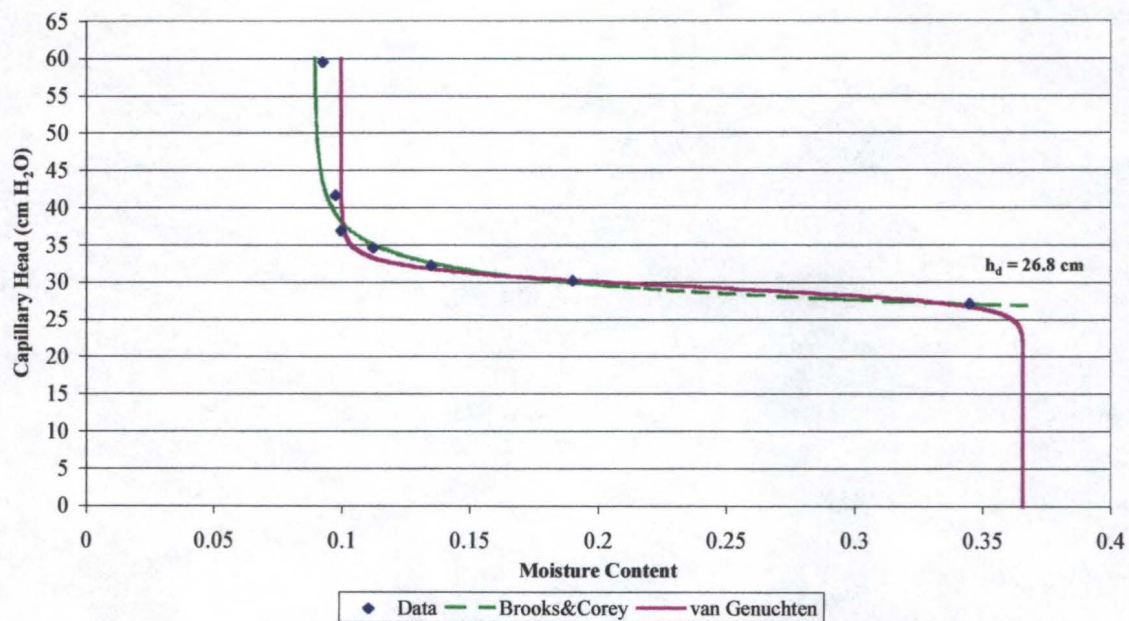


Figure A-7. Moisture release curve for Nos. 60-70 sand.

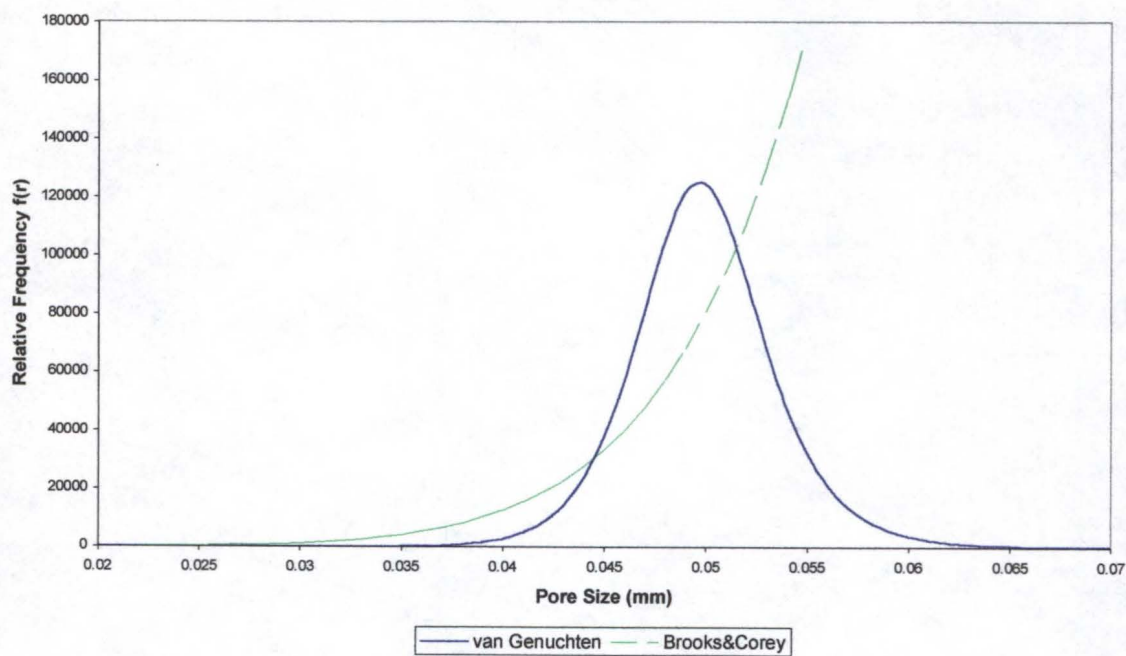


Figure A-8. Pore size frequency distribution of Nos. 60-70 sand.

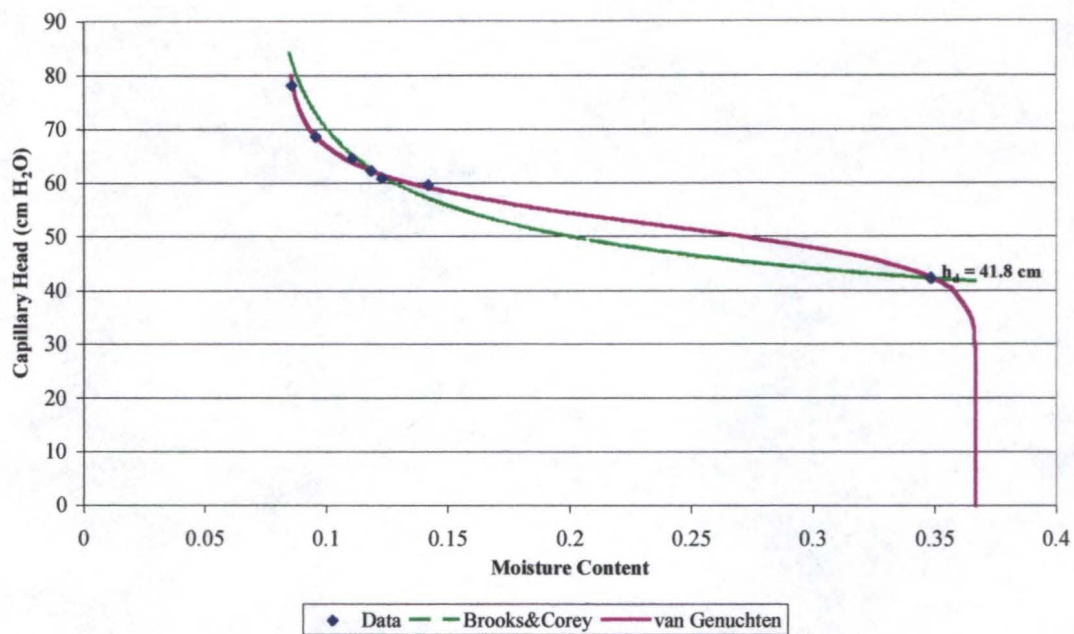


Figure A-9. Moisture release curve for Nos. 100-140 sand.

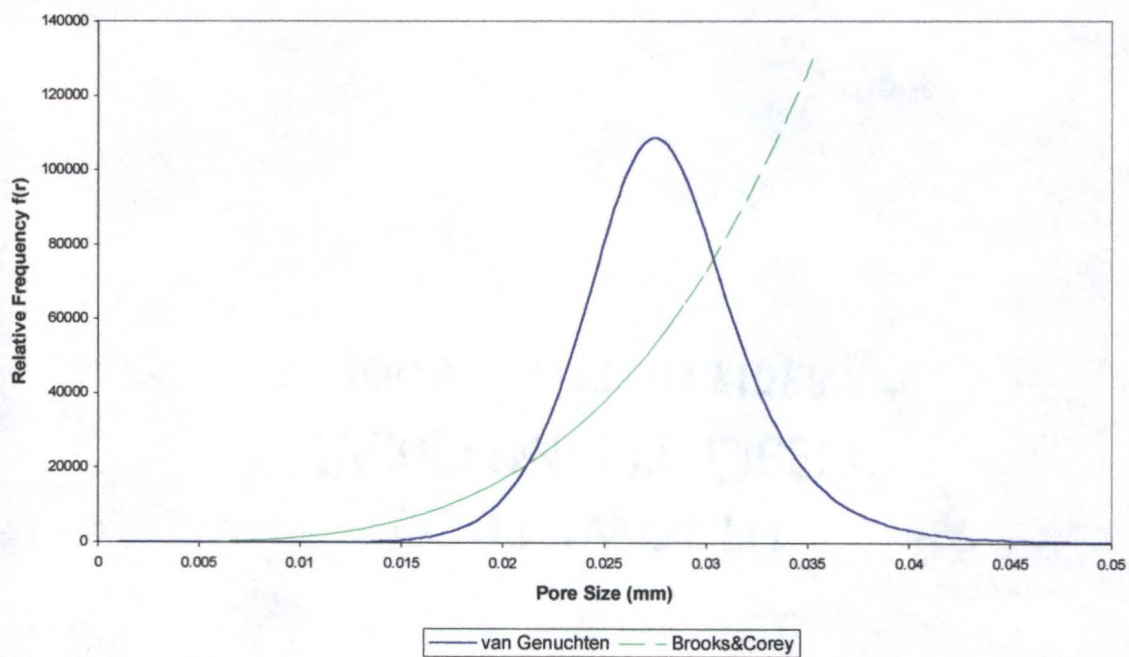


Figure A-10. Pore size distribution of Nos. 100-140 sand.

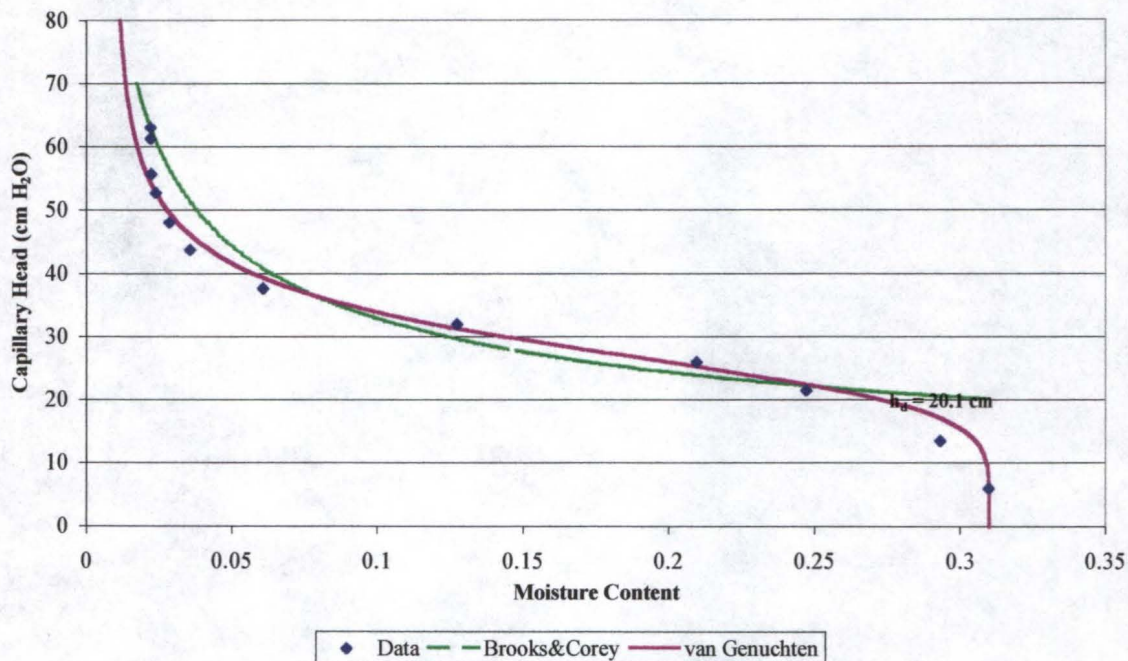


Figure A-6-11. Moisture release curve for wide distribution (#20-100) sand.

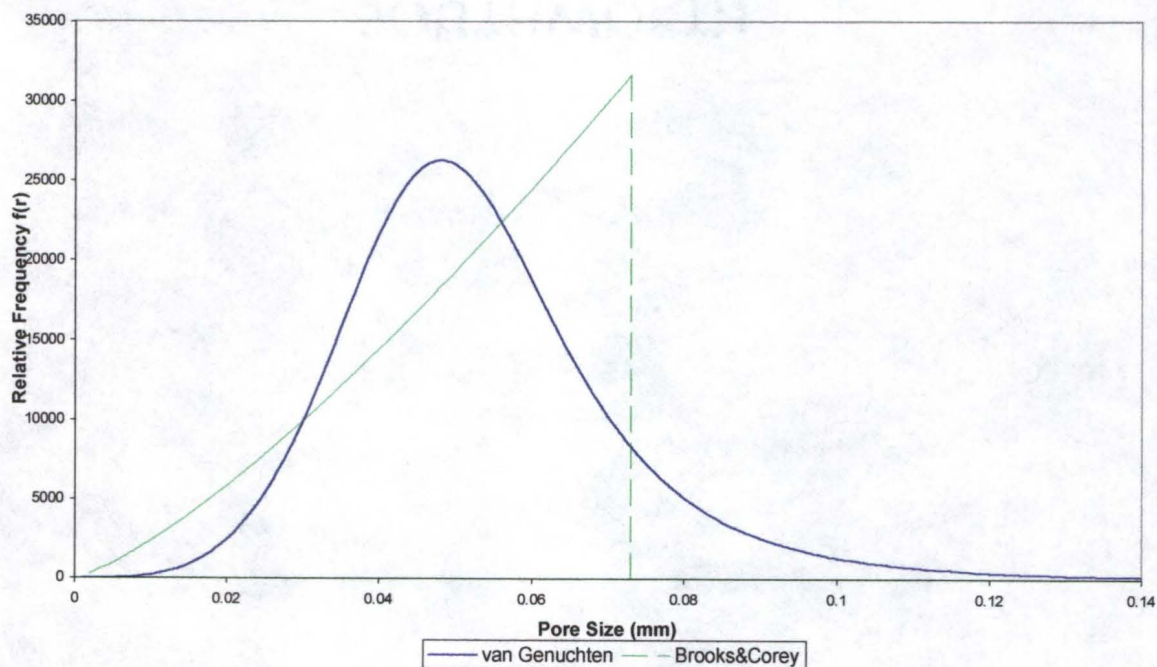
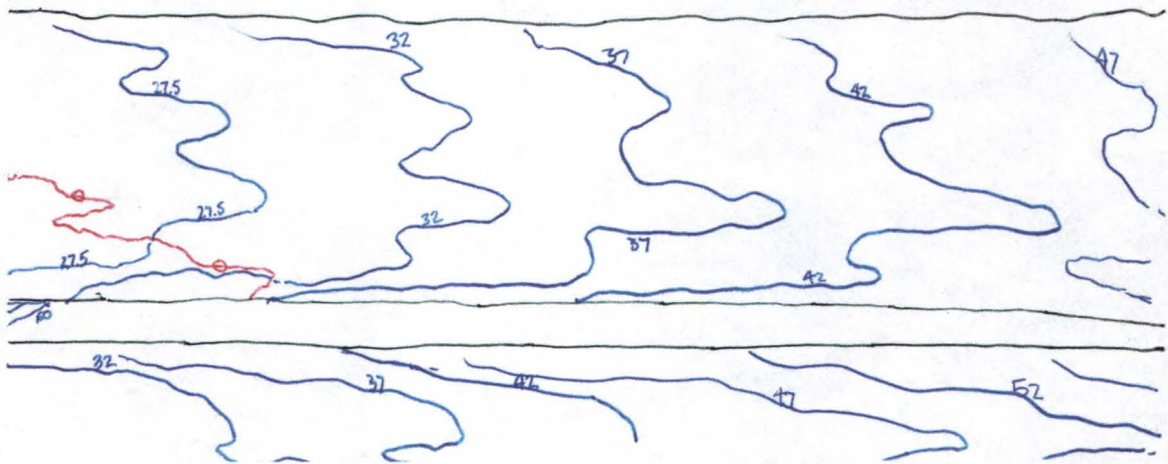
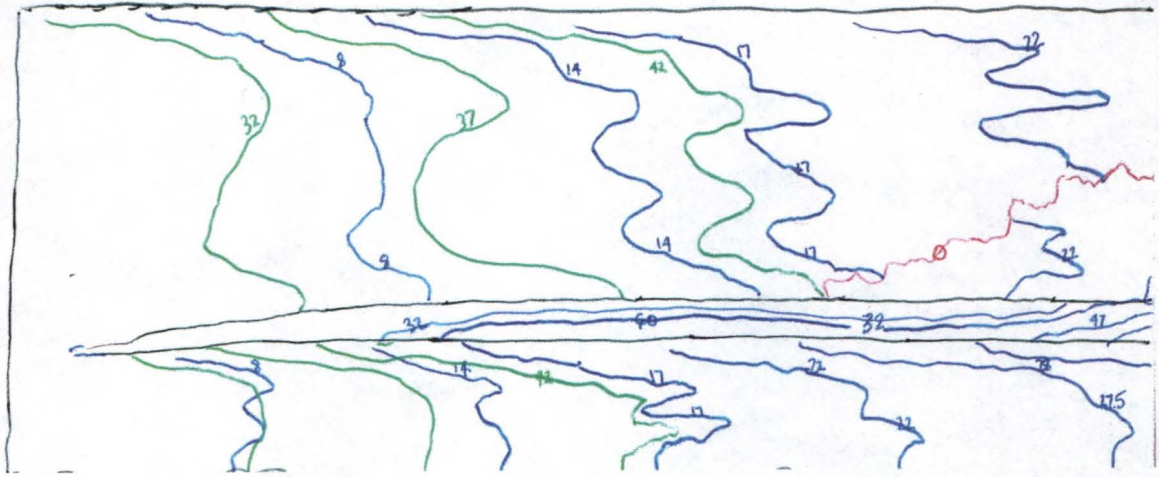


Figure A-12. Pore size distribution of wide distribution (#20-100) sand.

APPENDIX B
TWO-DIMENSIONAL BOX SCHEMATICS

The following pages contain the schematics drawn during each run discussed in the main body of the dissertation.



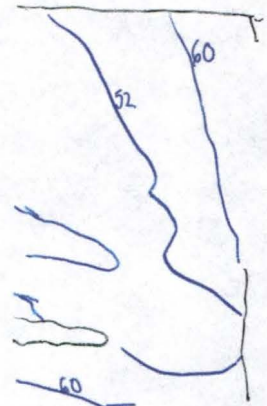
Water Tracer

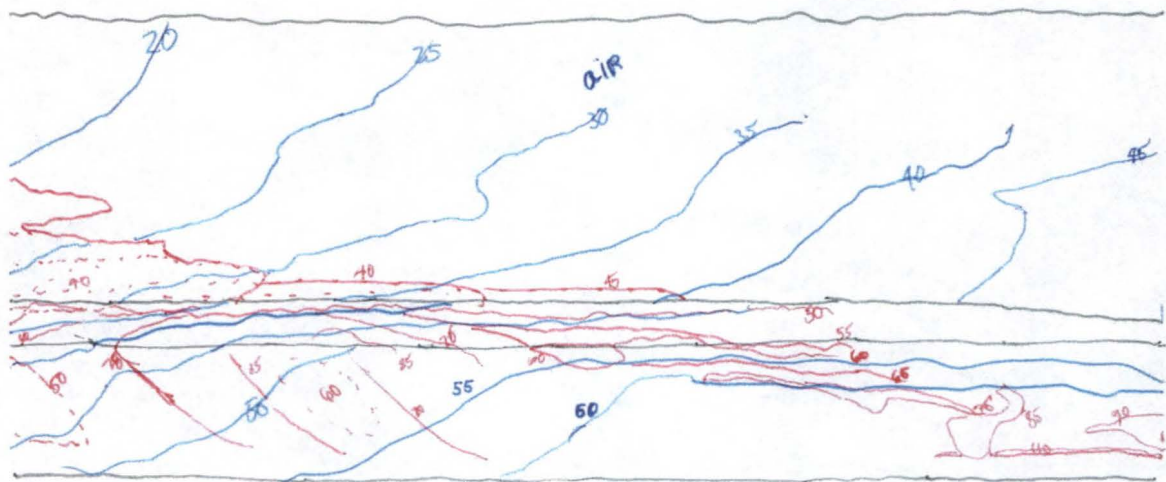
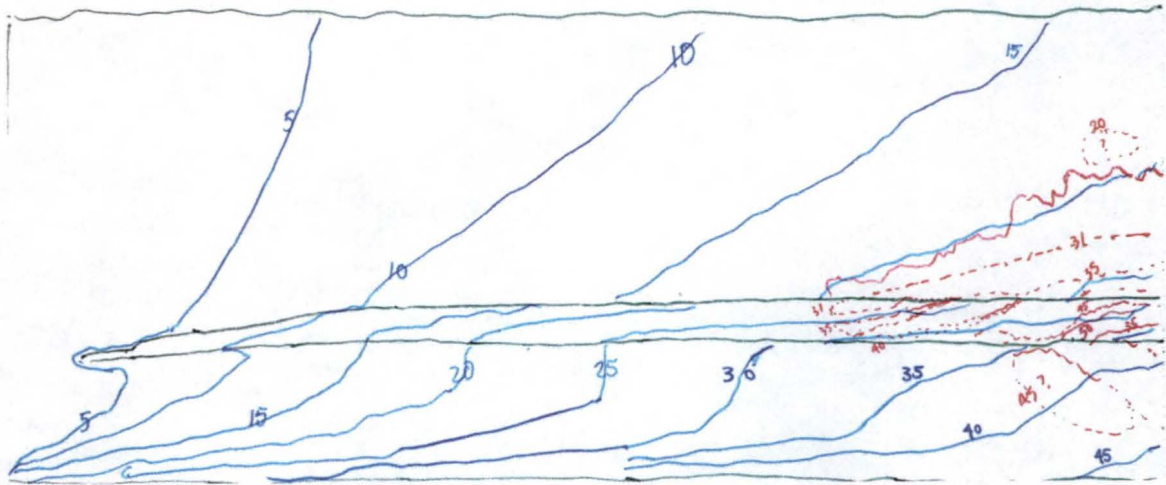
Media:

#20-30 Background

#100-140 Finer Layer

- Dye front
- Dye trailing edge
- DNAPL Pool





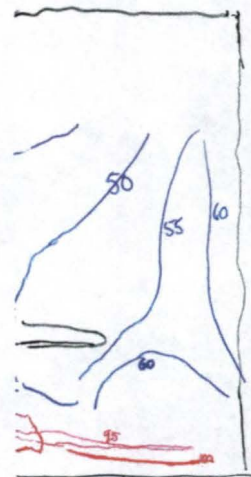
Step Injection 100% alcohol

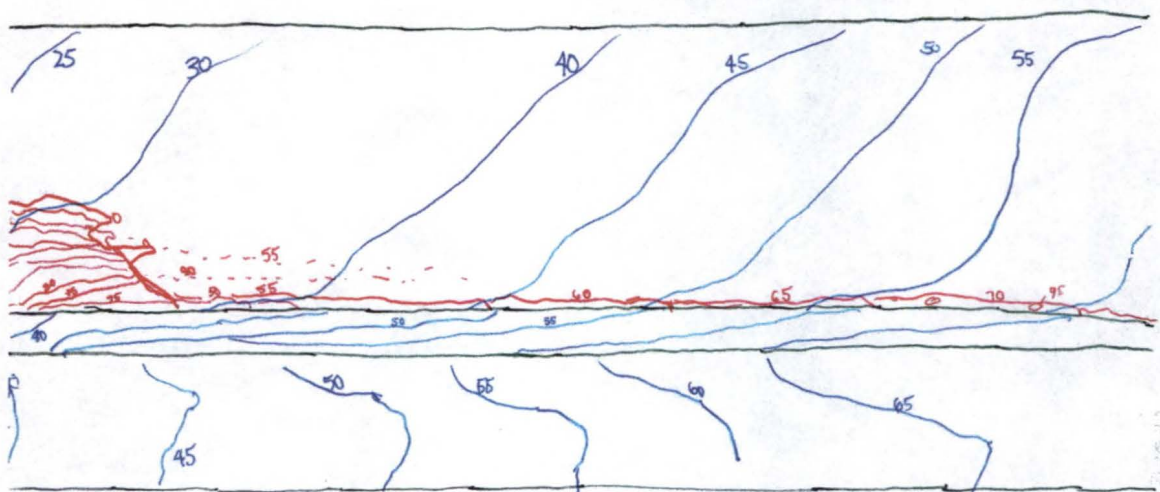
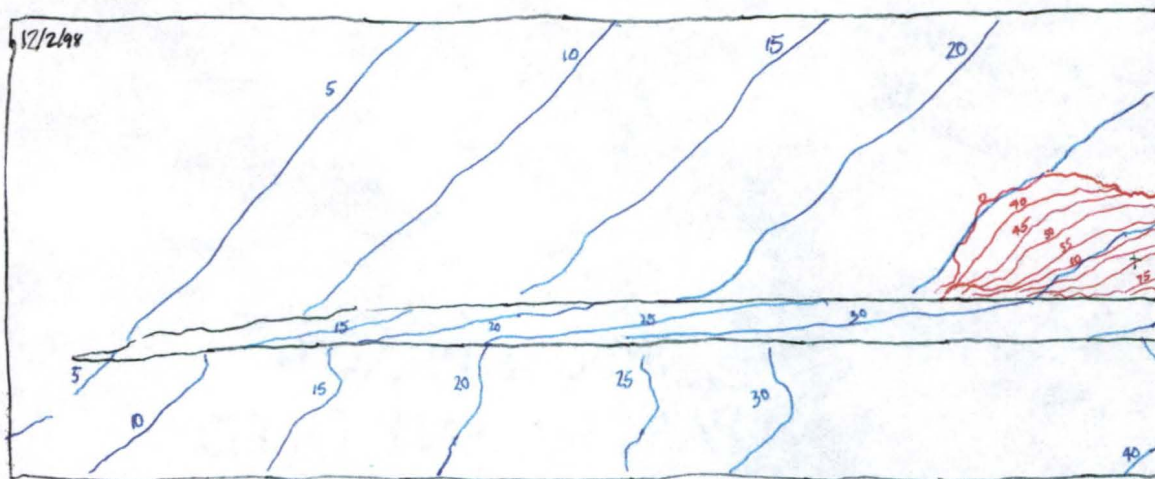
Media:

#20-30 Background

#100-140 Finer Layer

- 80% alcohol front
- DNAPL
- Shrinking DNAPL pool

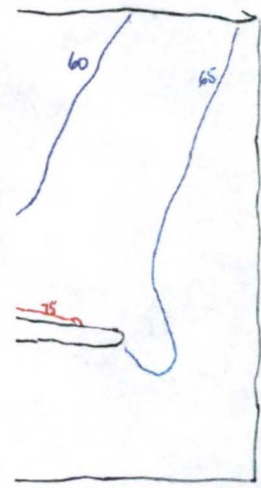


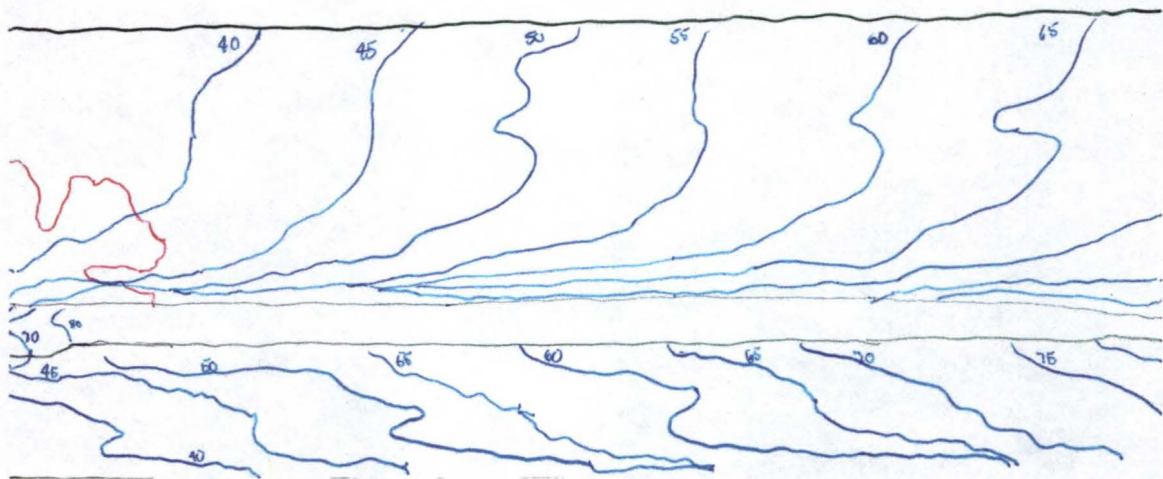
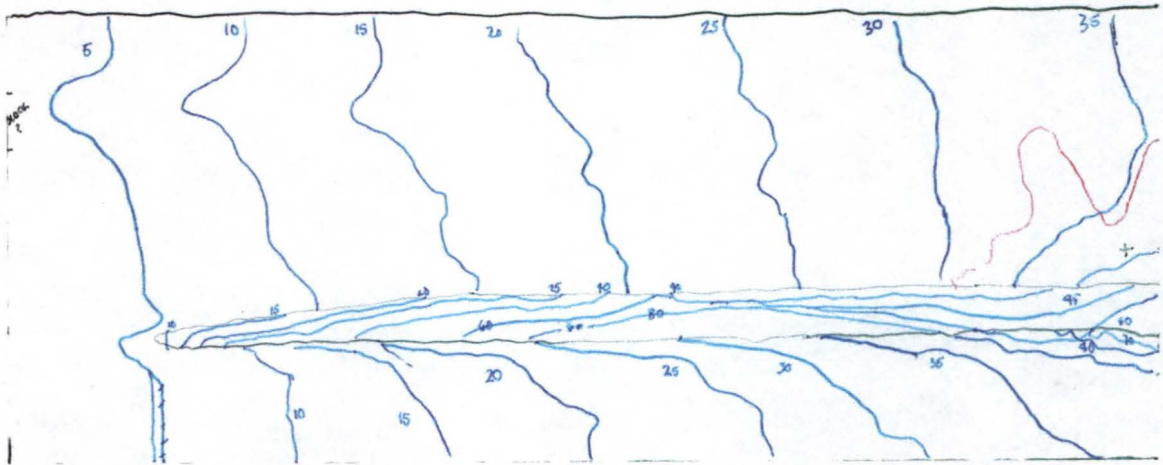


Step Injection 80% alcohol

Media:
 #20-30 Background
 #100-140 Finer Layer

— Dye front
 — DNAPL Pool





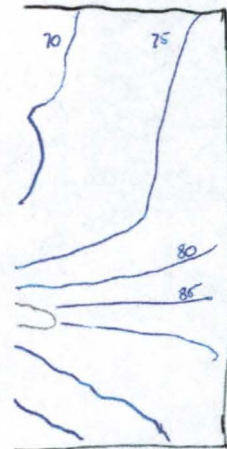
Water Tracer

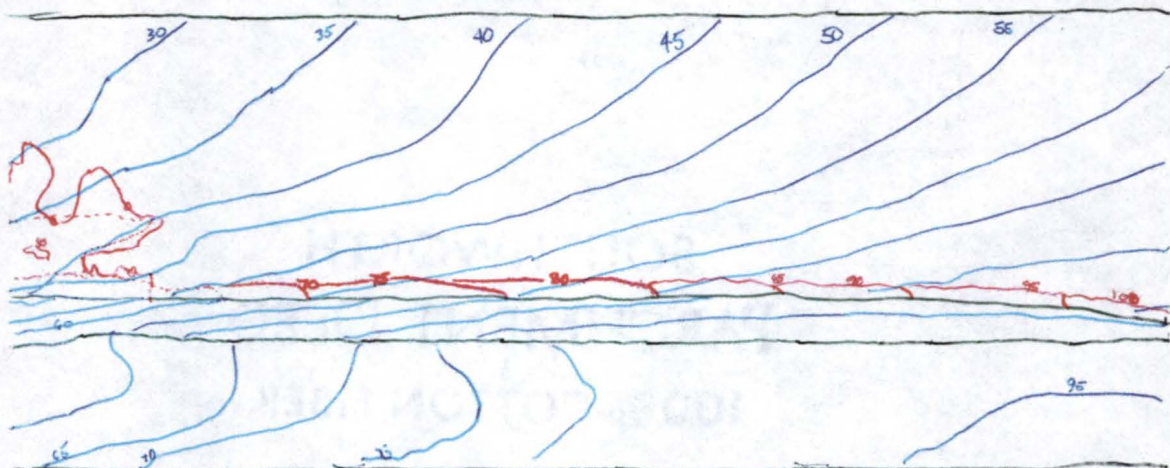
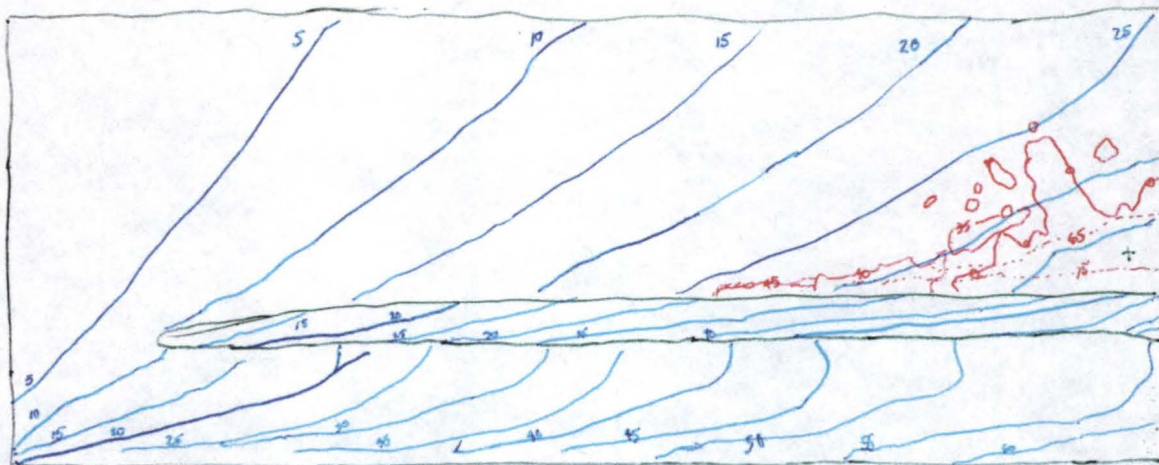
Media:

#20-30 Background

#60-70 Finer Layer

- Dye front
- DNAPL Pool





Step Injection 80% alcohol

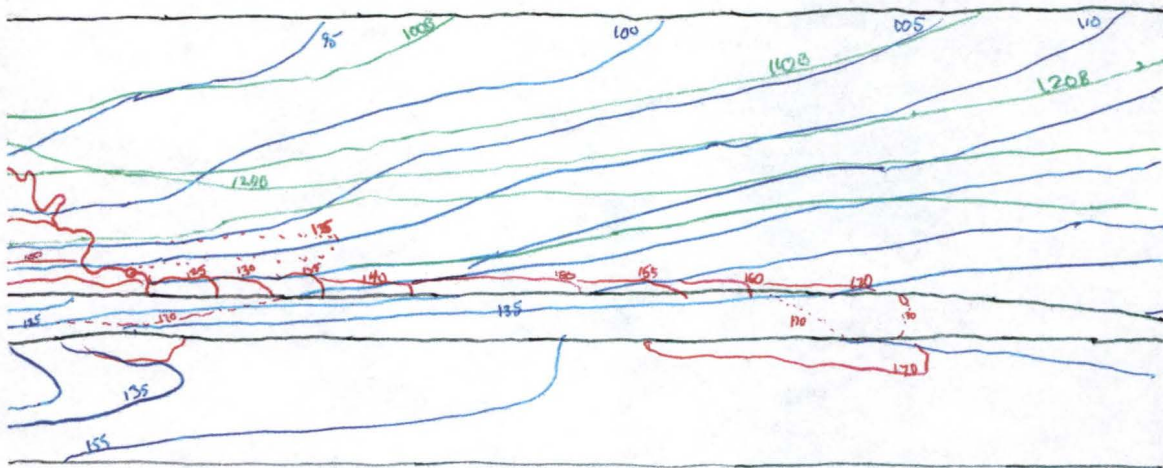
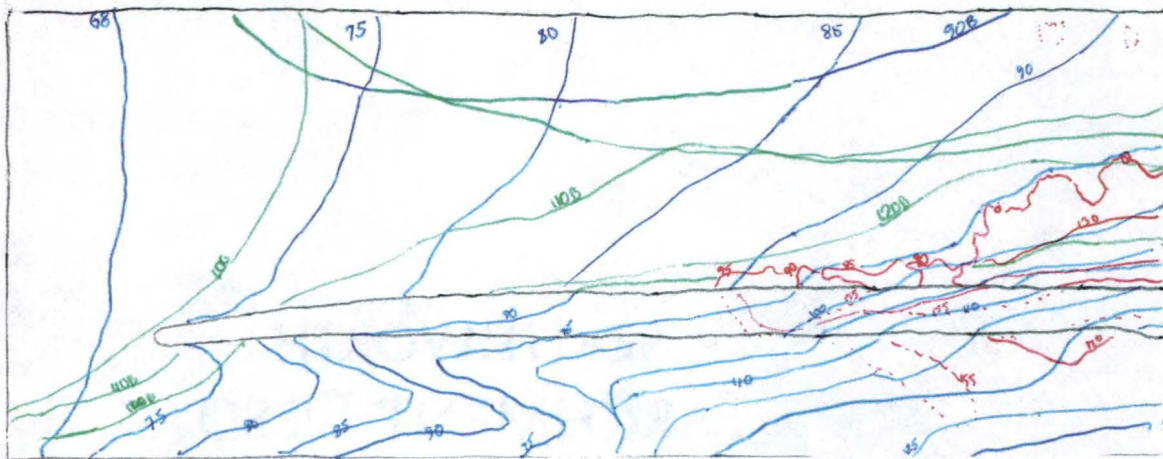
Media:

#20-30 Background

#60-70 Finer Layer

- 80% alcohol front
- DNAPL
- Shrinking DNAPL pool





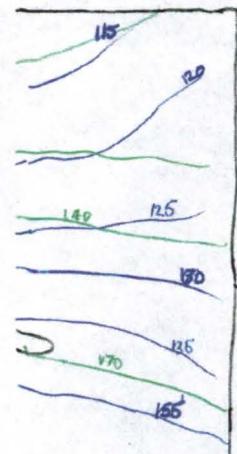
Gradient Injection

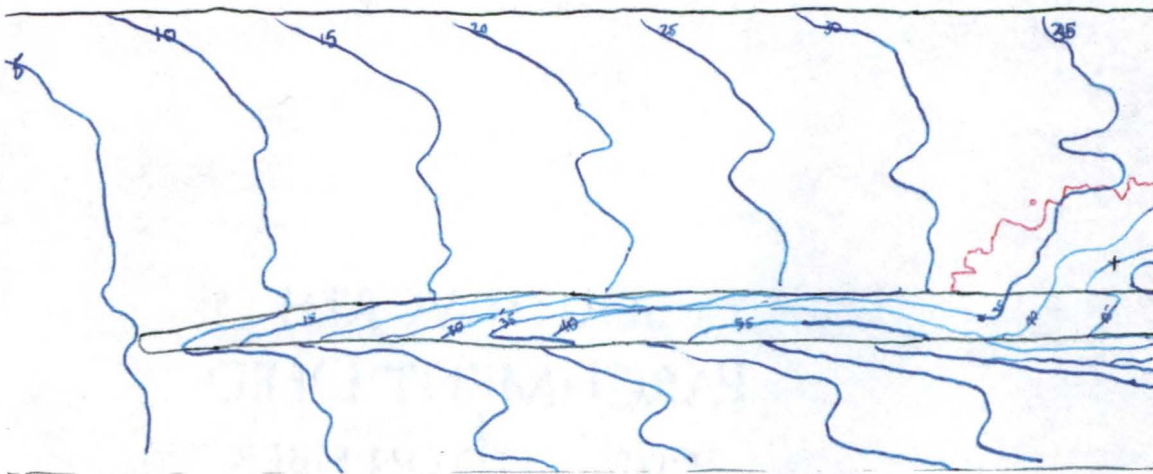
Media:

#20-30 Background

#60-70 Finer Layer

- 60% Alcohol front
- Dye trailing edge (74%)
- DNAPL
- Shrinkng DNAPL Pool





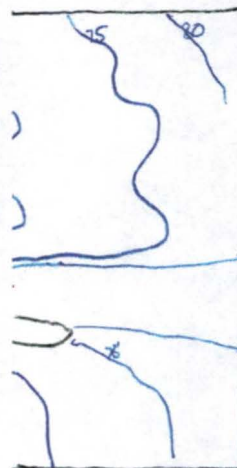
Water Tracer

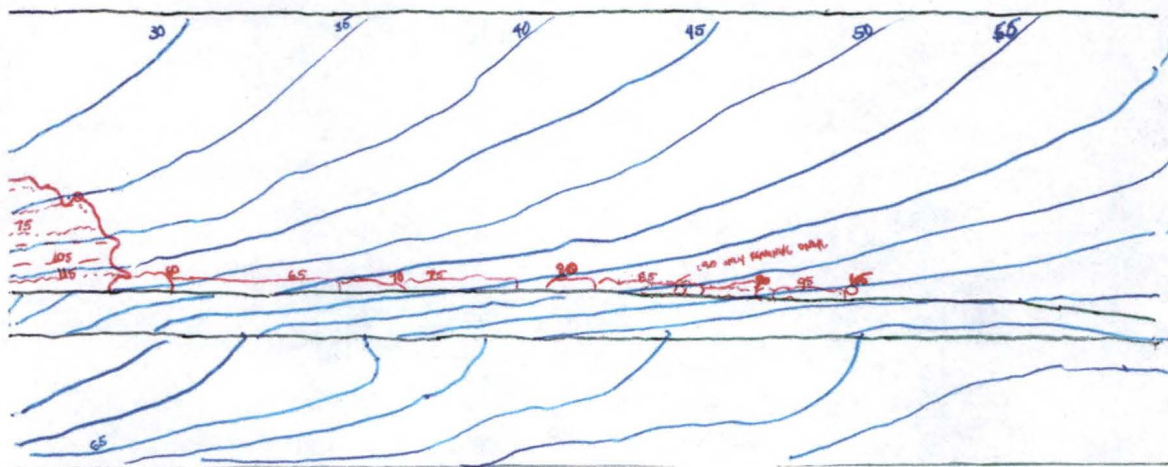
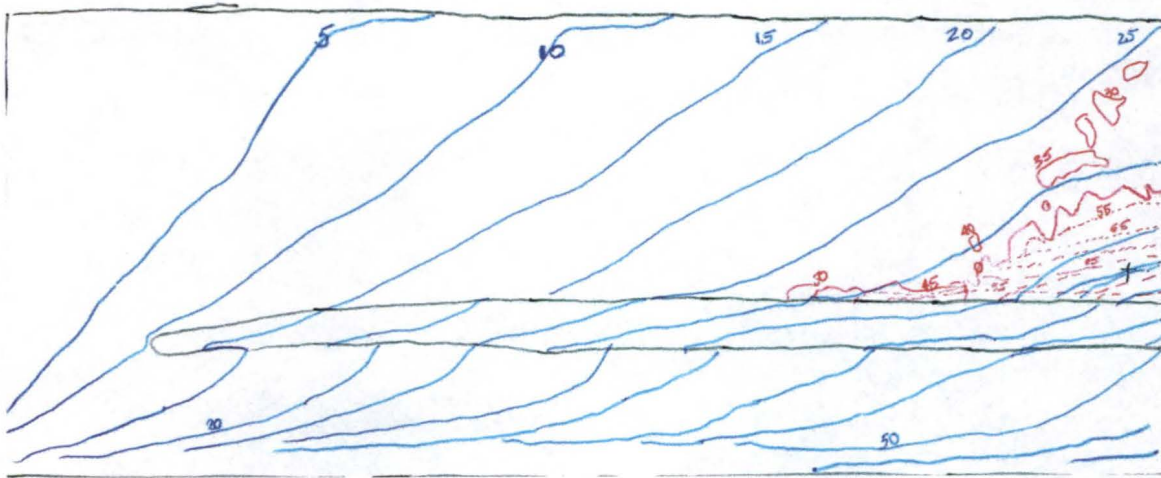
Media:

#20-30 Background

#40-50 Finer Layer

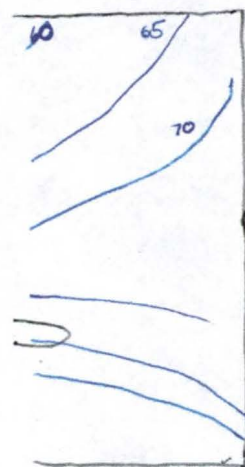
- Dye front
- DNAPL Pool

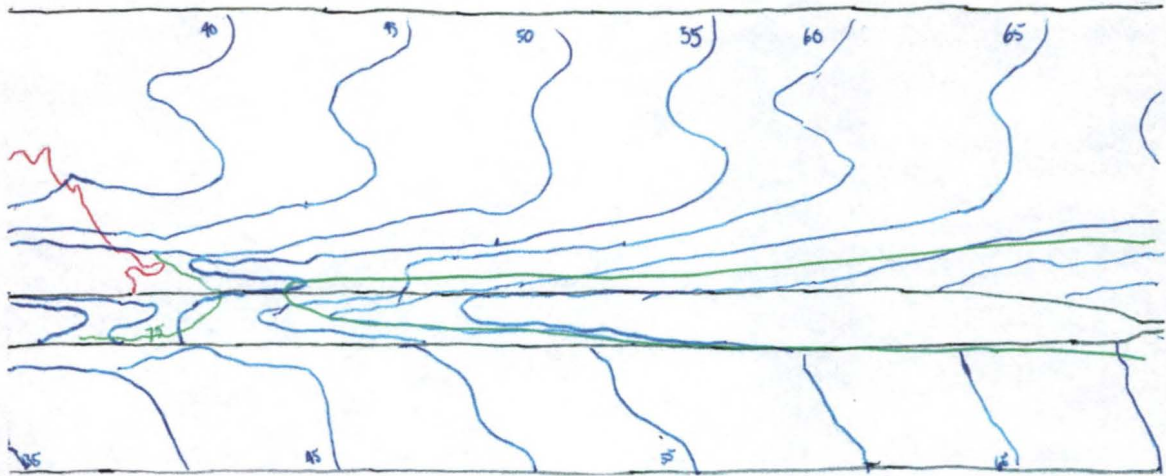
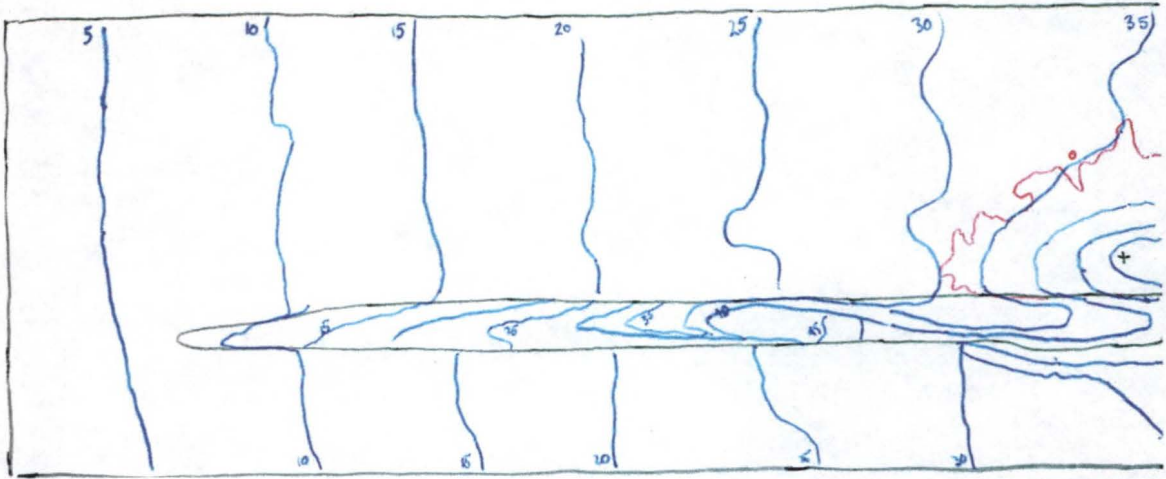




Step Injection 80% alcohol
Media:
 #20-30 Background
 #40-50 Finer Layer

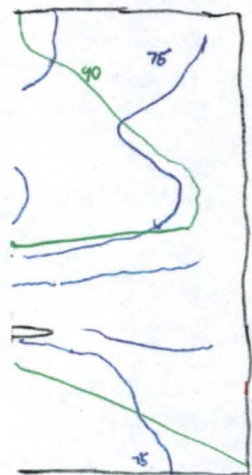
- 80% alcohol front
- DNAPL
- Shrinking DNAPL pool

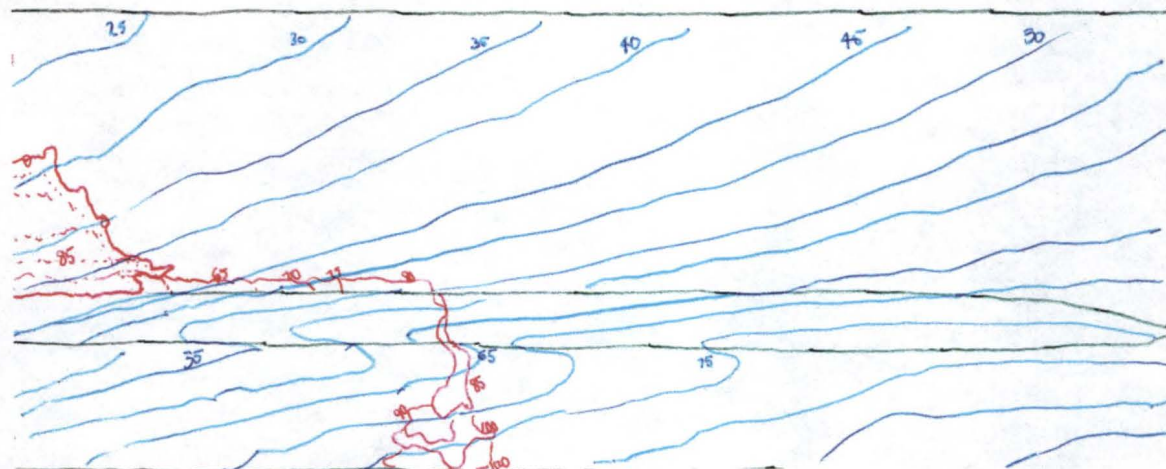
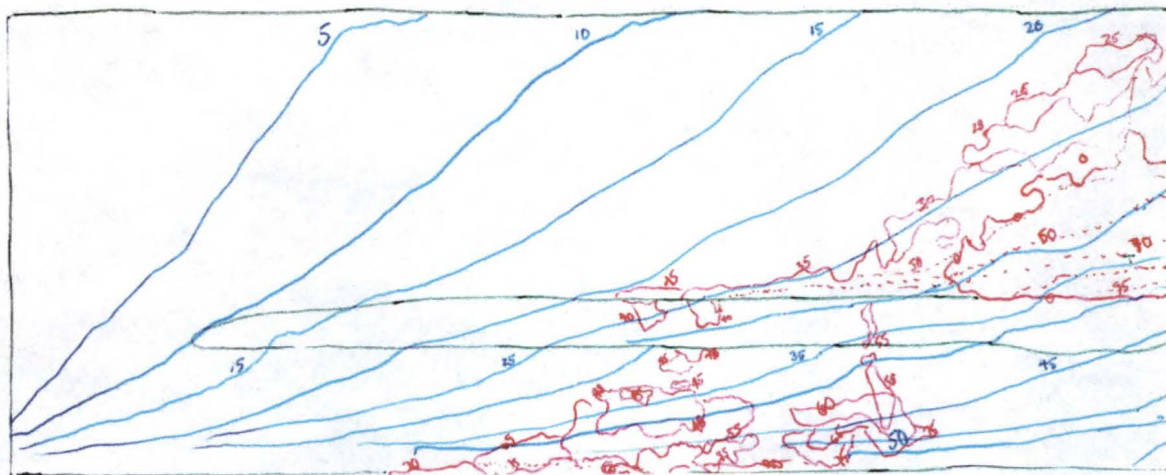




Water Tracer
Media:
 #20-30 Background
 #30-40 Finer Layer

- Dye front
- Dye trailing edge
- DNAPL Pool





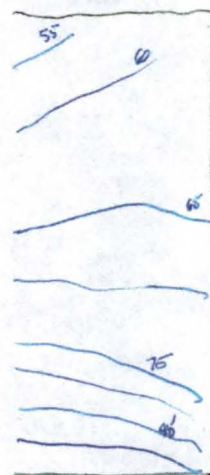
Step Injection 80% alcohol

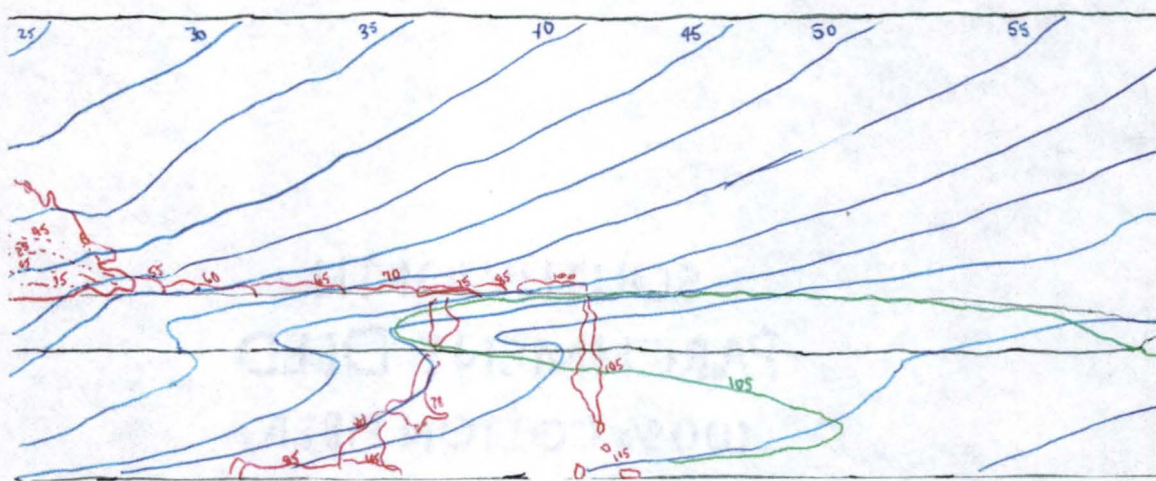
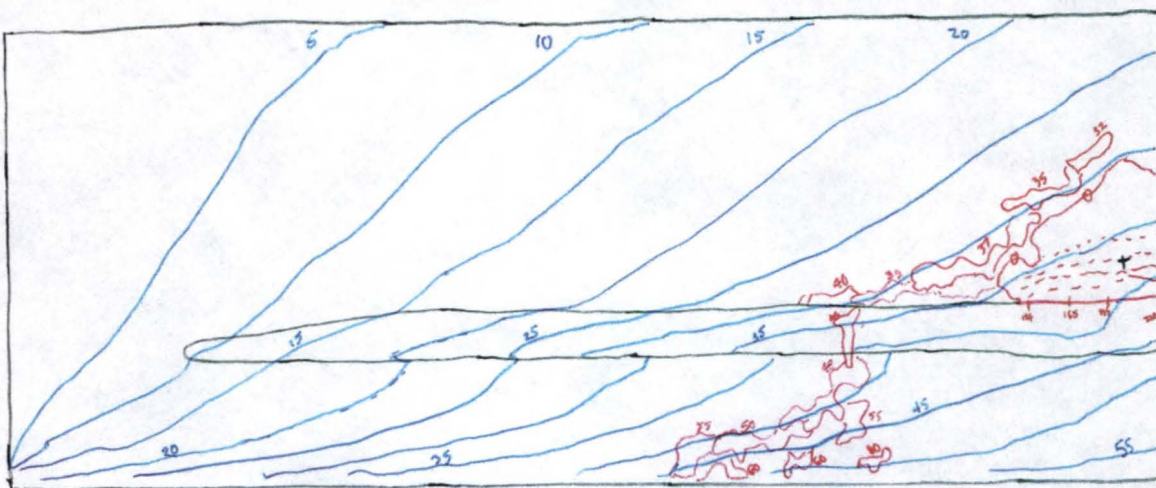
Media:

#20-30 Background

#30-40 Finer Layer

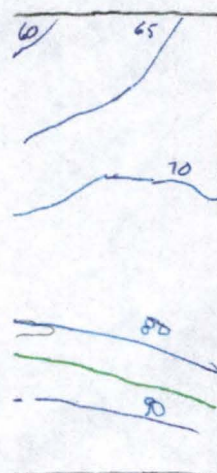
- 80% alcohol front
- DNAPL
- Shrinking DNAPL pool

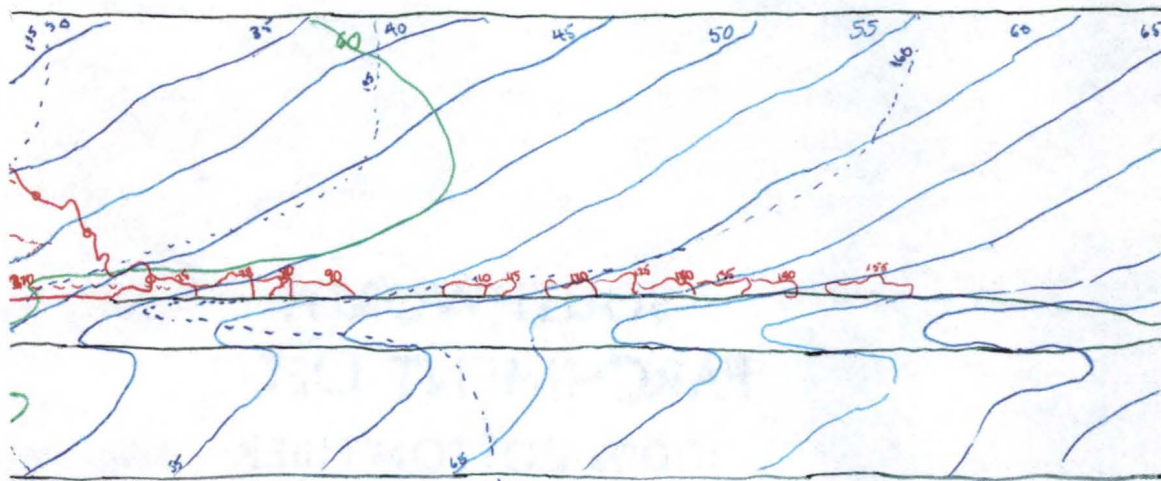
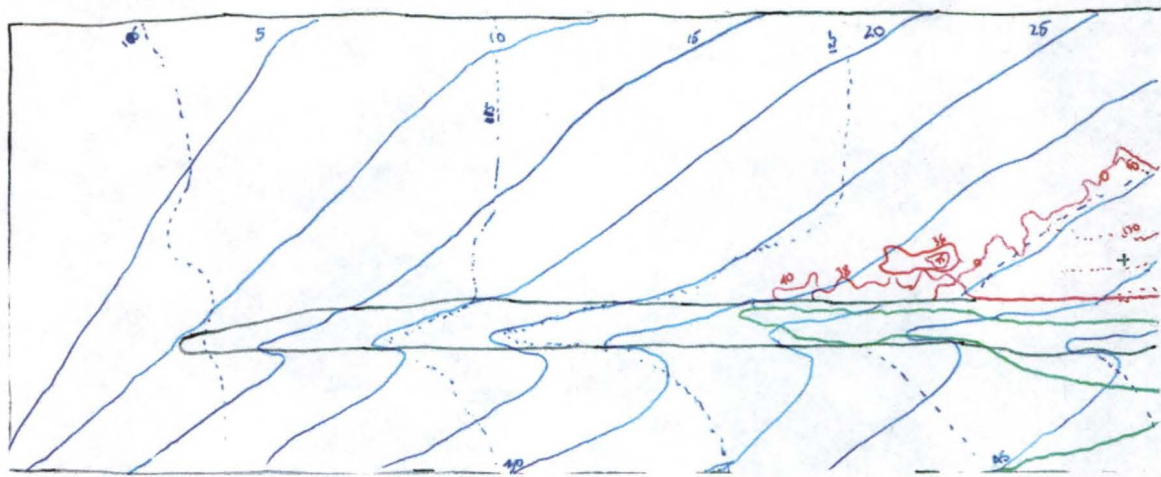




Step Injection 70% alcohol
Media:
 #20-30 Background
 #30-40 Finer Layer

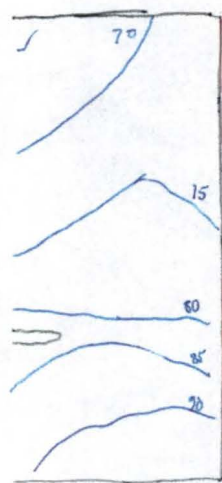
- 70% alcohol front
- Dye trailing edge
- DNAPL
- Shrinking DNAPL pool





Multi-Step Injection
Media:
 #20-30 Background
 #30-40 Finer Layer

- 50% Alcohol front (1PV)
- 60% Alcohol front (1PV)
- Dye trailing edge (50%)
- DNAPL
- Shrinking DNAPL Pool



REFERENCES

- Abrams, A., and Prausnitz. (1975). "The influence of fluid viscosity, interfacial tension, and flow velocity on residual oil saturation left by waterflood." *Society of Petroleum Engineers Journal* (October), 437-443.
- Amidon, G. L., Yalkowsky, S. H., and Leung, S. (1974). "Solubility of nonelectrolytes in polar solvents II: solubility of aliphatic alcohols in water." *Journal of Pharmaceutical Sciences*, 63(12), 1859-1866.
- Annable, M. D., Rao, P. S. C., Sillan, R. K., Hatfield, K., Graham, W. D., Wood, A. L., and Enfield, C. G. (1996). "Field-scale application of in-situ cosolvent flushing: Evaluation approach." *Proceedings of Non-Aqueous Phase Liquids (NAPLs) in Subsurface Environment: Assessment and Remediation*, ASCE, Washington, DC, 212-220.
- Antonov, G. N. (1907). *J. Chim. Phys.*, 8, 372.
- Atkins, P. W. (1994). *Physical Chemistry*, 5, W. H. Freeman, New York, 995.
- Atkinson, H. (1927). U.S. Patent No. 1,651,311, United States.
- Augustijn, D. C. M., Jessup, R. E., Rao, P. S. C., and Wood, A. L. (1994). "Remediation of contaminated soils by solvent flushing." *Journal of Environmental Engineering*, 120(1), 42-57.
- Augustijn, D. C. M., Lee, L. S., Jessup, R. E., Rao, P., Annable, M. D., and Wood, A. L. (1997). "Remediation of soils contaminated with hydrophobic organic chemicals: Theoretical basis for the use of cosolvents." *Subsurface Remediation*, C. H. Ward, J. A. Cherry, and M. R. Scaif, eds., Ann Arbor Press, Chelsea, MI, 231-270.
- Banerjee, S., and Yalkowsky, S. H. (1988). "Cosolvent-induced solubilization of hydrophobic compounds into water." *Analytical Chemistry*, 60, 2153-2155.
- Barton, A. F. M. (1975). "Solubility parameters." *Chemical Reviews*, 75(6), 731-753.
- Brandes, D. (1992). "Effect of phase behavior on residual DNAPL displacement from porous media by alcohol flooding," Master's thesis, Clemson University, 122.

- Brandes, D., and Farley, K. J. (1993). "Importance of phase behavior on the removal of residual DNAPLs from porous media by alcohol flooding." *Water Environment Research*, 65(7), 869-878.
- Brooks, R. H., and Corey, A. T. (1964). "Hydraulic properties of porous media", *Hydrology Paper No. 3*, Department of Civil Engineering, Colorado State University, Ft. Collins, CO, 27.
- Chaudhry, G. R. (1994). *Biological Degradation and Bioremediation of Toxic Chemicals*, Discorides Press, Portland, 515.
- Chen, C. S., and Delfino, J. J. (1997). "Cosolvent effects of oxygenated fuels on PAH solubility." *Journal of Environmental Engineering*, 123(4), 354-363.
- Chevalier, L. R., and Peterson, J. (1999). "Literature review of 2-D laboratory experiments in NAPL flow, transport, and remediation." *Journal of Soil Contamination*, 8(1), 149-167.
- Dawson, H. E., and Roberts, P. V. (1997). "Influence of viscous, gravitational and capillary forces on DNAPL saturation." *Ground Water*, 35(2), 261-269.
- Demond, A. H., and Lindner, A. S. (1993). "Estimation of interfacial tension between organic liquids and water." *Environmental Science and Technology*, 27(12), 2318-2331.
- Dickhut, R. M., Andren, A. W., and Armstrong, D. E. (1989). "Naphthalene solubility in selected organic solvent/water mixtures." *Journal of Chemical Engineering Data*, 34(4), 438-443.
- Dickhut, R. M., Armstrong, D. E., and Andren, A. W. (1991). "The solubility of hydrophobic aromatic chemicals in organic solvent/water mixtures: Evaluation of four mixed solvent solubility estimation methods." *Environmental Toxicology and Chemistry ETOCDK*, 10(7), 881-889.
- Donahue, D. J., and Bartell, F. E. (1958). "The boundary tension at water-organic liquid interfaces." *Journal of Physical Chemistry*, 56, 480-484.
- Falta, R. W., Brame, S. E., and Roeder, E. (1997). "The application of density controlled flooding solutions for remediation. GSA Abstract No. 51134." Proceedings of *GSA Annual Meeting*, Salt Lake City.
- Feenstra, S., and Cherry, J. A. (1988). "Subsurface contamination by dense non-aqueous phase liquids (DNAPL) chemicals." Proceedings of *International Groundwater Symposium*, Halifax, Nova Scotia.

- Flury, M., and Fluhler, H. (1995). "Tracer characteristics of Brilliant Blue FCF." *Soil Science Society of America Journal*, 59(1), 22-27.
- Fortin, J., Jury, W. A., and Anderson, M. A. (1997). "Enhanced removal of trapped non-aqueous phase liquids from saturated soil using surfactant solutions." *Journal of Contaminant Hydrology*, 24(3-4), 247-267.
- Fountain, J. C., Klimek, A., Beikirch, M. G., and Middleton, T. M. (1991). "Use of surfactants for in situ extraction of organic pollutants from a contaminated aquifer." *Journal of Hazardous Materials*, 28(3), 295-311.
- Frank, H. S., and Wen, W. Y. (1957). "Untitled." *Discussions of the Faraday Society*, 24, 133.
- Franks, F., and Ives, D. J. G. (1966). "The structural properties of alcohol-water mixtures." *Quarterly Reviews*, 20, 1-44.
- Fredenslund, A., Jones, R. L., and Prausnitz, J. M. (1977). "Group-contribution estimation of activity coefficients in non-ideal liquid mixtures." *American Institute of Chemical Engineering Journal*, 21, 1086-1099.
- Fu, J., Li, B., and Wang, Z. (1986). "Estimation of fluid-fluid interfacial tensions of multicomponent mixtures." *Chemical Engineering Science*, 41(10), 2673-2679.
- Gatlin, C. (1959). "The Miscible Displacement of Oil and Water from Porous Media by Various Alcohols," Ph. D. dissertation, Pennsylvania State University.
- Gatlin, C., and Slobod, R. L. (1960). "The alcohol slug process for increasing oil recovery." *Transactions of the American Institute of Mechanical Engineers*, 219, 46.
- Geller, J. T., and Hunt, J. R. (1993). "Mass transfer from nonaqueous phase organic liquids in water-saturated porous media." *Water Resources Research*, 29(4), 833-845.
- Girifalco, L. A., and Good, R. J. (1957). "A theory for the estimation of surface and interfacial energies. I. Derivation and application to interfacial tension." *Journal of Physical Chemistry*, 61, 904-909.
- Gliniski, J., Chavepeyer, G., and Platten, J. (1994). "An empirical relation between mutual solubilities and interface tension for two partially miscible liquids." *Physica B: Condensed Matter*, 193, 154-160.

- Groves, F. R., Jr. (1988). "Effect of cosolvents on the solubility of hydrocarbons in water." *Environmental Science and Technology*, 22(3), 282-286.
- Grubb, D. G., Empie, L. E., Hudock, G. W., Davies, R. N., and Lathrop, S. B. (1996). "Two-dimensional ethanol floods of toluene in homogeneous, unconfined aquifer media." Proceedings of *In Situ Remediation of the Geoenvironment*, ASCE, Minneapolis, MN.
- Grunwald, E. J. (1986). "Thermodynamic properties of non-polar solutes in water and the structure of hydrophobic hydration shells." *Journal of the American Chemical Society*, 108(19), 5726-5731.
- Hansen, H. K., Rasmussen, P., Fredenslund, A., Schiller, M., and Gmehling, J. (1991). "Vapor-liquid equilibria by UNIFAC group contribution. 5. Revision and extension." *Industrial Engineering Chemical Research*, 30(10), 2352-2355.
- Held, R. J., and Illangasekare, T. H. (1995). "Fingering of dense non-aqueous phase liquids in porous media, 1. Experimental investigation." *Water Resources Research*, 31(5), 1213-1222.
- Hildebrand, J. H., and Scott, R. L. (1950). *Solubility of Non-Electrolytes*, 3rd ed., Reinhold, New York.
- Hirasaki, G. J. (1980). "Scaling of nonequilibrium phenomena in surfactant flooding." Paper SPE 8841. Proceedings of *SPE/DOE Enhanced Oil Recovery Symposium*, Tulsa, OK.
- Illangasekare, T. H., Ramsey, J. L., Jensen, K. H., and Butts, M. (1995). "Experimental study of movement and distribution of dense organic chemicals in heterogeneous aquifers." *Journal of Contaminant Hydrology*, 20, 1-25.
- Imhoff, P. T., Giezyer, S. N., McBride, J. F., Vancho, L. A., Okuda, I., and Miller, C. T. (1995). "Cosolvent-enhanced remediation of residual dense nonaqueous phase liquids: Experimental investigation." *Environmental Science and Technology*, 29(8), 1966-1976.
- Jawitz, J., W, Annable, M., D, and Rao, P. S. C. (1998a). "Miscible fluid displacement stability in unconfined porous media: two-dimensional flow experiments and simulations." *Journal of Contaminant Hydrology*, 31, 211-230.
- Jawitz, J. W., Annable, M. D., Rao, P. S. C., and Rhue, R. (1998b). "Field implementation of a Winsor Type I surfactant/alcohol mixture for in situ solubilization of a complex LNAPL as a single-phase microemulsion." *Environmental Science and Technology*, 32(4), 523-530.

- Johnson, R. L., and Pankow, J. F. (1992). "Dissolution of dense chlorinated solvents into groundwater. 2. Source functions for pools of solvent." *Environmental Science and Technology*, 26(5), 896-901.
- Kamath, I. S. K. (1960). "Transfer and Movement of Materials during the Recovery of Oil and Water from a Porous Medium by an Alcohol," Ph. D. Dissertation, Pennsylvania State University.
- Kueper, B. H., and Frind, E. O. (1988). "Overview of immiscible fingering in porous media." *Journal of Contaminant Hydrology*, 2(2), 95-110.
- Lam, A. C., Schechter, R. S., and Wade, W. H. (1983). "Mobilization of residual oil under equilibrium and nonequilibrium conditions." *Society of Petroleum Engineers Journal*, 23(5), 781-790.
- Li, A., and Andren, A. W. (1994). "Solubility of polychlorinated biphenyls in water/alcohol mixtures. 1. Experimental data." *Environmental Science and Technology*, 28(1), 47-52.
- Li, A., and Andren, A. W. (1995). "Solubility of polychlorinated biphenyls in water/alcohol mixtures. 2. Predictive methods." *Environmental Science and Technology*, 29(12), 3001-3006.
- Li, A., Andren, A. W., and Yalkowsky, S. H. (1996). "Choosing a cosolvent: solubilization of naphthalene and cosolvent property." *Environmental Toxicology and Chemistry*, 15(12), 2233-2239.
- Lide, D. R. (1996). *Handbook of Chemistry and Physics*. 77th ed., CRC Press, Boca Raton.
- Lunn, S. R. D., and Kueper, B. H. (1997). "Removal of pooled dense, nonaqueous phase liquid from saturated porous media using upward gradient alcohol floods." *Water Resources Research*, 33(10), 2207-2219.
- Magat, M. (1959). In *Hydrogen bonding*, D. Hadzi and H. W. Thompson, eds., Pergamon Press, London.
- Martin, A., Newburger, J., and Adjei, A. J. (1979). "New solubility equation." *Journal of Pharmaceutical Sciences*, 68, IV-V.
- Martin, A., Wu, P. L., Adjei, R. E., Lindstrom, R. E., and Elworthy, P. H. (1982). "Extended Hildebrand solubility approach and the log linear solubility equation." *Journal of Pharmaceutical Sciences*, 71(8), 849-856.

- McWhorter, D. B., and Kueper, B. H. (1996). "Mechanics and mathematics of the movement of dense non-aqueous phase liquids (DNAPLs) in porous media." *Dense Chlorinated Solvents and other DNAPLs in Groundwater: History, Behavior, and Remediation*, J. F. Pankow and J. A. Cherry, eds., Waterloo Press, Portland.
- Miller, C. T., Poirier-McNeill, M. M., and Mayer, A. S. (1990). "Dissolution of trapped nonaqueous phase liquids: mass transfer characteristics." *Water Resources Research*, 26, 2783-2796.
- Moore, T. R., and Slobod, R. L. (1956). "The effect of viscosity and capillarity on the displacement of oil by water." *Producers Monthly*, 20, 20-30.
- Morris, K. R., Abramowitz, R., Pinal, R., Davis, P., and Yalkowsky, S. H. (1988). "Solubility of aromatic pollutants in mixed solvents." *Chemosphere*, 17(2), 285-298.
- Morrow, N. R. (1987). "A review of the effects of initial saturation, pore structure and wettability on oil recovery by waterflooding." *North Sea Oil and Gas Reservoirs*, Graham and Troutman, eds., Norwegian Institute of Technology, 179-192.
- Morrow, N. R., Chatzis, I., and Taber, J. J. (1988). "Entrapment and mobilization of residual oil in bead packs." *SPE Reservoir Engineering*, 3(3), 927-934.
- Morrow, N. R., and Songkran, B. (1981). "Effect of viscous and buoyancy forces on nonwetting phase trapping in porous media." *Surface Phenomena in Enhanced Oil Recovery*, D. O. Shah, ed., Plenum Press, New York, 387-411.
- Morse, R. A. (1952). German Patent No. 849,534, Germany.
- Mualem, Y. (1976). "A new model for predicting the hydraulic conductivity of unsaturated porous media." *Water Resources Research*, 12(3), 513-522.
- Ng, K. M., Davis, H. T., and Scriven, L. E. (1978). "Visualization of blob mechanics in flow through porous media." *Chemical Engineering Science*, 33, 1009-1017.
- Padgett, P. K., and Hayden, N. J. (1999). "Mobilization of residual tetrachloroethylene during alcohol flushing of clay-containing porous media." submitted to *Journal of Contaminant Hydrology*.
- Patel, K., and Greaves, M. (1987). "Role of capillary and viscous forces in mobilization of residual oil." *The Canadian Journal of Chemical Engineering*, 65 (August), 676-679.

- Paulsell, W. G. (1953). "The Effect of a Mutually Miscible Intermediate Phase on Immiscible Fluid Displacement in a Porous Medium," Master's Thesis, University of Oklahoma, Norman.
- Pennell, K. D., and Abriola, L. M. (1996). "Surfactant enhanced aquifer remediation: Fundamental processes and practical implications." *Bioremediation: Principles and Practice*, S. K. Sikdar and R. L. Irvine, eds., Technomic Publishers, Lancaster, PA (in press).
- Pennell, K. D., Abriola, L. M., and Loverde, L. E. (1996a). "The use of surfactants to remediate NAPL-contaminated aquifers." Proceedings of *Non-Aqueous Phase Liquids (NAPLs) in Subsurface Environment: Assessment and Remediation*, ASCE, Washington, DC, 221-232.
- Pennell, K. D., Abriola, L. M., and Pope, G. A. (1996b). "Influence of viscous and buoyancy forces on the mobilization of residual tetrachloroethylene during surfactant flushing." *Environmental Science and Technology*, 30, 1328-1335.
- Pennell, K. D., Abriola, L. M., and Weber, W. J., Jr. (1993). "Surfactant enhanced solubilization of residual dodecane in soil columns. 1. Experimental investigation." *Environmental Science and Technology*, 27(12), 2332-2340.
- Pennell, K. D., Jin, M., Abriola, L. M., and Pope, G. A. (1994). "Surfactant enhanced remediation of soil columns contaminated by residual tetrachloroethylene." *Journal of Contaminant Hydrology*, 16(1), 35-53.
- Pinal, R., Rao, P. S. C., Lee, L. S., Cline, P. V., and Yalkowsky, S. H. (1990). "Cosolvency of partially miscible organic solvents on the solubility of hydrophobic organic chemicals." *Environmental Science and Technology*, 24(5), 639-647.
- Pope, G. A., and Wade, W. H. (1995). "Lessons from enhanced oil recovery research for surfactant-enhanced aquifer remediation." *Surfactant Enhanced Subsurface Remediation, ACS Symposium Series 594*, D. A. Sabatini, R. C. Knox, and J. H. Harwell, eds., American Chemical Society, Washington, DC.
- Powers, S. E., Abriola, L. M., and Weber, W. J. (1994). "An experimental investigation of nonaqueous phase liquid dissolution in saturated subsurface systems: transient mass transfer rates." *Water Resources Research*, 30(2), 321-332.
- Ramamohan, T. R., and Slattery, J. C. (1984). "Effects of surface viscoelasticity in the entrapment and displacement of residual oil." *Chemical Engineering Communications*, 26, 241-263.

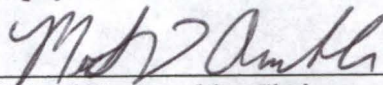
- Rao, P. S. C., Annable, M. D., Sillan, R. K., Dai, D., Hatfield, K., and Graham, W. D. (1997). "Field-scale evaluation of in situ cosolvent flushing for enhanced aquifer remediation." *Water Resources Research*, 33(12), 2673-2686.
- Ryan, R. G., and Dhir, V. K. (1996). "The effect of interfacial tension on hydrocarbon entrapment and mobilization near a dynamic water table." *Journal of Soil Contamination*, 5(1).
- Scatchard, G. (1931). "Equilibria in non-electrolyte solutions in relation to the vapor pressures and densities of the components." *Chemical Reviews*, 8, 321-328.
- Scatchard, G. (1949). "Equilibrium in non-electrolyte mixtures." *Chemical Reviews*, 44, 7-35.
- Schwille, F. (1988). *Dense Chlorinated Solvents in Porous and Fractured Media*, Lewis, Chelsea, MI, 146 pp.
- Shincariol, R. A., and Schwartz, F. W. (1990). "An experimental investigation of variable density flow and mixing in homogeneous and heterogeneous media." *Water Resources Research*, 26(10), 2317-2329.
- Sievert, J. A., Dew, J. N., and Conley, F. R. (1958). "The deterioration of miscible zones in porous media." *Transactions of the American Institute of Mechanical Engineers*, 213, 228.
- Sillan, R. K. (1999). "Field-scale evaluation of in situ cosolvent flushing for enhanced aquifer remediation," Ph.D. dissertation, University of Florida, Gainesville, 181 pp.
- Slobod, R. L. (1958). "A review of methods used to increase oil recovery." *Producers Monthly*, 22(4), 24.
- Sorenson, J., and Arlt, W. (1980). *Liquid-Liquid Equilibrium Data Collection-Ternary Systems*, 2. DECHEMA Chemistry Data Series, D. Behrens and R. Eckermann, eds., DECHEMA, Frankfurt.
- Stegemeier, G. L. (1977). "Mechanisms of entrapment and mobilization of oil in porous media." *Improved Oil Recovery by Surfactant and Polymer Flushing*, D. O. Shah, ed., Academic Press, New York, 55-91.
- Stumm, W., and Morgan, J. J. (1981). *Aquatic Chemistry: An Introduction Emphasizing Chemical Equilibria in Natural Waters*, 2nd ed., John Wiley & Sons, Inc., New York, 780 pp.

- Taber, J. J. (1969). "Dynamic and static forces required to remove a discontinuous oil phase from porous media containing both water and oil." *SPE Journal*, March, 3-12.
- Taber, J. J. (1981). "Research on enhanced oil recovery: Past, present and future." *Surface Phenomena in Enhanced Oil Recovery*, D. O. Shah, ed., Plenum Press, New York, 13-52.
- Valvani, S. C., Yalkowsky, S. H., and Amidon, G. L. (1976). "Solubility of nonelectrolytes in polar solvents. VI. Refinements in molecular surface area computations." *Journal of Physical Chemistry*, 80, 829-835.
- van Genuchten, M. T. (1980). "A closed-form equation for predicting the hydraulic conductivity of unsaturated soils." *Soil Science Society of America Journal*, 44, 892-898.
- Williams, N. A., and Amidon, G. L. (1984a). "Excess free energy approach to the estimation of solubility in mixed solvent systems. I: Theory." *Journal of Pharmaceutical Science*, 73, 9-13.
- Williams, N. A., and Amidon, G. L. (1984b). "Excess free energy approach to the estimation of solubility in mixed solvent systems. II: Ethanol water mixtures." *Journal of Pharmaceutical Science*, 73, 14-18.
- Wilson, J. L., Conrad, S. H., and Mason, W. R. (1990). "Laboratory Investigation of Residual Liquid Organics." *EPA/600/6-90/004*, Robert S. Kerr Environmental Research Laboratory, Environmental Protection Agency, Ada.
- Wise, W. R. (1992). "A new insight on pore structure and permeability." *Water Resources Research*, 28(1), 189-198.
- Yalkowsky, S. H., Valvani, S. C., and Amidon, G. L. (1976). "Solubility of nonelectrolytes in polar solvents. IV. Nonpolar drugs in mixed solvents." *Journal of Pharmaceutical Science*, 65, 1488-1494.
- Young, S. R. (1999). "Cosolvent Effects on the Phase Behavior of NAPL Mixtures," Masters of Science, University of Florida, Gainesville.

BIOGRAPHICAL SKETCH

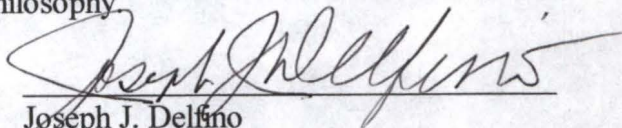
Michael E. Van Valkenburg was born at the U.S. Military Academy, West Point, New York, on October 23, 1963. He graduated from Amphitheater High School, Tucson, Arizona, in May 1981, and immediately attended Washington University in St. Louis. In May 1985, he was awarded a Bachelor of Science degree in chemical engineering. On the same day, he was commissioned a second lieutenant in the U.S. Air Force as a bioenvironmental engineer. His first duty location was at Williams Air Force Base (AFB), Mesa, Arizona, where he held the position of Chief, Bioenvironmental Engineering Services. In June 1997 he was transferred to Ellsworth AFB, Rapid City, South Dakota, where he was Chief, Environmental Protection and Monitoring Programs. Upon acceptance to an Air Force-sponsored graduate program, he attended South Dakota School of Mines and Technology from August 1989 to June 1991, and received a Master of Science degree in civil (environmental) engineering. Upon completion, he transferred to the United States Air Force Academy, Colorado Springs, Colorado, to become a member of the Department of Chemistry. Here he taught general, analytical, and environmental chemistry to undergraduate Air Force Cadets. From June 1994 to August 1996 he was assigned to the Air Force Center for Environmental Excellence (AFCEE), Brooks AFB, Texas, where he was Deputy Chief, Pollution Prevention Programs Division. Upon acceptance of an Air Force sponsored Ph.D. program, he moved to Gainesville, Florida. Mike has a wife, Kim, and three children, Joseph, Lauryn, and Kelley.

I certify that I have read this study and that in my opinion it conforms to acceptable standards of scholarly presentation and is fully adequate, in scope and quality, as a dissertation for the degree of Doctor of Philosophy.



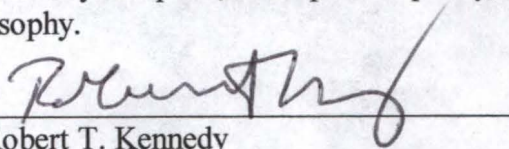
Michael D. Annable, Chair
Associate Professor of
Environmental Engineering Sciences

I certify that I have read this study and that in my opinion it conforms to acceptable standards of scholarly presentation and is fully adequate, in scope and quality, as a dissertation for the degree of Doctor of Philosophy.



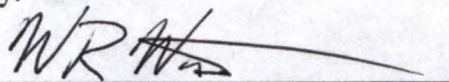
Joseph J. Delfino
Professor of Environmental Engineering
Sciences

I certify that I have read this study and that in my opinion it conforms to acceptable standards of scholarly presentation and is fully adequate, in scope and quality, as a dissertation for the degree of Doctor of Philosophy.



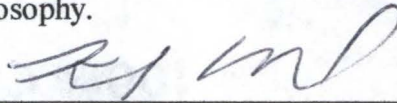
Robert T. Kennedy
Professor of Chemistry

I certify that I have read this study and that in my opinion it conforms to acceptable standards of scholarly presentation and is fully adequate, in scope and quality, as a dissertation for the degree of Doctor of Philosophy.



William R. Wise
Associate Professor of Environmental
Engineering Sciences

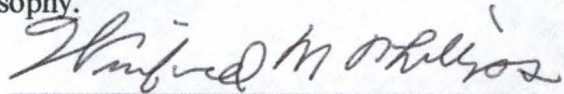
I certify that I have read this study and that in my opinion it conforms to acceptable standards of scholarly presentation and is fully adequate, in scope and quality, as a dissertation for the degree of Doctor of Philosophy.



Kirk Hatfield
Associate Professor of Civil
Engineering

This dissertation was submitted to the Graduate Faculty of the College of Engineering and to the Graduate School and was accepted as partial fulfillment of the requirements for the degree of Doctor of Philosophy.

May 1999



Winfred M. Phillips
Dean, College of Engineering

M. J. Ohanian
Dean, Graduate School

CORRELATION AND MODIFICATION OF PERCHLORATE BY
SOLUBILITY IN POROUS MEDIA

LD
1780
199g
V217

MICHAEL EDWARD VAN VALKENBURG

STATE SCHOOL
FULFILLMENT
OF THE R



A DISSERTATION
OF THE UNIVERSITY
OF THE R

DOCTOR OF PHILOSOPHY

UNIVERSITY OF FLORIDA

1999
MICHAEL EDWARD VAN VALKENBURG
DOCTOR OF PHILOSOPHY